BRILL *Insect Systematics & Evolution (2022) DOI 10.1163/1876312X-bja10034* brill.com/ise

Neoponera Emery, 1901 (Hymenoptera: Formicidae) revisited: 1. The *N. laevigata* species-group

Adrian Troya[a,b,*] and John Lattke[a,*]

[a]Departamento de Zoologia, Universidade Federal do Paraná, CP 19020, Curitiba, PR, 81531–980, Brazil
[b]Departamento de Biología, Escuela Politécnica Nacional, Ladrón de Guevara E11-253, P.O.Box 17-01-2759, Quito, Ecuador
*Corresponding authors; e-mails: adrian.troya77@gmail.com; piquihuye@gmail.com

ORCID iDs: Troya: 0000-0002-1548-3215; Lattke: 0000-0002-6793-3003

Abstract
The Neotropical *Neoponera laevigata* species-group is revised. This group can be separated from others in the genus by means of a new key to *Neoponera* species–groups. We propose two new species, *N. gojira* **sp. nov.**, and *N. mashpi* **sp. nov.**, the latter being usually confused with its putative sister species, *N. laevigata* (Smith). This small, termite-feeding species-group now contains five taxa. We provide comprehensive redescriptions for the known castes of the three previously known species, together with images and notes about intraspecific morphological variation, biology, and distribution of the taxa here treated. We reveal the external morphological features of the genitalia of the known males. This is the first contribution en route to a better understanding of the systematics of this charismatic ponerine genus.

Keywords
Neotropical region; polymorphism; Ponerinae; termite-hunting; Termitopone

ZooBank: https://zoobank.org/490A02AE-77DC-435E-A673-E87C2C288A7A

Introduction

Neoponera Emery is a behaviorally and morphologically diverse group of ground and mostly arboreal, solitary hunting ants which inhabit exclusively tropical and subtemperate regions of the Americas (Schmidt & Shattuck 2014). A few species, like *N. apicalis* (Latreille) and *N. villosa* (Fabricius) are recognizable at a glance, whereas most of the remaining taxa require detailed examination, and little is known about the natural history of most species. Schmidt and Shattuck (2014) provide a good primer about various aspects of their social and reproductive behavior, nesting ecology,

 10.1163/1876312X-bja10034DOI

chemical communication, and some other details on the biology of a few well–studied *Neoponera*.

Neoponera is closely related to *Pachycondyla* Smith, with which it shares numerous morphological features (Schmidt & Shattuck 2014). Emery (1901) erected *Neoponera*, and in his work he described the genus as "the American *Pachycondyla* with keeled cheeks" (p. 43), i.e., with malar carina, which separated them from the true *Pachycondyla* and other related Neotropical forms, like *Mayaponera* Schmidt and Shattuck. Although this character probably proved useful for earlier researchers distinguishing *Neoponera* species from similar ponerines, a number of taxonomic issues emerged as the material increased in collections. The apparent lack of synapomorphies among several *Pachycondyla*–related groups probably led Brown (1973) to synonymize all of them under *Pachycondyla*. Prior to Schmidt (2013), who provided a phylogenetic classification framework for the whole subfamily Ponerinae based on molecular data, *Pachycondyla*, as formerly considered, remained broadly accepted (Bolton 1995; Mackay & Mackay 2010; Fernandes et al. 2014).

Schmidt and Shattuck (2014) revived *Neoponera* from synonymy and transferred to it some species previously considered in *Eumecopone*, *Mesoponera, Pachycondyla*, and *Termitopone*. This latter is composed of termite feeding specialists which is considered a unique behavioral trait within the genus. Mackay and Mackay (2010) assigned them to the *N. laevigata* species–complex, but here we treat it as a species–group. Despite being revised twice (see details below), in the last years, as part of a complete revision of the genus which is currently ongoing, we have found new information about this small, but certainly iconic clade. In addition, we detected that most of the material which is frequently assigned to the commonly collected *N. laevigata* (Smith), in fact belongs to a new species which we describe here. Also, based on new morphological information we provide detailed descriptions for all known castes, along with notes, in most cases, about intra– and interspecific morphological variation, biology and distribution.

Materials and methods

Repositories of examined material

Morphological observations are based on close to 400 specimens which are deposited in the following institutions. Within that number, 16 specimens were examined through high quality images available online on AntWeb (www.antweb.org). Museum abbreviations are based on Arnett et al. (2019).

ALWC	Alex L. Wild Collection, TX, USA
BMNH	The British Museum of Natural History, London, UK
CASC	California Academy of Sciences, San Francisco, CA, USA
CPDC	Coleção do Laboratório de Mirmecologia, Centro de Pesquisas do Cacau, Ilhéus, Bahia, Brazil

DZUP	Coleção Entomológica Padre Jesus Santiago Moure, Universidade Federal do Paraná, Curitiba, Paraná, Brazil
ECOFOG	EcoFoG–Joint Research Unit Ecology of Guianan Forests, Kourou, French Guiana
ICN	Instituto de Ciencias Naturales, Universidad Nacional de Colombia, Bogotá, Colombia
INBC	Instituto Nacional de Biodiversidad, Heredia, Costa Rica
INPA	Instituto Nacional de Pesquisas da Amazônia, Manaus, Amazonas, Brazil
JTLC	John T. Longino Collection, University of Utah, Salt Lake City, UT, USA
LACM	Los Angeles County Museum, LA, USA
MECN	Museo Ecuatoriano de Ciencias Naturales, Instituto Nacional de Biodiversidad, Quito, Ecuador
MPEG	Museu Paraense Emílio Goeldi, Belém, Pará, Brazil
MEPN	Museo de Historia Natural "Gustavo Orcés V.", Escuela Politécnica Nacional, Quito, Ecuador
MIZA	Museo del Instituto de Zoología Agrícola, Universidad Central de Venezuela, Maracay, Venezuela
MUCR	Colección de Insectos, Universidad de Costa Rica, San Pedro, Costa Rica
MUSENUV	Museo de Entomología de la Universidad del Valle, Cali, Colombia
PSWC	Philip S. Ward Collection, University of California, Davis, CA, USA
QCAZ	Museo de Zoología de la Pontificia Universidad Católica del Ecuador, Quito, Ecuador
UFVLABECOL	Laboratório de Ecologia de Comunidades, Universidade Federal de Viçosa, Viçosa, Minas Gerais, Brazil

Imaging

Images were taken using a Canon® EOS DSLR 70D with a Laowa® 25mm F2.8, 2.5X – 5.0X macro lens, coupled to a Cognisys StackShot® macro rail system which enabled depth–focus shooting through Helicon Remote v. 3.9.9, and posterior stacking in Helicon Focus v. 7.5.6 (Helicon Soft Ltd.). A dome–shaped, cold–light (LED) source was used for illumination. Images of type material and some non–type specimens, as well as collection data of all examined specimens with unique specimen identifiers are available online on AntWeb (but see further below in "Material examined").

Images and illustrations by A. Troya, except those in figures: Fig. 5b (by Júlio Chaul), Fig. 8a (by April Nobile), and Fig. 20a, b, c, f (by Will Ericson), available on

AntWeb.org. SEM images in Figs 14a, b and 18b by Paula Carolina Ferreira, Centro de Microscopia Eletrônica, Universidade Federal do Paraná.

Morphometric variables

All observations and measurements of the following morphological variables (Fig. 1 and Supplementary Material S1) were taken using a pin–holding stage, allowing rotations around the X, Y, and Z axes at magnifications from 8X to 50X with an ocular micrometer incorporated to a Zeiss® Stemi SV6 stereo microscope.

Measurements are presented in mm with an accuracy of two decimal places, minimum and maximum values are indicated when more than one specimen was measured. Most of our measurements are in line with those previously used in other ponerine taxonomic studies, e.g., Lattke (2012), Rakotonirina and Fisher (2013), Fernandes et al. (2014), and Longino and Branstetter (2020). Other measurements, e.g., length of gastral sclerites, are less common in Formicidae taxonomy and its use is intended to support the body of typically used morphological variables in discriminating difficult–to–discern variations across populations in a given species. Criteria for selecting specimens for measurement follow each species' known distribution, by picking up a number of differently sized specimens per collection site, when available. Morphometric variables facilitate, to a certain degree, examining across the morphospace the intra– and inter–population variability in the set of treated species. This is also useful as another line of evidence for testing and/or supporting species hypotheses.

HL	Head length. In frontal view, maximum distance from the posterior margin of head to the anterior margin of clypeus.
HW	Head width. In frontal view, maximum width of head, excluding the eyes.
EL	Eye length. In lateral view, measured along its maximum length.
SL	Scape length. In frontal view, maximum length of scape excluding its basal condyle and neck.
PrW	Pronotum width. In dorsal view, maximum width of pronotum.
WL	Weber's length. In lateral view, distance between the anterior margin of pronotum, excluding collar, to the posteroventral margin of metapleuron.
MsW	Mesonotum width. In dorsal view, maximum width of mesonotum.
MsL	Mesonotum length. In dorsal view, the maximum distance from the anterior margin of mesonotum to its posterior margin.
PW	Petiolar width. In dorsal view, maximum width of the petiolar node.
PH	Petiolar height. In lateral view, the perpendicular distance from the posteroventral lobe of the petiolar tergite to its maximum dorsal margin.
PL	Petiolar length. In lateral view, the distance between the anteriormost margin of petiole to its posterior margin, excluding the posteroventral ridge.
GL	Gaster length. In lateral view, the oblique distance between the anterior margin of abdominal segment III to the posterior margin of pygidium, excluding the stinger. This is a relative measure since it can vary in relation to the extension or contraction of abdominal segments IV to VII.

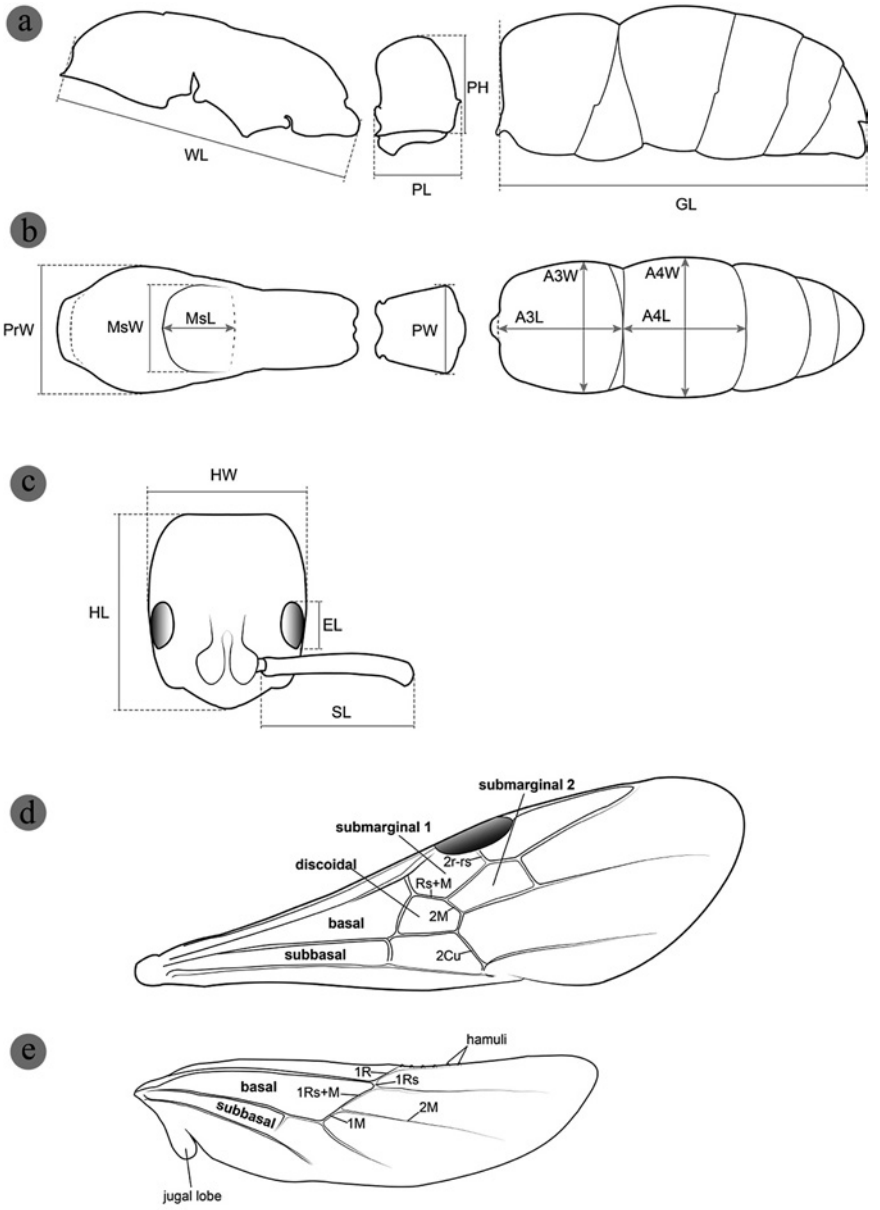

Fig. 1. Morphometric variables and wing venation (valid for male & female). **a.** GL: gaster length, PH: petiolar height, PL: petiolar length, WL: Weber's length; **b.** A3L: Abdominal segment III length, A3W: Abdominal segment III width, A4L: Abdominal segment IV length, A4W: Abdominal segment IV width, MsL: mesonotum length, MsW: mesonotum width, PW: petiolar width, PrW: pronotum width; **c.** EL: eye length, HL: head length, HW: head width, SL: scape length; **d.** Fore wing; **e.** Hind wing. Only some cells (in bold) and veins are shown since these are cited in the species descriptions.

A3L Abdominal segment III length. In dorsal view, the distance between the anterior and posterior margin of abdominal tergite III.
A3W Abdominal segment III width. In dorsal view, maximum width of tergite of abdominal segment III.
A4L Abdominal segment IV length. In dorsal view, the distance between the anterior and posterior margins of abdominal tergite IV.
A4W Abdominal segment IV width. In dorsal view, maximum width of tergite of abdominal segment IV.
TLa Total accurate length of body: HL + WL + PL + A3L + A4L.
TLr Total relative length of body: HL + WL + PL + GL.

Indices

The following ratios were multiplied by 100:

CI Cephalic index: HW/HL
OI Ocular index: EL/HW
SI Scape index: SL/HW
MsI Mesonotum index: MsW/MsL
LPI Lateral petiolar index: PL/PH
DPI Dorsal petiolar index: PW/PL

Distribution maps

We used the open–source package Quantum GIS 2.18 to generate maps of distribution, based on coordinates written on specimen labels and from notes recorded in field books from the authors. All localities were transformed to decimal degrees. Google Earth (Google.com 2021), and the online conversion tool NCAT (National Geodetic Survey 2021) were used as information sources to check and confirm locality names. In regards to unusual records without specific localities which were below the administrative circumscription of state, province, or similar, the center of the next most specific site was georeferenced. We also included in the maps, appropriately labeled AntWeb records of *N. commutata* Roger and *N. marginata* Roger for which we were confident on their taxonomic and geographic information. Selected AntWeb records belonging to these two common taxa were identified by ant taxonomists, for example, Alex Wild, Bryan Fisher, Flavia Esteves, Jack Longino. Due to their unique morphology within *Neoponera* these are easily identifiable species, showing low morphological variation across their range of distribution, thus making misidentifications unlikely.

Jack Longino (lead researcher in several Central American ant survey campaigns) aided in examining diagnostic characters from representative AntWeb records of *N. laevigata* from Costa Rica and Panama. This was required since we believe most *N. laevigata* specimens from these countries are confused with *N. mashpi* **sp. nov.** (see below under each species treatment).

Morphometric analysis

Due to imbalance among the number of measured specimens per caste, namely 59 workers vs 15 reproductives, we chose only the former caste for creating the data matrix which incorporates 24 morphological variables.

Using the package vegan v2.5–7 (Oksanen et al. 2015) implemented in R (R Core Team 2021), we first analyzed the data using principal components analysis (PCA) to visually explore the relative quality of each morphometric variable as shown in the factor map of a circular correlation plot (Fig. 1, Supplementary Material S2). We also calculated the amount of retained variance by each of the 10 dimensions in the PCA by means of the eigenvalues (Fig. 2, Supplementary Material S2). The eigenvalues are useful for determining the number of principal components to retain in a PCA (Kaiser 1961). Since our main goal for using ordination techniques is to statistically discern differences among our species set, particularly between the highly similar *N. mashpi* **sp. nov.** and *N. laevigata* with respect to the morphometric variables, we chose to use non–metric multidimensional scaling (NMDS) for representing the final plot due to its robustness in handling non–parametric data, as well as its versatility in allowing the use of a range of dissimilarity indices. We used the following basic parameters for generating the NMDS ordination: No. of dimensions (*K*): 2–4 (though, the final result is represented in dimensions 1–2, since dimensions 3–4 returned unrealistic results); method for calculating the dissimilarity matrix (*distance*): *euclidean*; No. of permutations (*trymax*) set to 1000. In order to examine potential global differences among the whole set of species we ran a permutational multivariate analysis of variance (PERMANOVA), using the *adonis* function, with 1000 permutations, and the *gower* method (Gower 1971) for calculating *pairwise distances*. Finally, for examining statistical differences between each species pair, we ran a pairwise contrast analysis using the function *pairwise.adonis* (Pedro Martinez Arbizu, unpubl. data) with a *Bonferroni* adjustment. The user can find the annotated script containing the full commands for performing and plotting the statistical analyses in the Supplementary Material S3.

Morphological terms

General morphological terminology follows mainly Bolton (1994), Keller (2011), Boudinot (2015), Silva and Feitosa (2019), and the Hymenoptera Anatomy Ontology – HAO (Yoder et al. 2010). Surface sculpture is based mainly on Harris (1979). Male and female forewing venation on Ogata (1991), and Cantone (2017); hind wing venation on Cantone and Von Zuben (2019). Degree of pilosity inclination follows Wilson (1955), Serna and Mackay (2010): 0°–5° for appressed hairs running parallel or nearly parallel to body surface; 10°–20° for decumbent hairs slightly standing from surface; 20°–40° for subdecumbent hairs; 40°–70° for suberect hairs; and more than 70° for erect hairs when these stand vertical or nearly vertical. For male genitalia we followed Boudinot (2013) and Tozetto and Lattke (2020). Palp formula is denoted by "PF" followed by the number of maxillary and labial segments, for example, PF: 4, 4, which means that both appendices have four segments. Tibial spur formula is denoted by "s" – simple,

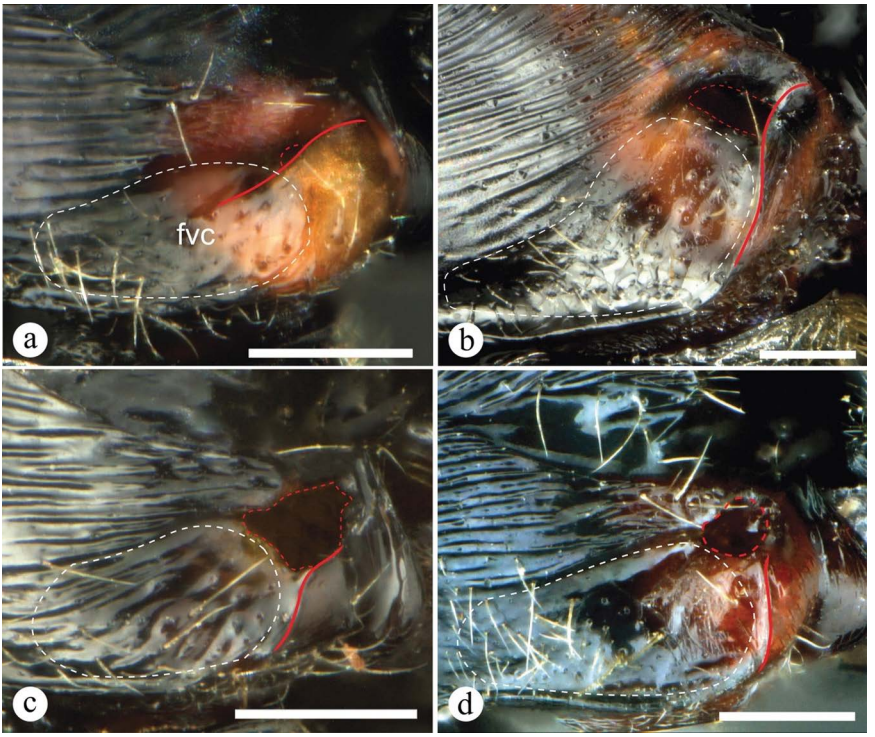

Fig. 2. Cuticular flap variations (solid red line) at the orifice of metapleural gland (dashed red line) in queens and workers of the *N. laevigata* species–group, as seen in lateral view. **a**. *Neoponera mashpi* **sp. nov.** (CPDC: ATPFOR2054–2), the flap is well–developed, strongly curved anterad so that it conceals most of the gland opening, this variation is almost identical to that present in *N. laevigata*; **b**. *Neoponera commutata* (DZUP: DZUP549422), the flap is well–developed, barely curved anterad and slightly hides the orifice of the gland; **c**. *Neoponera marginata* (MEPN: ATPFOR1988), the flap is present but is less developed than in *N. commutata*, the orifice of the gland is almost entirely visible; **d**. *Neoponera gojira* **sp. nov.** (DZUP: DZUP549444), the flap is strongly reduced and modified into a carina, the orifice of the gland is completely visible. Dashed white lines represent the approximate area of the pheromone venting canal (fvc). Scale bars: 0.2 mm.

and "p" – pectinate, for example, 2(1s, 1p) which means that two spurs are present, one simple, and 1 pectinate.

Descriptions and material examined

We used the computer package DELTA (Dallwitz 1980) for encoding the attributes of species (character states) and subsequently translating them into natural language (RTF–rich text files) taxonomic descriptions, requiring only posterior final editing from the user. Transcription of the collection information of examined specimens, from a spreadsheet data matrix to correspondent RTF file, was mostly done using AUTOMATEX (Brown 2013).

Under "status as species" in the taxonomic history of each species, only their first appearance in the taxonomic literature is cited, as well as relevant redescriptions which

are usually part of revisionary studies. The user can access the complete history of literature mentions for each species on the Online Catalogue of the Ants of the World – AntCat (AntCat by B. Bolton 2022).

Although the "material examined" section represents the complete set of recorded localities in this work, it does not contain the whole list of specimens/locality. We have included, however, at the beginning of each section the total number of specimens/caste/species examined. The reader can freely download from the Supplementary Material S4 the full list of specimen records containing collection and geographic information, most of which have unique specimen identifiers.

The format of type material follows: [# specimens examined], [country], [first administrative region], [second administrative region or, if known, specific locality], [coordinates in decimal degrees], [elevation in meters], [collection date in format yyyy–mm–dd], [collector], [method of collection (if known)], [habitat (if known)], and [institution where the material is located, usually represented by a unique specimen identifier composed of capitalized letters and numbers]. The format for "Other material examined" is essentially equal except that unique specimen identifiers are not shown, but museum acronyms are.

Relationships among taxa

In this work we have chosen to add brief comments about the relationships between species within the *N. laevigata* group, and also between *Neoponera* and a newly recognized clade (see further below). Our statements are grounded on prior studies by Schmidt (2013) and Branstetter and Longino (2022), as well as on molecular-based preliminary results (A. Troya, J. Longino, M. Branstetter et al. unpublished) which are part of a larger ongoing collaborative study about the phylogeny of the genus *Neoponera* which will be published separately. This additional information is not to be treated as conclusive, nevertheless we think it adds support to our morphology–based arguments around the species hypotheses shown here.

Species delimitation

We follow the biological species concept *sensu* Mayr (1942) by considering species as population assemblages which are under presumed continuous gene flow. Since we did not directly assess this process, our criterion for species delimitation was to detect a continuum of expected character gradations lacking discontinuities among distinctive populations. In sympatry, interspecific gene flow can obscure populational distinctness (Arnold 1992; Field et al. 2011). In such case species can be detected by consistently grouping morphologically similar individuals assumed to belong to structured populations, which is a proxy for gene flow (Wild 2005).

The species hypotheses presently proposed, especially the newly described taxa, should be evaluated in further studies using additional information criteria, e.g., population genetics, natural history observations. These will add more objective evidence aiding in the discrimination of species boundaries among cryptic populations which

may potentially be under differing selective pressures that are suspected, yet untested in this study.

Results

Morphology

The following few terms are defined in detail to aid in the comprehension of this treatment. In regards to the comparatively complex male external morphological terminology the user can consult Boudinot (2013, 2015), and HAO.

Mesosternal (msp) and metasternal (mtp) processes (Figs 16d, 19f, 20e, 22f, 25e): also called articular coxal processes of the meso- and metapectus (see HAO): in ants, especially in the Ponerinae, a pair of ventrally directed extensions of the cuticle, usually with acute or blunt apices, emerge medially from the meso- and metasternon. Each of these emerge either immediately posterior- or just around the mesosternal and metasternal pits, respectively, approximately in between the coxal cavities. When present, these structures may vary considerably in size, external shape and orientation, though probably the most generalized is the triangular-shaped form with acute apices, easily discernible in posteroventral view when the posterior coxae are oriented laterally (not posterad as is usual). In *Neoponera*, their presence/absence, as well as their size and shape, are considered useful character–states aiding in species and species-groups distinction.

Pheromone venting canal (fvc) at the metapleural gland opening (Fig. 2): a depression of the cuticle located just anteriorly and below the orifice of the metapleural gland. This structure is present in virtually all Ponerinae and is located at the posteroventral margin of the propodeum. It varies in depth, being clearly concave, e.g., *Neoponera commutata*, to shallowly concave, e.g., *Megaponera analis* (Latreille). In most *Neoponera* it is flanged posteriorly by a cuticular flap, and dorsally by an excavated edge of the propodeum.

Anteroventral petiolar carina: a transverse ridge located near the ventral part of the anterior face of tergite of A2 (petiolar node), relatively close to the petiolar condyle which articulates with the propodeal foramen, as seen in dorsal view. In Ponerinae, when well–developed, this carina usually extends anterolaterad forming salient, either acute or blunt projections ("spiracular horns" in Mackay & Mackay 2010). Two variations are recognized: complete and incomplete carina. In the first state, the carina runs horizontally uninterrupted connecting both anterolateral nodal projections, e.g., *Leptogenys luederwalti* Forel, *Loboponera nasica* (Santschi). When it is incomplete, it disappears medially on the petiolar tergite, leaving the nodal projections virtually unconnected, in which case these usually are notoriously salient. An incomplete carina is the norm in *Neoponera*, e.g., *N. crenata* Roger, *N. commutata*, *N. villosa*, as well as in most ponerines. In *Neoponera*, a complete carina is found for example, in *N. apicalis*, *N. rostrata* (Emery).

Morphometrics

The PCA circular plot (Fig. 1, Supplementary Material S2) shows that most variables are positively correlated and also most of them are well–represented in the factor map (= they are close to the circumference margin), which means they are important in explaining the total morphometric variance (ca. 92%) represented in the first two dimensions of the ordination. The quality of representation of the variables is calculated using the square cosine and expressed through the eigenvalues as shown in Fig. 1 for dimensions 1 and 2 (Supplementary Material S4). On the other hand, the NMDS ordination was supported by a robust stress value of 0.01826, which according to the criteria of Kruskal (1964), indicates a strong correlation between ranked observed dissimilarities and ordinated distances. This value also suggests that our observations, i.e., measured specimens, are not grouped randomly. The graph shows a small cluster of convergent observations representing most taxa, except *N. commutata*, which is suggestive of morphometric similarity as these share a significant fraction of their morphospace. As expected, this is evident between *N. mashpi* **sp. nov.** and *N. laevigata* since their measured characters are more similar in size between each other than with the remaining species (Fig. 3). The PERMANOVA, however, rejected the null hypothesis that all the observations are equal ($p < 0.000999$; 85% of variance explained, see the full output statistics in Supplementary Material S2), and the pairwise contrast test was significant for some species pairs, including *N. mashpi* **sp. nov.** and *N. laevigata* (p adjusted = 0.03), thus supporting our hypothesis that these belong to distinct, though phylogenetically close lineages (Troya et al. unpubl. data). Except for the dorsal petiolar index (DPI), which is shown in the ordination plot relatively distanced apart from all the species groupings, the remaining indices are comparatively important in explaining the morphometric differences between *N. mashpi* **sp. nov.** and the rest of related taxa. Whereas, most of the other variables are important for distinguishing between *N. commutata* and its congeners. In regards to *N. gojira* **sp. nov**., for which a single individual was identified, the ordination shows that it is more similar to *N. laevigata* than to *N. marginata* and *N. mashpi* **sp. nov.** The morphospecies *Neoponera* nr. *gojira*, which is supposed to be closer (or perhaps conspecific) to *N. gojira* **sp. nov.**, is placed within the morphospace of *N. laevigata*, *N. marginata*, and *N. mashpi* **sp. nov.** Since the sample size of both *N. gojira* **sp. nov.** and *Neoponera* nr. *gojira* is currently insufficient for making solid conclusions about the potential place occupied by them in the morphospace of the *N. laevigata* group, further specimens are required to confirm current assumptions. However, as detailed in its corresponding species treatment, we do have valid reasons to treat *N. gojira* **sp. nov.** as a good species.

Worker– and queen–based key to Neoponera species–groups

The following key allows distinguishing species–groups within *Neoponera*, as well as a newly recognized genus lineage which is apparently sister to *Neoponera* (Troya et al. unpubl. data). For practical reasons only we here refer to this new genus as "*N. emiliae* 2", since the three species composing this clade, *Neoponera concava* Mackay & Mackay, *N. schultzi* Mackay & Mackay, and *N. venusta* Forel, are currently assigned

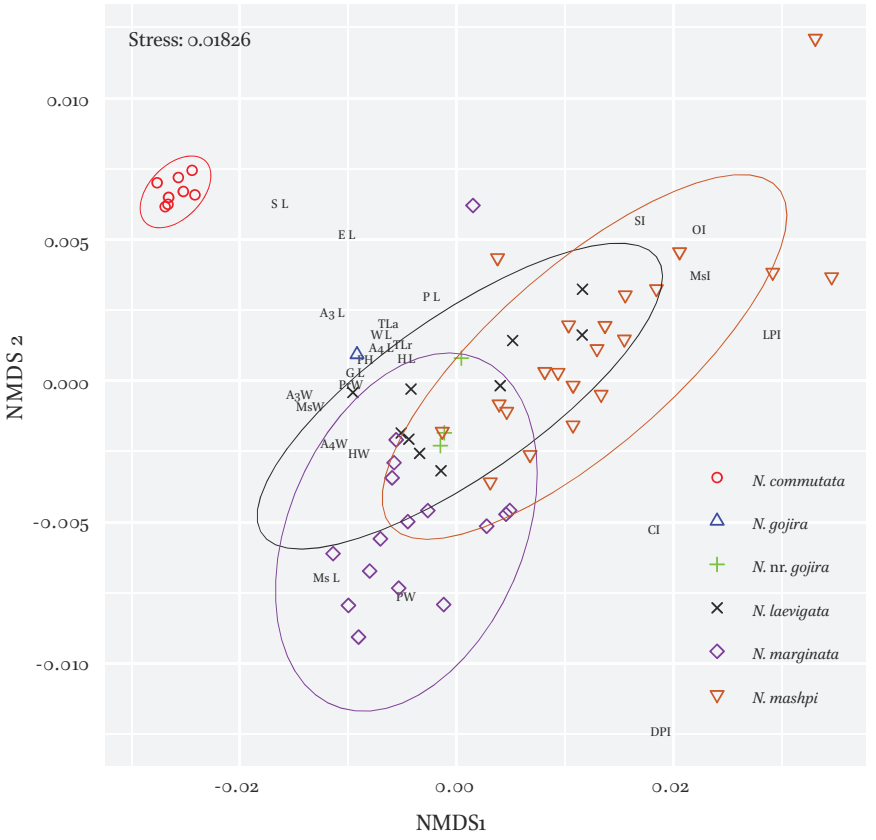

Fig. 3. Non–metric multidimensional scaling (NMDS) plot depicting the 24 morphometric variables shown in abbreviated letters (see materials and methods) which best contribute to explain the morphological variance among the observations (N= 59 workers) across the morphospace which is composed of five species and one morphospecies in the *N. laevigata* group. The ellipses margins represent the 95% confidence intervals. See extended explanation under results.

to the *Neoponera emiliae* group *sensu* Mackay & Mackay (2010). In addition, we have evidence that *N. bucki* Borgmeier does not belong to *Neoponera* but it is distantly related to it, probably another new genus lineage. Nevertheless, as we are not proposing new nomenclatural acts in this regard, we have included both *N. bucki* and the "*N. emiliae* 2" group in the present key until formalizing their new status in a coming contribution.

Character states in each statement appear in relative order of importance for the identification of a given group.

1. Propodeal spiracle circular (Fig. 4a); malar carina present, running over anterointernal eye region, in lateral view (Fig. 4d); body black, while legs usually yellowish to brownish; workers comparatively small (WL = 1.4–2.1 mm); ground living; eastern Brazil (mostly Atlantic Forest), Southern Colombia (?), Rondônia (?), Pará (?)..... **"*N. emiliae 2*"**

Propodeal spiracle either oval (Fig. 4b) or slit-shaped (Fig. 4c); malar carina present or absent, when present never running over anterointernal eye region but in front of it, in lateral view (Fig. 4e); body (including legs) varying in color from black, to brownish, to yellowish, to iridescent bluish-greenish; size of workers may vary greatly, but in general, significantly larger than in previous statement (WL usually > 2 mm up to about 6 mm); Neotropical Region: southern United States to central – northern Argentina..... **2 *Neoponera***

2(1). Ventrolateral pronotal margin with well-impressed, usually cross ribbed groove (Fig. 5f); propodeal spiracle oval to suboval (Fig. 4b) and, in only two species (*N. magnifica* Borgmeier and the undescribed "*N. magnifica*-5" DZUP549389, image on AntWeb.org) this spiracle is slit-shaped; mesonotum and propodeum divided by feeble notopropodeal suture which *never* forms a groove (Fig.5c); malar carina present or absent, when present always tenuously impressed and hard to discern at first sight; ground living; northern Venezuela, eastern Colombia (Amazonia), and eastern Brazil (Amazonia and Atlantic Forest)..... ***N. emiliae* group**

Ventrolateral pronotal margin without well-impressed groove, if a groove if present, then always shallow and never sculpted (Fig. 5e); propodeal spiracle always slit-shaped (Fig. 4c); mesonotum and propodeum either fused, although a vestigial line can be present (Fig. 5a, b), or divided by notopropodeal groove (Fig. 5d); malar carina either present or absent..... **3**

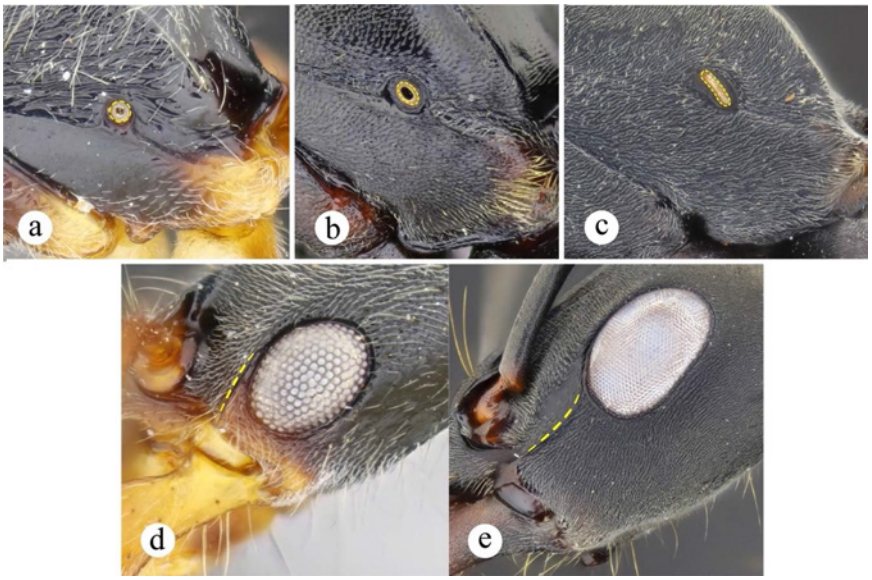

Fig. 4. Propodeal spiracle (**a**–**c**). **a**. Circular (*Neoponera schultzi*, MEPN: ATPFOR2024); **b.** Oval (*N. metanotalis*, CPDC: ATPFOR1997); **c.** Slit–shaped (*N.verenae*, DZUP: DZUP549670). Malar carina (**d**, **e**, highlighted by yellow dashed line). **d**. Running over anterointernal eye region (*N. schultzi*, MEPN: ATPFOR2024); **e**. Placed in front of anterointernal eye margin (*N.verenae*, DZUP: DZUP549670).

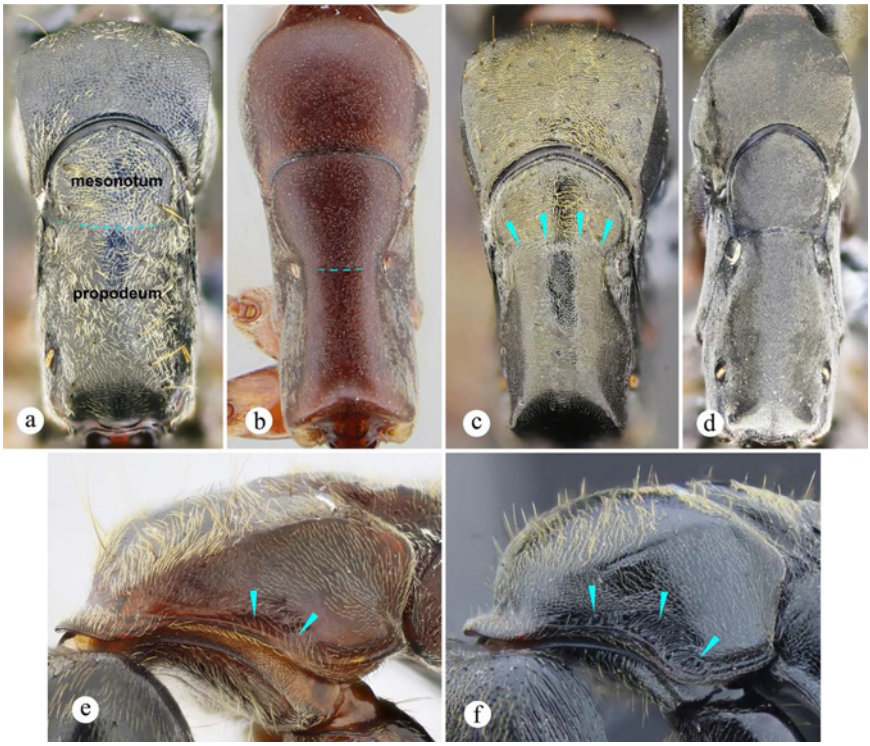

Fig. 5. Notopropodeal suture (**a**–**d**). In **a** and **b**, dashed, cyan lines demarcate the approximate region where the mesonotum and propodeum converge, in these cases the suture is either vestigial or tenuously impressed and the mesonotum and propodeum are fused; in **c**, the suture (as pointed by cyan arrowheads) is more discernible than in **a** and **b**, so that mesonotum and propodeum appear slightly separated; while in **d**, the suture is clearly visible, forming a shallow groove, so that mesonotum and propodeum are clearly separated. Ventrolateral pronotal margin (**e**, **f**). In **e**, with a shallow groove (as pointed by cyan arrowheads), while in **f**, the groove is strongly impressed and cross ribbed. **a**. *Neoponera carinulata* Roger (DZUP: DZUP549576), **b.** *N. bucki* (UFV: UFV-LABECOL007493), **c.** *N. metanotalis* (CPDC: ATPFOR1997), **d.** *N. verenae* (DZUP: DZUP549670), **e.** *N. goeldii* (MEPN: MEPNINV37890), **f.** *N. metanotalis* (UFV: UFVLABECOL000625).

3(2). Body integument jet-black and polished, with scarce appressed hairs (Fig. 6a); anterior mandibular region strongly bent ventrad in lateral view (Fig. 6c); ground (and arboreal?) living; Central America to Northern Argentina..... ***N. laevigata* group**
Body integument varying in color and surface sculpture, but never jet-black, usually with abundant appressed hairs which may vary in size and thickness (Fig. 6b); anterior mandibular region not strongly bent ventrad in lateral view (Fig. 6d)..... **4**

4(3). Clypeus, in lateral view, with convex, longitudinal carina medially, tip of carina acute (Fig. 7a, b); eye relatively flat, not surpassing lateral head margin, in frontal view (Fig. 7b); body with pruinose pilosity (tiny appressed hairs

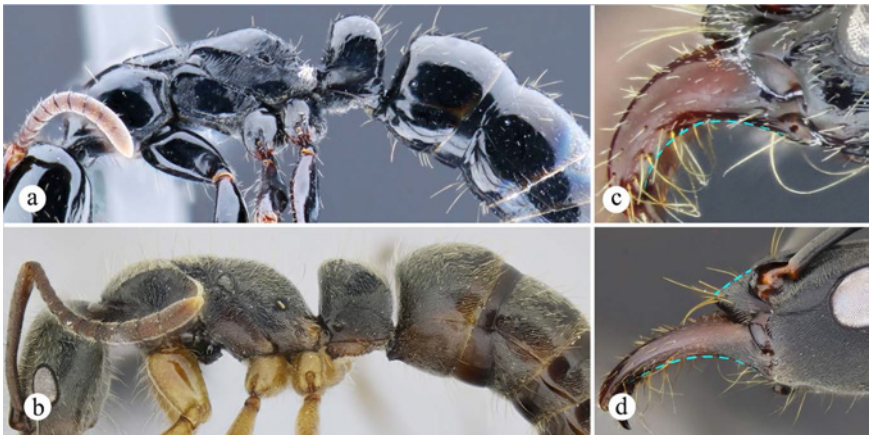

Fig. 6. Overall integument (**a**, **b**) and mandible curvature (**c**, **d**). **a.** Body with scarce appressed hairs (*Neoponera marginata*, MEPN: CASENT0649897); **b.** Body with abundant appressed hairs (*N. unidentata* Mayr, DZUP: DZUP549462); **c.** Mandible strongly curved ventrad (*N. laevigata*, CPDC: ATPFOR2040); **d.** Mandible not strongly curved ventrad (*N. verenae*, DZUP: DZUP549670).

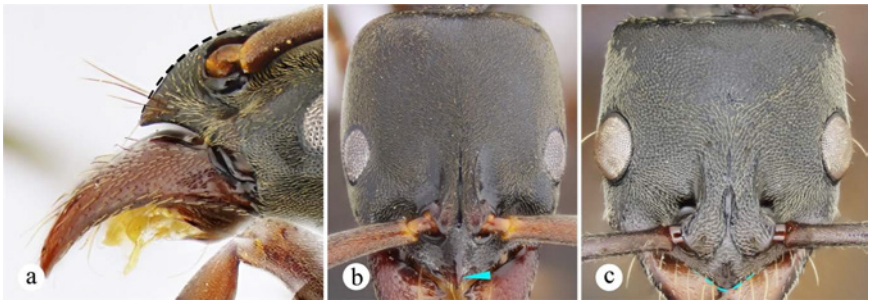

Fig. 7. Clypeus (**a**) and eye format (**b**, **c**). **a.** Clypeus with convex longitudinal carina medially (dashed black line) (*Neoponera bucki*, DZUP: DZUP549473); **b.** Eyes relatively flat, not surpassing lateral head margins; the cyan arrowhead points to the clypeal carina (*N. bucki*, DZUP: DZUP549473); **c.** Eyes convex, surpassing lateral head margins (*N. carinulata*, DZUP: DZUP549576).

forming a dusty-looking coat) and completely devoid of erect hairs on dorsum (Fig. 5b, d); mesonotum and propodeum fused, but usually a vestigial line is discernible dorsally (Fig. 5a, b); ground living; eastern Brazil (mostly Atlantic Forest) and eastern Venezuela..... ***N. bucki***

Clypeus, in lateral view, without convex longitudinal carina medially (shown in dashed cyan line, Fig. 6d); eye convex to globose, surpassing lateral head margin, in frontal view (Fig. 7c); body either with pruinose pilosity (few species) or with moderate to abundant appressed hairs (most species) (Fig. 6b); mesonotum and propodeum either fused (though a vestigial line can be discernible) or separated by notopropodeal groove..... **5**

5(4). Mesonotum and propodeum fused, and in many species a vestigial line is present (Fig. 5a, b); anterior mid clypeal region with usually blunt, subtriangular

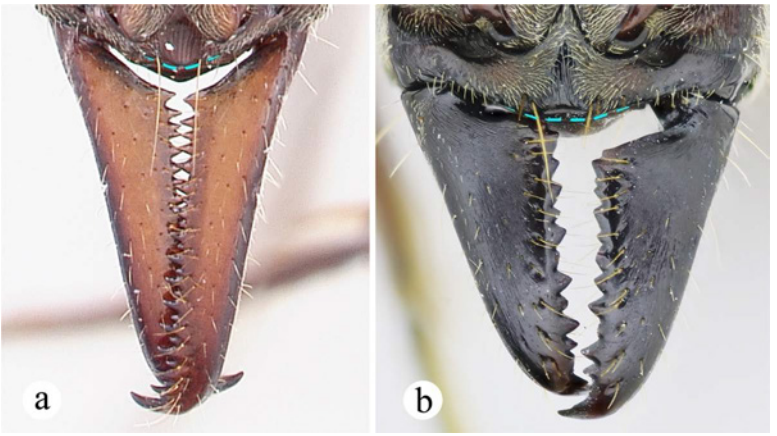

Fig. 8. Mandible. **a.** Very long, bearing about 18–19 teeth, alternating with denticles (*Neoponera rostrata*, MIZA: CASENT0178713); **b.** Bearing about 10–13 teeth alternating with denticles (*N. villosa*, MEPN: MEPN2930).

cuticular extension (dashed cyan line, Fig. 7c); arboreal living; southern Mexico to central – northern Argentina..... ***N. crenata*** **group**

Mesonotum and propodeum separated by shallow, but distinct notopropodeal groove (Fig. 5d); anterior mid clypeal region without subtriangular cuticular extension, it may be convex, flat or concave but never as described above (Fig. 8a, b); ground and arboreal species..... **6**

6(5). Mandible narrow at base, very long, usually three fourths or slightly more of head length, armed with 18–19 teeth alternating with 8–10 denticles (Fig. 8a); arboreal living mostly; South America: northwestern Venezuela to northwestern Argentina..... ***N. rostrata*** **group**

Mandible relatively wide at base, always shorter than three fourths of head length, armed with 10–13 teeth alternating with denticles (Fig. 8b)..... **7**

7(6). Body with white, pruinose pilosity, combined with scattered erect hairs (except *N. cooki* Mackay & Mackay, which bears abundant, black erect hairs); integument always black and in most species opaque (Fig. 9a); ground living; northern Mexico to northern Argentina..... ***N. apicalis*** **group**

Body without pruinose pilosity, but bearing abundant appressed hairs, and usually abundant erect hairs (Fig. 9b); integument varying in color from black, to brownish black, to iridescent bluish-greenish..... **8**

8(7). Malar carina absent (Fig. 10a); ground living; some species with iridescent, bluish-greenish integument; Central America to Northwest Argentina..... ***N. aenescens*** **group**

Malar carina present (Fig. 10b); body integument black to brownish black, but never iridescent bluish-greenish; arboreal living mostly; southern United States to northern Argentina..... ***N. foetida*** **group**

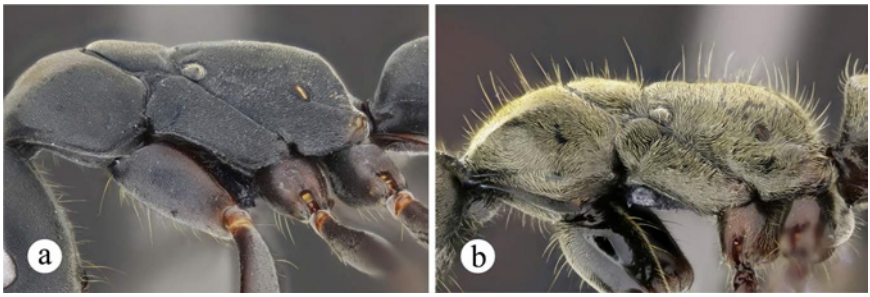

Fig. 9. Pilosity. **a.** Body surface pruinose with scattered erect hairs mostly ventrally (*Neoponera verenae*, DZUP: DZUP549670); **b.** Body surface with abundant appressed and erect hairs (*N. villosa*, DZUP: DZUP549448).

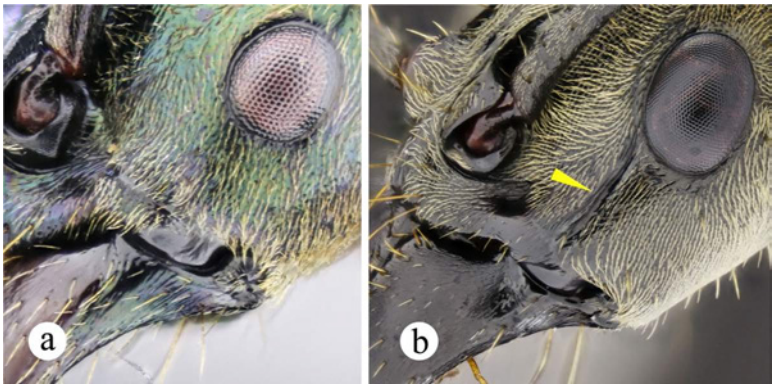

Fig. 10. Malar carina. **a.** Absent (*Neoponera carbonaria* Smith, MEPN: CASENT0649889); **b.** Well-developed (pointed by yellow arrowhead), usually reaching anterointernal eye margin (*N. villosa*, DZUP: DZUP549448).

Taxonomy

Neoponera laevigata *species–group brief taxonomic notes*

Probably based mainly on the presence of the malar carina of *Neoponera commutata* Roger, Emery (1911) created the "*Commutata* group" and placed it within *Neoponera*. Later, Wheeler (1936) in a treatment of the ecological relations of ants and termites, with a focus on ponerines, created *Termitopone* to accommodate *N. commutata*, *N. laevigata*, and *N. marginata* Roger. This author based his decision on morphological and ecological observations related to specialized termite predation which is common to all three species. Wheeler's *Termitopone* remained valid for a relatively long time until its synonymy under *Pachycondyla* by Brown (1973). Mackay and Mackay (2010) included these three termitophagous species, again under *Pachycondyla* within the "*P. laevigata* species–complex", providing a new key to its species, distribution, and brief field and literature notes on their biology and ecology. Schmidt and Shattuck (2014) included these taxa in *Neoponera*, and according to their molecular phylogeny the *N. laevigata* group is sister to the *N. aenescens* group.

We found the following combination of morphological and behavioral characters useful for diagnosing this clade of above–ground termite–raiding species. In addition to the strongly ventrally bent mandibles, we consider such behavioral traits as being synapomorphic for the species here treated. The sole exception to confirmed termite–raiding is *N. gojira* **sp. nov.**, for which we found a single worker and information about its natural history is unknown. Most of the following character states will not be repeated in the general synoptic description, nor in the diagnoses and descriptions of individual species, and apply to all castes except where otherwise stated.

Neoponera laevigata *species–group differential diagnosis*

Known species in the *N. laevigata* group are easily recognized from other species in the genus by the following: 1) the integument of workers and queens is entirely black and exceptionally lustrous (reflecting objects very much like a mirror), bearing scant piligerous punctae, usually with whitish to pale yellowish tiny appressed pilosity, and erect golden hairs. Although the integument of the males is also black and lustrous, it shows significantly more piligerous punctae than in the other castes within this species–group. Workers and queens in some species of the *N. aenescens* group (for example, *N. carbonaria* Smith), *N. crenata* group (for example, *N. moesta* Mayr), and *N. emiliae* group (for example, *N. magnifica* Borgmeier) also show lustrous integuments but these are covered with abundant piligerous punctae, especially on the head dorsum and mesosoma, and with the exception of *N. magnifica*, the body surface is on average dark brownish to bluish–greenish, never jet–black as in all species of the *N. laevigata* group. The integument of *N. magnifica* is also jet-black and the gaster is lustrous, without sculpture, but this species is easily distinguished from all species in the *N. laevigata* group since it bears costae on the dorsum of head, pronotum and mesonotum. 2) Except for *N. commutata*, the distal region of the mandibles in workers and queens is strongly bent ventrad in lateral view, clearly more than in any other *Neoponera* species. Although the mandibles of workers and queens in *N. commutata* are similarly bent ventrad as in most *Neoponera*, the lustrous black integument of the body and their large size (maximum relative body length of workers: 19 mm, and queens: 20 mm, the largest species in the genus), are the easiest clues to separate it from all other *Neoponera* species. The male caste of *N. commutata* is the only case within the genus showing well–developed torular lobes (Fig. 14a), and maxillary palps with segments 4 th to 6th fused (Fig. 18b) (see extended details under the comments section for this species).

Following, is a set of traits which together provide a detailed characterization of the species of the *N. laevigata* group.

1. Compound eye relatively large, ca. one fourth of head length; in most species flat with its external margin not surpassing lateral margin of head in frontal view. In *Neoponera commutata* the eye is globose and surpasses the lateral head margin. In males the eye is slightly notched anterodorsally, globose, and occupies ca. two–fourths or more of head length; its external margin clearly surpasses the lateral head margin in frontal view.

2. Torular lobe subtriangular with rounded lateral margins, covering approximately 90% of acetabulum of antennal socket in frontal view. Known males of *N. mashpi* **sp. nov.** and *N. marginata* with strongly reduced torular lobe, while the male of *N. commutata* shows a small, but well–developed lobe covering approximately less than 10% of the antennal socket.
3. Frontal carina surpassing ocular mid–length in frontal view. In *N. commutata* this carina just reaches ocular mid–length.
4. Malar carina, absent in most species, instead a swelling is present and usually bears foveae and striae. Only *N. commutata* exhibits a strongly developed malar carina which reaches the anterior eye margin. Males lack this character.
5. Mandibles strongly bent ventrad in lateral view, with external margin weakly sinuous medially in full–face view. Males bear the typical Ponerini spatulate to semi–triangular, small, toothless mandibles, always bearing the oval–shaped groove dorsally near the mandibular base.
6. Pronotum lacking a distinct humeral carina, though a very tenuous, blunt, almost indistinguishable border may be present in workers and queens of all species, except for *N. commutata* and males of all species where the humerus is completely rounded.
7. Notauli absent on mesoscutum (males only).
8. Notopropodeal suture present, forming groove, not depressed though (*N. laevigata*, *N. mashpi* **sp. nov.**, and *N. gojira* **sp. nov.**), or slightly depressed (*N. commutata* and *N. marginata*) in dorsal view. This groove is usually cross ribbed. In males and queens the metanotum is clearly separated from the mesonotum anteriorly, and from the tergum of A1 posteriorly, by well–defined grooves.
9. Mesosternal and metasternal processes well–developed, fang–shaped, anteroposteriorly flattened.
10. Posteroventral cuticular flap at metapleural gland opening and its relative visibility in posterolateral view: strongly reduced, gland orifice entirely visible (worker of *N. gojira* **sp. nov.**); well–developed, strongly bent anterad, gland orifice barely visible (worker and queen of *N. laevigata* and *N. mashpi* **sp. nov.**); well–developed, bent dorsad nearly vertically straight, gland orifice almost entirely visible (worker and queen of *N. commutata*, *N. marginata*). In males of examined species this structure varies from well–developed, slightly bent dorsad, gland orifice clearly visible (*N. mashpi* **sp. nov.**, *N. marginata*), to absent, instead forming a vertically–oriented, salient carina, gland orifice completely visible (*N. commutata*).
11. Petiolar node cuboid, usually subquadrate in lateral view, or slightly tapering dorsad, the latter state only seen in *N. commutata*. In males of all examined species the petiolar node also tapers dorsad with both anterior and posterior margins relatively straight in lateral view.
12. Prora either well–developed, with a blunt tip projecting ventrad (*N. mashpi* **sp. nov**., *N. commutata*, *N. marginata*), or poorly developed with only a small cuticular lip that is usually hardly discernible laterally (*N. laevigata*, *N. gojira* **sp. nov.**).
13. Cinctus moderate (most species) to absent or barely distinguishable (only in *N. commutata*). All examined males showed a moderate cinctus.

14. Stridulitrum present on presclerite of A4, sometimes poorly developed, faint and narrow.
15. Arolium present, small, roughly half length or less of pretarsal claw. In males the arolium is slightly longer than half–length of pretarsal claw.
16. General body appearance jet–black, surface with sparse erect golden hairs interspersed with few scattered, piligerous punctures from which golden, appressed tiny hairs emerge, most of which do not touch each other. Queens show relatively more erect pilosity than workers, particularly ventrally on head and on abdominal segments 5–7. Males depart from this in showing a body surface with less erect hairs and significantly more piligerous punctures bearing appressed pale–yellowish pubescence.
17. All species show striae on the head, mesosoma and petiolar node, that varies interspecifically in abundance, thickness and complexity. The petiolar node of *N. gojira* **sp. nov.**, and that of most populations of *N. mashpi* **sp. nov.** are almost devoid of striae. Subpetiolar process covered with transverse, strongly impressed, irregular striae. The head, petiole, and subpetiolar process in males are usually significantly less sculptured than in workers and queens.
18. Worker caste either monomorphic (only *N. commutata*), or polymorphic (*N. mashpi* **sp. nov.**, *N. laevigata*, *N. marginata*). Evidence is lacking for *N. gojira* **sp. nov.**, though probably also polymorphic.
19. This is the only clade within *Neoponera* with all constituent species being specialized in termite–raiding. The feeding biology of *N. gojira* **sp. nov.** is unknown, but probably it raids on termites too.

Synonymic list

In square brackets the known distribution by political and administrative regions, and in parentheses the studied castes: ☿ – worker; ♀ – queen; ♂ – male.

Neoponera commutata (Roger, 1860) [Colombia to southeast Brazil: São Paulo, to southern Paraguay] (☿, ♀, ♂)

Neoponera gojira Troya & Lattke, **sp. nov.** [Brazil: Minas Gerais] (☿)

Neoponera laevigata (Smith, 1858) [Northwestern Colombia to Brazil: São Paulo] (☿, ♀)

= *Neoponera gagatina* (Emery, 1890: 75) (synonymy by Emery 1892: 9)

= *Neoponera laevigata whelpleyi* (Wheeler, 1922: 3) (synonymy by Wheeler 1936: 164)

Neoponera marginata (Roger, 1861) [Trinidad & Tobago to eastern Ecuador, to southern Brazil: Rio Grande do Sul] (☿, ♀, ♂)

Neoponera mashpi Troya & Lattke, **sp. nov.** [Costa Rica to Brazil: Bahia] (☿, ♀, ♂)

Worker– and queen–based key to species of the* Neoponera laevigata *species–group

1. Eye globose, surpassing lateral margin of head, and placed approximately at cephalic mid–length in frontal view (Fig. 11b)..... ***Neoponera commutata***

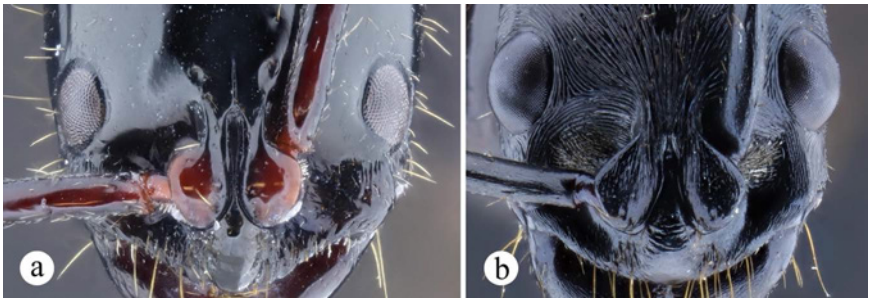

Fig. 11. Eyes. **a.** Flattened, not surpassing lateral margin of head (*Neoponera. marginata* MEPN: CASENT0649897); **b.** Globose, surpassing lateral margin of head (*N. commutata* DZUP: DZUP549422).

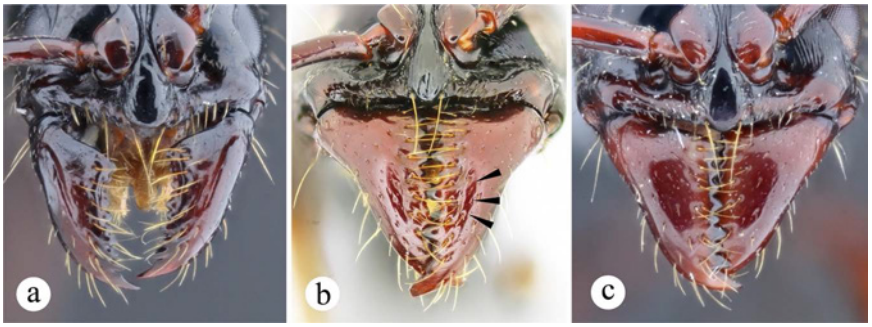

Fig. 12. Mandibular dorsum **a.** Strongly carved longitudinal groove (*Neoponera marginata*, MEPN: ATPFOR1988), **b.** Shallow longitudinal rim (black arrowheads show part of the structure) (*N. gojira* **sp. nov.**, DZUP: DZUP549444); **c.** Even surface, without groove or rim (*N. laevigata*, CPDC: ATPFOR2054-2).

Eye relatively flattened, not surpassing lateral margin of head, and placed anterior to cephalic mid–length in frontal view (Fig.11a)..... **2**

2. Mandibular dorsum, near masticatory margin with a strongly carved longitudinal groove in frontal view (Fig. 12a); posterior flap at metapleural gland orifice well–developed, the gland orifice is almost completely visible in posterolateral view (Fig. 2c)..... ***Neoponera marginata***

Mandibular dorsum, near masticatory margin with shallow, somewhat irregular, longitudinal rim in frontal view (Fig. 12b); posterior flap at metapleural gland orifice strongly reduced to a narrow carina, the gland orifice is completely visible in posterolateral view (Figure 2d)..... ***Neoponera gojira* sp. nov.**

Mandibular dorsum, near masticatory margin without the structures mentioned above, though hair–bearing small fossulae and punctae are present (Fig. 12c); posterior flap at metapleural gland orifice well–developed though strongly curved anterad so that it conceals most of the gland orifice in posterolateral view (Fig. 2a)..... **3**

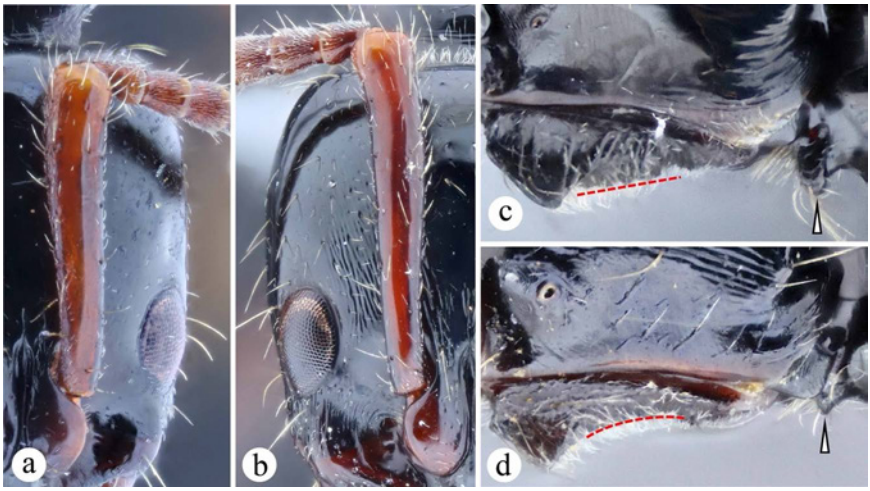

Fig. 13. Scape length, subpetiolar process and prora. **a.** Scape not surpassing posterior margin of head (*Neoponera mashpi* **sp. nov**., CPDC: ATPFOR2054-2); **b.** Scape surpassing posterior margin of head (*N. laevigata*, MPEG: ATPFOR2027); **c.** Subpetiolar process subtriangular, robust with a straight slope (dashed line); prora well–developed (white arrowhead), keel–shaped (*N. mashpi* **sp. nov.**, CPDC: ATPFOR2054-2); **d.** Subpetiolar process subtriangular, less robust than in Figure 13c, with relatively concave to flattened slope (dashed line); prora very small (white arrowhead), lip–shaped (*N. laevigata*, MPEG: ATPFOR2027).

3. Scape fails to reach posterior head margin (smallest workers and queen, Fig. 13a), or barely reaches it (largest workers) in frontal view; prora well–developed, keel–shaped, clearly discernible in lateral view (Fig. 13c); subpetiolar process *usually* with a straight, robust, ca. 45° posterior slope in lateral view (Fig. 13c)..... ***Neoponera mashpi* sp. nov.**
Scape surpassing posterior margin of head by approximately one apical scape width (sometimes slightly less) in frontal view (Fig. 13b); prora very small, lip–shaped, not easily discernible in lateral view (Fig. 13d); subpetiolar process *usually* with a relatively concave to flattened, less robust, posterior slope in lateral view (Fig. 13d) ..... ***Neoponera laevigata***

Male–based key to known species of the Neoponera laevigata *species–group*

1. Torular lobe comparatively small but well–developed, covering ca. less than 10% of antennal socket acetabulum in frontal view (Fig. 14a); posterior face of propodeum weakly concave in lateral view, bearing strong rugae and striae, outline carinate and usually salient (Fig. 18a, c)..... ***Neoponera commutata***
Torular lobe strongly reduced, almost vestigial, cuticle not extending over antennal socket acetabulum (frontal view) (Fig. 14b); posterior face of propodeum straight in lateral view (Figs 24a, c, 27a, b), sculpture present or absent but never strongly impressed, outline not carinate..... **2**

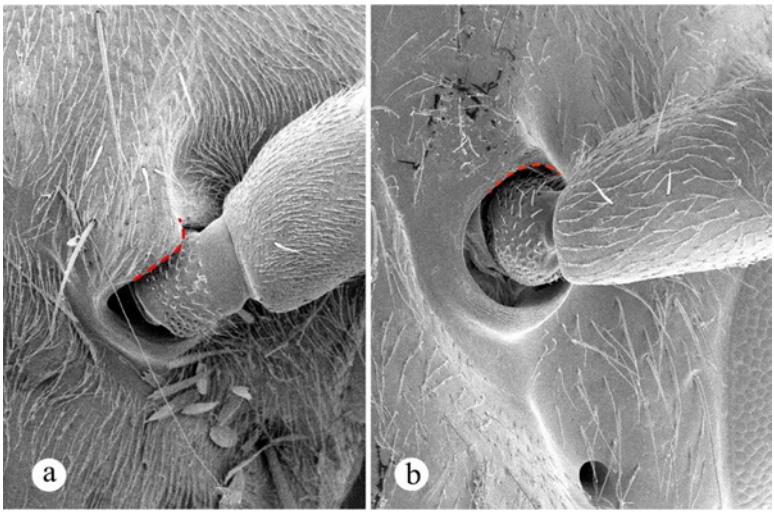

Fig. 14. Torular lobes (demarcated by red dashed lines). **a.** Well–developed though comparatively small, covering ca. less than 10% of antennal socket acetabulum (*Neoponera commutata*, DZUP: DZUP549398); **b.** Strongly reduced, not extending over antennal socket acetabulum (*N. marginata*, CPDC: ATPFOR2011).

2. Pretarsal claw armed with well–developed median tooth; mesoscutum with weakly impressed, median longitudinal line in dorsal view (Fig. 15a); spine at sternum of A8 dorsoventrally depressed with round tip..... ***Neoponera marginata***
Pretarsal claw unarmed, without any accessory tooth; mesoscutum smooth, without median longitudinal line in dorsal view (Fig. 15b); spine at sternum of A8 subconical, not dorsoventrally depressed, with acute tip..... ***Neoponera mashpi*** **sp. nov.**

Neoponera laevigata *species–group description*

The following describes the morphological traits shared by all examined species in each caste: worker, queen and male. Species–specific traits are shown under each species description in the "Species accounts" section. The male of *N. laevigata*, and the queen and male of *N. gojira* **sp. nov.** are unknown.

Worker

Head. *Frontal view*: Mandible triangular, longer than wide, strongly bent ventrad, dorsolateral margin weakly sinuous medially. PF: 4,4. Stipes mostly smooth with strong longitudinal internal groove. Clypeus anteromedially convex, slightly projecting over base of mandibles when closed. Posterior margin of frontoclypeal sulcus just reaching ocular mid–length (except *N. commutata* where the sulcus barely reaches anterior horizontal ocular length). Frontal carina surpassing ocular mid–length. Eye suboval, maximum length ca. one–fourth of head length, in workers placed anterior to cephalic mid–length while in males is slightly anterior to it (except *N. commutata* where the eye

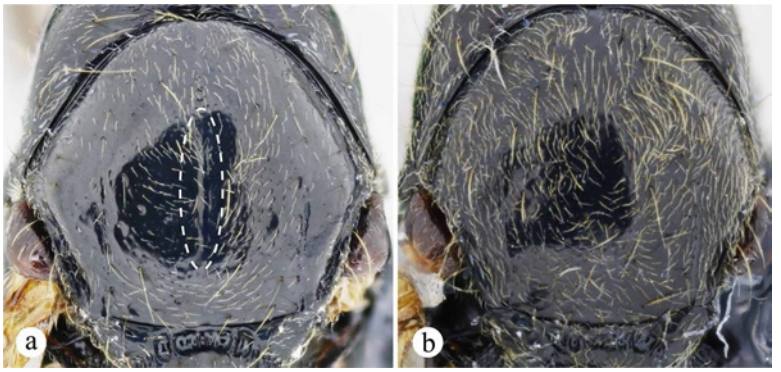

Fig. 15. Male mesoscutum in dorsal view. **a.** Weakly impressed longitudinal line (marked by dashed white ellipse), or shallow groove (*Neoponera marginata*, UFVLABECOL: UFV–LABECOL010414) present in the center of the sclerite; **b.** Mid surface of mesoscutum devoid of grooves and/or striae (*N. mashpi* **sp. nov.,** CPDC: ATPFOR2054–2).

is placed at cephalic mid–length). **Mesosoma**. *Lateral view*: Dorsal margin straight. Propodeal spiracle slit–shaped. *Ventral view*: probasisternum shield–shaped, strongly grooved. Meso– and metasternal processes well–developed, fang–shaped, relatively flattened anteroposteriorly, with internal margins running parallel; space between apices approximately equal to– or shorter than width of each apex. Metasternal process inclined posterad 20°–30° in lateral view (except for *N. commutata* where the process is inclined ca. 45°). Apices of metasternal processes slightly higher than half height of metacoxal internal margin. *Lateral view*: Pheromone venting canal at metapleural gland opening usually well–developed with few interspecific variations. **Petiole**. *Lateral view*: Subpetiolar process covered with transverse, usually well–impressed, irregular striae. *Dorsal view*: anteroventral nodal carina incomplete, with feeble concavity medially. **Gaster**. *Lateral view*: Anterior margin of tergum of A3 straight. Dorsalmost limit of anterior tergal margin of A3 nearly as high as maximum height of petiolar node margin. **Legs**. Tibial spur formula 2(1s, 1p), 2(1s, 1p). Internal mid tibial spur half-length of external spur. Internal hind tibial spur close to one–third length of external spur. Arolium present, roughly 0.5 times length of pretarsal claw. Pretarsal claw arched, unarmed (without accessory teeth on its surface). Metabasitarsal gland present on basalanterior face. **Pilosity**. Body with sparse, flexuous, golden, erect and suberect hairs; appressed pubescence almost absent on entire body (only smallest workers of *N. laevigata*, and *N. mashpi* **sp. nov.**) to slightly more abundant (remaining workers of all species); subpetiolar process always with a combination of fine, relatively abundant whitish (all species except *N. commutata*) to light golden (only *N. commutata*) appressed and suberect hairs. Scape hairs mostly erect and suberect with sparse appressed pubescence. Posterior ventrolateral margin of hypopygium (just next to the base of stinger) bearing flexuous hairs. **Sculpture**. Integument polished, mostly smooth.

Queen

Head. Morphology as in worker except for: *Frontal view*: Ocelli approximately equidistant to each other. Ocellar area not protruding from cuticle. **Mesosoma**. Morphology as in worker except for: Dorsal margin convex in lateral view. *Dorsal view*: Parapsidal lines weakly impressed, slightly divergent; scutoscutellar sulcus present, slightly arched posterad, not separating mesoscutum from mesoscutellum. Anterior subalar area shorter than tegular maximum width in lateral view. Metanotum well–developed, clearly discernible dorsally, surface even, slightly flat. *Lateral view*: Metanotal trough deeply impressed; anapleural sulcus present, almost completely dividing anepisternum from katepisternum; metapleural sulcus present. Metapleuropropodeal groove vestigial in dorsal view. **Wings**. Hyaline, weakly infuscated, moderately setose. Forewing venation: Ogata type Ia: submarginal cells 1 and 2, and discoidal cell present, vein 2M present, 2r–rs offset from 2rs–m. Hindwing venation: Cantone Type I: basal and subbasal cells, and vein 2M present, 1R well–developed. Jugal lobe present. **Petiole**. Morphology as in worker except for: *Dorsal view*: Node of petiole proportionally shorter and wider than in worker. **Gaster and legs.** Morphology as in worker. **Pilosity and sculpture.** As in worker.

Male

Head. *Frontal and/or lateral view*: Subrhomboid. Mandible spatulate, longer than wide, blunt apically, close to 1.5 oval pits (maximum length) fit on mandibular dorsum. Stipes mostly smooth with feeble longitudinal internal groove. Malar carina absent. Eye convex, globose. Ocellar area not protruding from cuticle. Anterior ocellus maximum length subequal to posterior ocelli. Ocelli approximately equidistant. Occipital carina reduced. Length of first flagellomere subequal to second flagellomere. **Mesosoma**. Morphology as in queen except for: *Lateral and/or dorsal view*: Pronotum lacking humeral carina, completely rounded. Mesoscutum about as long as broad. Notauli absent. Transscutal line well–developed. Scutoscutellar sulcus present, strongly impressed, cross ribbed. Mesoscutellum subtrapezoidal, convex. Anapleural sulcus present in just a short pleural portion, not reaching midpleural region. Metapleural sulcus present. Anterolateral propodeal corner rounded. Propodeal lateral margins subparallel in posterodorsal view. The morphology of probasisternum and metasternal process is almost identical to that of the worker and queen. Posteroventral cuticular flap at propodeal posterolateral corner present, though reduced and not bent dorsad. **Wings**. Morphology as in queen. **Petiole**. *Lateral view*: subtriangular, shorter than that of worker and queen, and with rounded nodal dorsum (except for *N. commutata* worker and queen which show relatively round node, dorsally). Lateral and/or posterolateral carinae absent on node. **Gaster**. Morphology as in worker and queen except for: *Lateral and/or ventral view*: Prora well–developed, with blunt tip projecting ventrad. Spine at posterior margin of tergum of A8 well–developed, usually surpassing length of sternum of A9. Posterior margin of sternum of A9 convex. Pygostyles present. **Legs**. Morphology as in worker and queen except for the presence of medial tooth (only *N. commutata* and *N. marginata*) on pretarsal claw, which is absent in *N. mashpi* **sp. nov. Genitalia**. Dorsointernal margins of basimeres slightly touching each other.

Basivolsella setose. Internal and external margins of cuspis nearly straight, its apex very close to posterior margin of digitus. Penial scleritess dorsomedially fused up to approximately one–half or less their length. **Pilosity and sculpture**. As in worker and queen except for: Appressed pubescence abundant mostly on body dorsum. Erect hairs smaller than maximum eye length. Scape hairs mostly with abundant appressed pubescence, mostly shorter than apical scape width. Meso– and metatarsi bearing abundant stiff setae interspersed with abundant suberect and appressed hairs.

Species accounts

***Neoponera commutata* (Roger, 1860)**

Figs 16: e (☿); 17: a–d (♀); 18: a–d (♂); 28: a–c, j (♂ genitalia); 29: b (distribution)

Ponera commutata Roger, 1860: 311 (☿). South America. Unconfirmed type locality [but *sensu* Smith, 1858, possibly Brazil (Pará), and Guyana)]. Type material (syntypes): 1 ☿, 1 ♀ (MNHN) [not examined]. Combinations. In *Pachycondyla*: Emery, 1890: 72; Brown in Bolton, 1995: 304. In *Termitopone* (*Syntermitopone*): Wheeler, 1936: 169. In *Neoponera*: Emery, 1901a: 47; Schmidt & Shattuck, 2014: 151.

Status as species. Mayr, 1863: 447; Wheeler, 1936: 169 (redescription); Mackay & Mackay, 2010: 257 (redescription).

Worker and queen diagnosis. Head with strong, concentric striae ventrally; eye globose, surpassing lateral margin of head in frontal view (Fig. 11b); scape subtriangular in transverse plane (Fig. 17c); malar carina distinctive (Figs 11b, 16c); occipital (nuchal) carina present, though feebly developed (Figs 16c, 17c); posterolateral margin of propodeal declivity with blunt, salient, slightly crenulated carina (Figs 16a, b, 17d); petiolar node slightly tapering at top, posterolaterally bearing convex carina, in lateral view (Figs 16e, 17d); largest workers (WL $\bar{X}$ = 5.64 mm) and queens (WL $\bar{X}$ = 6.31 mm) of the *N. laevigata* group.

Worker description. Measurements (*n* = 8): HW: 2.97–3.18; HL: 3.56–3.73; EL: 0.93–1.02; SL: 3.39–3.73; WL: 5.59–5.68; PrW: 2.29–2.46; MsW: 1.53–1.74; MsL: 1.14–1.27; PW: 1.27–1.36; PH: 1.78–1.95; PL: 1.36–1.48; GL: 5.25–8.48; A3L: 2.2–2.46; A4L: 2.2–2.29; A3W: 2.58–2.88; A4W: 2.71–2.88; TLa: 15–15.51; TLr: 15.85–19.24. **Indices**. CI: 81.82–86.9; OI: 29.49–30.26; SI: 85.9–86.84; MsI: 79.55–84.15; LPI: 64.15–76; DPI: 131.58–155.88.

Head. *Frontal view*: Subquadrate. Masticatory margin of mandible with six to seven large teeth interspersed with five to nine denticles, basal margin edentate. Labrum dorsum mostly smooth, rugose basally. Posterolateral margin of torular lobe straight. Malar carina usually reaching anterior eye margin. Eye convex, relatively globose, placed at cephalic mid–length. Posterior margin of head straight to slightly concave. Scape when pulled back, surpasses posterior margin of head by close to three times apical scape width. *Ventral view*: Prementum with strong transverse carina. **Mesosoma**. *Lateral view*: Pronotum lacking humeral carina, completely rounded. Metanotal groove present, slightly depressed, mesonotum and propodeum clearly separated. Anapleural sulcus present, though usually merged with surrounding striae. Posterior

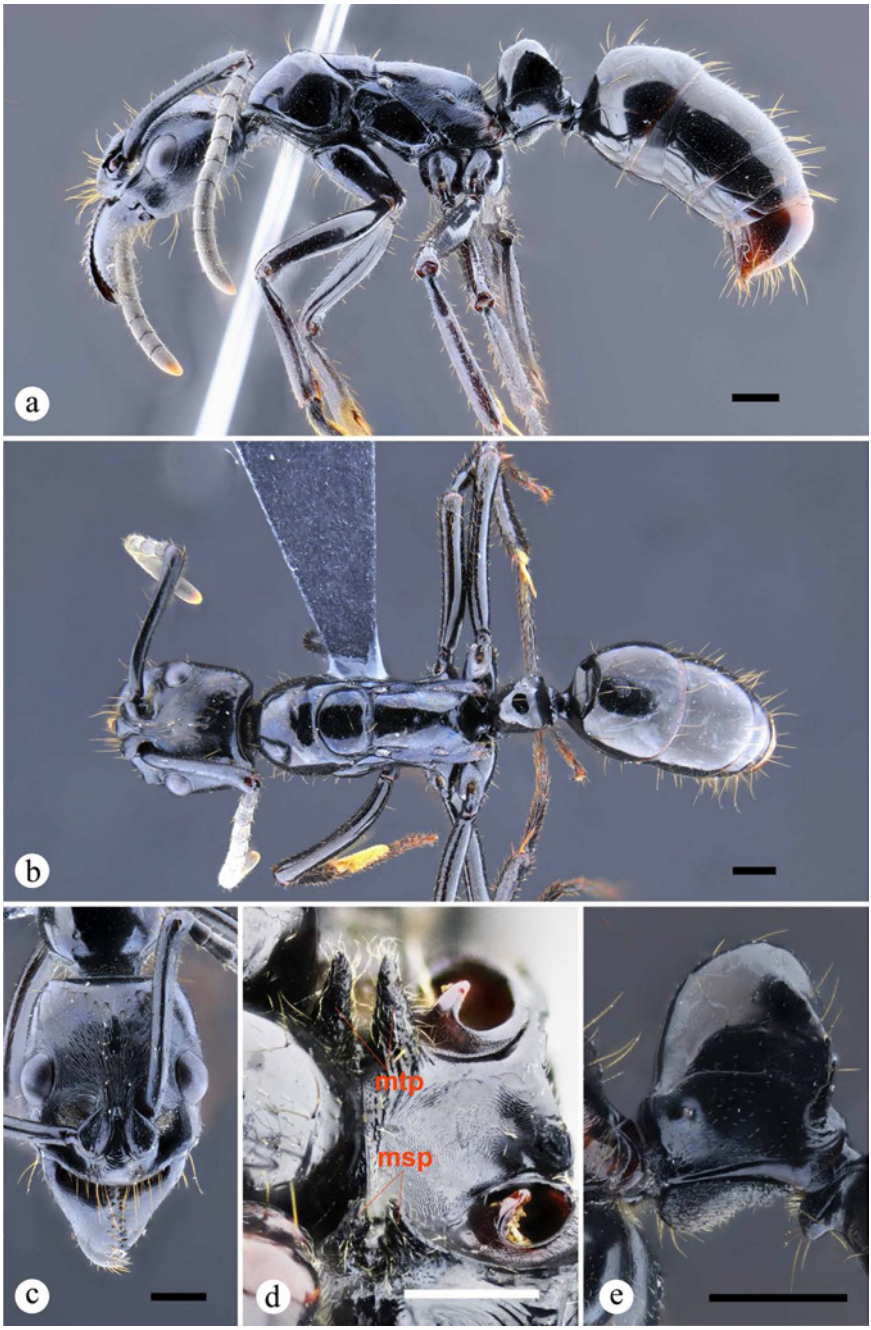

Fig. 16. *Neoponera commutata*. ♀ (DZUP: DZUP549422), Brazil, Acre. **a.** Lateral view; **b.** Dorsal view; **c.** Head in frontal view; **d.** Mesosternal (msp) and metasternal (mtp) processes in anteroventral view; **e.** Petiole in lateral view. Scale bars: 1 mm (**a**–**c**, **e**); 0.5 mm (**d**).

DOI 10.1163/1876312X-bja10034

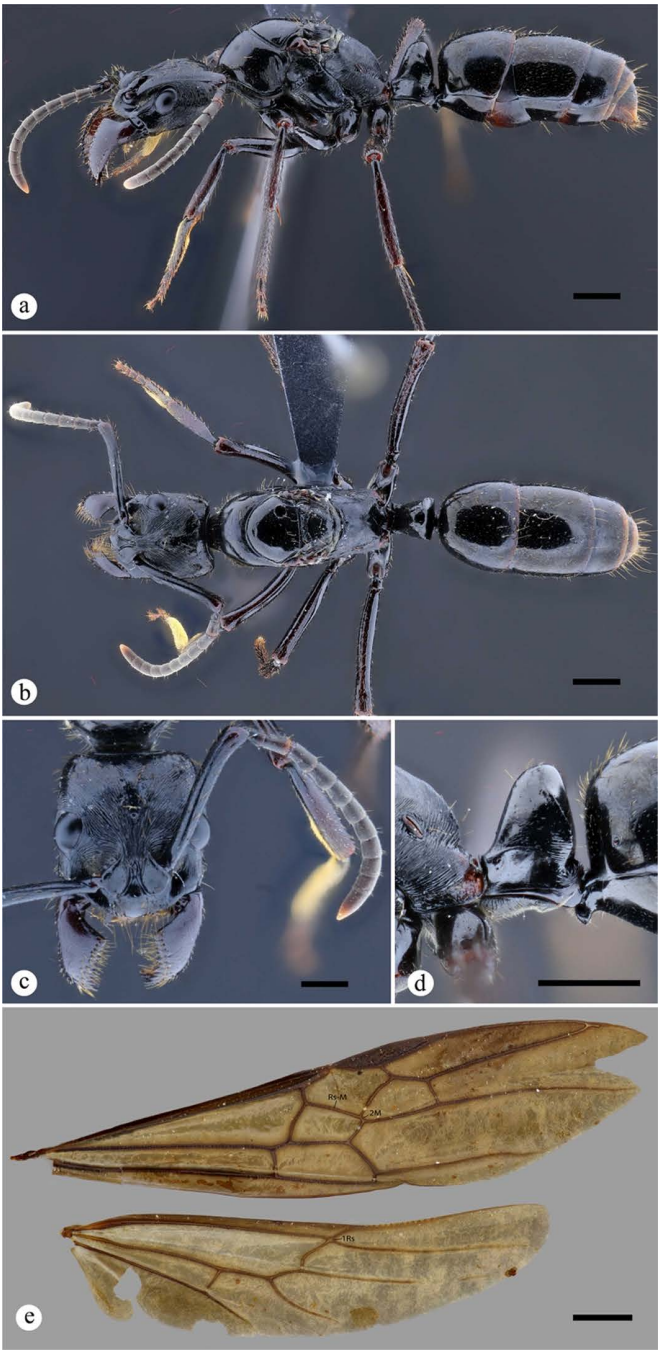

Fig. 17. *Neoponera commutata*. ♀ (INPA), Brazil, Amazonas. **a.** Lateral view; **b.** Dorsal view; **c.** Head in frontal view; **d.** Petiole in lateral view; **e.** Fore and hind wings. Scale bars: 1 mm.

face of propodeal declivity mostly flat. Propodeal lateral margins convergent dorsally in posterodorsal view. Pheromone venting canal at metapleural gland opening, well–developed, mostly smooth. Ventrolateral propodeal declivity without deep transverse groove. *Ventral view*: Probasisternal posterior projection with spine. Metasternal process inclined posterad, ca. 45° in lateral view. **Petiole**. *Lateral view*: anterior and posterior margins of node nearly straight at base and slightly tapering dorsad; dorsal margin convex, highest point posterior to nodal longitudinal midline. Lateral projection of anteroventral nodal carina well–developed, with stout acute tip moderately bent dorsad. *Dorsal view*: Anterior margin of petiolar node slightly shorter than width of posterior margin. Anteroventral nodal carina incomplete, feebly concave medially. *Lateral view*: Subpetiolar process subtriangular, with rounded anterior cusp, followed by posterior slightly concave slope (ca. 30°). **Gaster**. *Lateral view*: Prora well–developed, with blunt tip projecting ventrad. Meeting of anterior margin of abdominal tergum 3 with its dorsal margin rounded. Cinctus weak. *Dorsal view*: Tergum of A3 slightly longer than A4. Posterior dorsum of epipygium completely smooth. **Legs**. Mesofemur roughly equally thick as metafemur, in dorsal or ventral view. Ventral surface of meso- and metafemora almost entirely flattened from base to apex, without longitudinal groove. **Color**. Appendages including antennae and mandibles black to ferruginous black, mandibles feebly lighter than remaining integument of body. **Pilosity**. Erect hairs on body dorsum mostly shorter than maximum eye length. Scape hairs mostly shorter than apical scape width. Meso- and metatarsi bearing abundant spines interspersed with few suberect hairs. Posterior dorsum of epipygium surrounded by sparse, ca. 10, long flexuous hairs. **Sculpture**. Striae on head strongly impressed both dorsally and ventrally, covering most surface, longitudinal and slightly divergent on dorsum, roughly concentric ventrally; strong striae posterolaterally on pronotal margin, usually anepisternum and part of katepisternum, axillula, metapectus, and lateral side of propodeum; striae on petiolar node mostly absent.

Queen description. Measurements (n = 2). HW: 3.39; HL: 3.94–3.9; EL: 1.1–1.02; SL: 3.81–3.73; WL: 6.78–5.85; PrW: 2.92–2.67; MsW: 2.71–2.2; MsL: 3.39–2.8; PW: 1.61–1.44; PH: 2.29–1.95; PL: 1.53–1.53; GL: 7.8–5.85; A3L: 2.8–2.5; A4L: 2.88–2.46; A3W: 3.56–3.09; A4W: 3.52–3.05; TLa: 17.92–16.23; TLr: 20.04–17.12. **Indices**. CI: 86.02–86.96; OI: 30–32.5; SI: 110–112.5; MsI: 78.79–80; LPI: 66.67–78.26; DPI: 94.44–105.56.

Morphology mostly as in worker except for: **Head**. *Frontal view*: anterior ocellus maximum diameter subequal to that of posterior ocelli, though sometimes larger. Distance from posterior ocellar margin to posterior margin of head close to twice apical scape width. Distance between anterior and posterior ocellus approximately 1.8 times anterior ocellus maximum length. **Mesosoma**. *Dorsal view*: Mesoscutum broader than long, close to twice as long as mesoscutellum. Transscutal line well–developed. Scutoscutellar sulcus strongly impressed, cross–ribbed. Mesoscutellum subtrapezoidal, slightly flat dorsally. Anterodorsal median propodeal sulcus vestigial. *Lateral view*: Posterior face of propodeal declivity slightly concave. Posterolateral margin of propodeal declivity very similar as in worker though usually less salient and sometimes with crenulae. *Ventral view*: Mesosternal process with internal margins slightly divergent.

Wings. Forewing venation: Rs–M one–third longer than 2M. Forewing evenly covered by fine setose layer, except for subbasal and basal cells which are almost completely devoid of pilosity. Hindwing venation: 1Rs absent or highly reduced. Hindwing bearing 10–14 hamuli. **Petiole.** *Lateral view*: anterior nodal margin shows a more pronounced slope than posterior margin. **Color, pilosity and sculpture**. Mostly as in worker (but see general synoptic description).

Male diagnosis. Maxillary palpomeres 4 to 6 fused (Fig. 18b); posterior supraclypeal area round, followed by carinate swelling (Fig. 18e); torular lobe present, well–developed, small though compared to that of the worker and queen, covering ca. less than 10% of antennal socket acetabulum (Figs 14a, 18d); posterior face of propodeal declivity concave, its margin bearing relatively sharp carina (Fig. 18a); posteroventral cuticular flap at metapleural gland opening absent, replaced by strong vertical carina; pheromone venting canal absent at metapleural gland opening; forewing subbasal and basal cells almost completely devoid of pilosity (Fig. 18f).

Male description. Measurements (n = 3). HW: 1.94–2.04; HL: 2.04–2.19; EL: 1.02–1.08; SL: 0.44–0.48; WL: 4.95–5.14; PrW: 2.03–2.16; MsW: 2.29–2.3; MsL: 2.96–3.05; PW: 1.08–1.11; PH: 1.4–1.46; PL: 1.07–1.14; GL: 5.52–6.98; A3L: 1.84–2.14; A4L: 1.9–1.94; A3W: 2.04–2.16; A4W: 2.19–2.29; TLa: 12–12.35; TLr: 13.78–15.46. **Indices**. CI: 88.41–100; OI: 50–55.74; SI: 22.58–23.75; MsI: 75–77.59; LPI: 75–81.82; DPI: 94.44–102.38.

Head. *Frontal view*: Mandibular apex, when closed, slightly surpasses lateral margin of labrum. PF: pseudo 4, 4. Labral dorsum mostly rugose. Clypeus anteromedially straight to slightly concave. Area between posterior margin of clypeus and supraclypeal area without depression. Posterior supraclypeal area rounded, slightly protruding from cuticle, followed posteriorly by carinate swelling. Distance between internal margins of antennal sockets 1.5 times socket diameter. Ocellar area positioned slightly posterad to vertex. Distance from posterior ocellar margin to posterior margin of head equal to twice apical scape width. Distance between anterior and posterior ocelli close to one anterior ocellus maximum length. Scape cylindrical, twice as long as pedicel. *Ventral view*: Prementum with strong transverse carina. *Lateral view*: Dorsal surface of clypeus relatively straight to slightly convex, not inflated as in remaining known males of the *N. laevigata* group, always covering anterior clypeal margin. Eye suboval, located at cephalic mid–length, slightly notched in the dorsal third, maximum length slightly shorter than half head length. **Mesosoma**. *Dorsal view*: Mesoscutum close to twice as long as mesoscutellum, anterior triangular impression weakly impressed, lacking median longitudinal line. Parapsidal lines strongly impressed, slightly divergent. Scutoscutellar sulcus straight. Anterior subalar area approximately as broad as tegular maximum width. Metanotum surface even, slightly flat. Metapleuropropodeal groove deeply depressed. Anterodorsal median propodeal sulcus present, strongly impressed. *Lateral view*: Posterior face of propodeal declivity concave. Posterolateral margin of propodeal declivity with strong, sharp carina, running along the posterodorsal propodeal margin. Pheromone venting canal at metapleural gland opening absent, replaced by circular groove surrounded by strong, salient carinae. *Ventral view*: Probasisternal

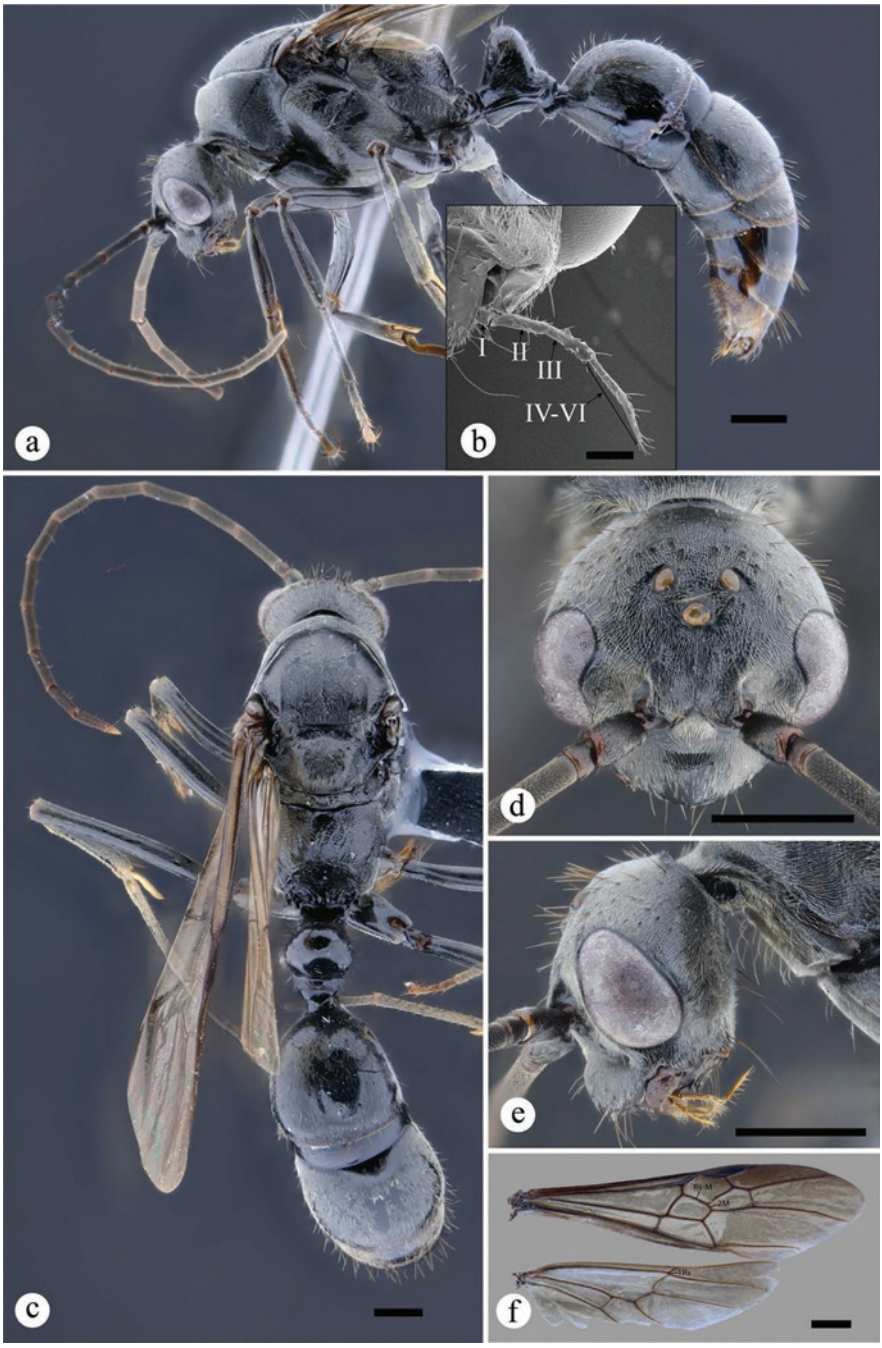

Fig. 18. *Neoponera commutata*. ♂ (MEPN: ATPFOR2051), Colombia, Chocó. **a.** Lateral view; **b.** Left maxillary palp showing fused IV-VI palpomeres; **c.** Dorsal view; **d.** Head in dorsal view; **e.** Head in lateral view; **f.** Fore and hind wings. Scale bars: 1 mm (**a**, –**f**); 0.2 mm (**b**).

posterior projection with minute spine. Mesosternal process well-developed, fang-shaped, with internal margins running parallel, relatively flattened anteroposteriorly, inclined posterad ca. 45° in lateral view, space between apices approximately equal to width of each apex. Metasternal process inclined posterad, ca. 45° in lateral view, space between apices wider than width of each apex. **Wings**. Forewing venation: Rs–M one-third longer than 2M. Forewing evenly covered by fine setose layer, except for subbasal and basal cells which are almost completely devoid of pilosity. Hindwing venation: as in queen. Hindwing bearing 10–14 hamuli. **Petiole**. *Lateral view*: Anterior and posterior margins of node nearly straight at base and tapering at top. Lateral projection of anteroventral nodal carina well–developed, with acute tip strongly bent dorsad. *Dorsal view*: Anterior margin of petiolar node slightly shorter than width of posterior margin. *Lateral view*: Subpetiolar process subtriangular, with rounded anterior cusp, followed by posterior, slightly concave slope (ca. 20° or less), usually with two slightly divergent longitudinal carinae bearing groove in between. **Gaster**. *Lateral view*: Meeting of anterior margin of abdominal tergum 3 with its dorsal margin rounded. Cinctus weak. Spine at posterior margin of tergum of A8 strongly acute, slightly flattened laterally, with sharp dorsal carina posteriorly. Abdominal sternum 9 longer than broad. Pygostyles close to four times longer than broad. *Dorsal view*: Tergum of A3 slightly shorter than A4. *Ventral view*: Abdominal sternum 7 showing uneven surface, with strong ditch initiating on second third, most surface bearing abundant erect and suberect hairs, ventrolaterally with long barbiculate hairs. **Legs**. Mesofemur roughly equally thick as metafemur, in dorsal view. Ventral surface of meso– and metafemora almost entirely flattened from base to apex, without longitudinal groove. Arolium roughly 0.7 times (two–thirds) length of pretarsal claw. Pretarsal claw with tiny, barely distinguishable median tooth. **Color**. Appendages, including antennae and mandibles, black to slightly yellowish black. **Genitalia**. *Dorsal view*: Cupula: posterior margin of medial invagination relatively broad. Lobular process well–developed. Gonopod dorsally elongated, with approximately subequal margins from base to apex, elongated in lateral view, with dorsal and ventral margins subparallel along its length, dorsolateral margin rounded medially, smooth surface. Gonostylus subrounded apically, dorsointernal margin mostly evenly continuous. Basivolsella externally convex. Digitus subrectangular, with outer margin nearly straight in ventral view. Penial sclerites, overall outline, subrectangular, dorsal surface mostly flat, though slightly convex posteriorly. Dorsoapical third of penial sclerite surface continuous, not modified. **Sculpture**. Head feebly rugulose mostly on dorsum; posterolateral pronotal margin slightly striated; axillula, metapleuron, and most of propodeum rugose; striae on petiolar node almost absent.

Natural history notes. This is a relatively common ground surface dweller, found mostly in a variety of habitats from the Amazon–Orinoco watershed, where the majority of the records are known, and have been examined in this study. Individuals of all castes have been collected throughout the year, however, research is still pending in regards to colony life cycle and production of alate forms (but see Schmidt & Overal 2009). Nothing is known in regards to its flight phenology. Several techniques have been used to collect this species including (from the most to the least effective) ground

surface pitfall traps, hand collections, Malaise (mostly males), litter sifting and Winkler, and very unusually with canopy fogging. *Neoponera commutata* nests underground (Wheeler 1936; Mill 1984; Schmidt & Overal 2009; A. Troya pers. obs.) with colonies varying in population size from approximately 400–1000 individuals (Mill 1984; Schmidt & Overal 2009). Adrian Troya observed various individuals of *N. commutata* coming in and out from an (apparently) empty, ca. 1m diameter, dome–shaped, termite nest. The structure was attached to a live tree trunk in a lowland Amazonian forest in Ecuador, and seemed to host an ant colony. After ca. 15 minutes of observation no prey of any kind was seen in the mandibles of the workers. Although no guarding behavior was recognized at what would be their nest entrance located laterally on the dome, the hypothesis of reutilization of termite nests by *N. commutata* needs further confirmation.

Mill (1982a, 1984), as part of his research on termites, registered the group recruitment, predatory behavior of *N. commutata* on several termite groups, including the genus *Syntermes* Holmgren, some of the species of which are considered exclusive prey of these ants, for example *S. calvus* Emerson, *S. molestus* (Burmeister), *S. spinosus* (Latreille) [= *S. solidus* Emerson] (Wheeler 1936; Hermann 1968?; Mill 1984), all of them broadly distributed in Amazonia, except for *S. calvus* which has only been found in Brazil, French Guiana, and Guyana (Constantino 2020). Most of this data was recorded in a few sites, such as Kartabo and Kaieteur in Guyana, and Vista Alegre, state of Amazonas and Ilha de Maracá state of Roraima, in Brazil. John Lattke observed nocturnal hunting of *Syntermes* in forests of Cerro Los Pijiguaos, southern Venezuela. A loose column of 6–8 workers making their way through the litter was seen, and a little over an hour later, presumably the same column was seen returning, each worker carrying 2–3 termites in their mandibles. Based on this pattern of specific predatory behavior Wheeler (1936) proposed that the distribution of *N. commutata* should follow that of their prey. Thus far, this hypothesis has not been challenged, nor tested. *N. commutata* is an efficient predator, according to Mill (1984) estimations, only three colonies can consume as much as three times the worker and soldier populations of the above–mentioned termite species per hectare, annually. Mill (1982b) also informed on the nest migration strategy of *N. commutata* in an Amazonian rain forest.

The venom of *N. commutata* contains antimicrobial, insecticidal and haemolytic peptides, according to Aili et al. (2016). These proteins are known as ponericins and it is assumed these help prevent diseases originated from the prey organisms brought by the ants inside their colonies (Orivel et al. 2001). Aili et al. (2016) also found in the venom of *N. commutata* the highest number of proteins as compared to the venoms of the ants *Ectatomma brunneum* Smith, *Myrmecia gulosa* (Fabricius), *Neoponera apicalis*, and *Odontomachus hastatus* (Fabricius). Schmidt and Overal (2009) found that raiders and nest defenders are equipped with more amounts of venom and that also this is more lethal than in other worker nest mates who do not get involved in foraging activities and colony defense.

Comments. Current morphological evidence allows an unequivocal evolutionary relatedness of *N. commutata* to the remaining species in the *N. laevigata* group. However, despite showing some apomorphies with other members in this clade, for

example, the mandibles strongly bent ventrad in workers and queens, mesoscutum lacking notauli in males (Fig. 17b), specialized termite–feeding, this lineage is an outlier from a morphological perspective. Traits like the subtriangular antennal scapes (transverse plane), the occipital and malar carinae in workers and queens, the presence of well–developed torular lobes in males, all of which are absent in the remaining species within the clade, provide signs of an evident separation of this lineage with respect to its more derived clade partners which thus far appear to form a closely related group (Troya et al. unpubl. data). This is also clearly depicted by the multivariate analysis in Fig. 3. In addition, we consider a striking feature in this species the (secondary?) fusion of the male maxillary palpomeres 4–6 (Fig. 18b), which is evidenced by the absence of a complete joint between the 4th and 5th, and the 5th and 6th segments. Thus far, this is the only known case in *Neoponera*, and to our knowledge unknown in ponerine males. Why and when this loss of segmentation occurred during the course of evolution in this caste, remain open questions.

Distribution notes. Based on our records and the literature, the populations of *N. commutata* are exclusively South American (Fig. 29b). The elevational range of the species extends from nearly the sea level up to approximately 1300 m. The northern geographic range reaches the Serranía de la Macarena, a Colombian mountainous region lying just at the transition zone between the Amazonian lowlands and the premountainous Andean forests, in the center of that country. The southernmost distribution of *N. commutata* appear to be marked by the Humid Chaco and the Atlantic Forest in Paraguay, whereas its eastern limit is the state of Paraíba in northeast Brazil, where we examined a single worker from a heavily anthropized zone with remains of stepic savannas, some of which are part of the threatened Caatinga biome. In northwestern South America the Andean Cordilleras may act as the ultimate barrier for *N. commutata* entering Mesoamerica. Except for an isolated record from the Department of Bolívar in northern Colombia (mined from Antmaps.org, Janicki et al. 2016), no other sightings or collections have been reported from the northern region of that country, nor in Atlantic or Pacific regions in Central America. The Costa Rican record in San José, reported by Mackay and Mackay (2010), is a possible interception of South American origin, as no individuals have been found so far after years of sampling in the region (J. Longino, pers. comm.).

Material examined. 117☿, 9♀, 12♂: **BRAZIL**: **Acre**: 24 km SE Río Branco, Fazenda Experimental Catuaba– UFAC, 10.0667°S, 67.6167°W, 214m, 2016–11–07, Lattke, J., hand collected (DZUP), 35 km NW of Plácido de Castro, 10.3333°S, 67.4833°W, 203m, 2014–08, Rufino, C. P. B.; Souza, C. S. (CPDC), Rio Branco–Res, 9.97454°S, 68.4299°W, 219m, 2007–01–07, Oliveira, M. A. (CPDC), Villa Thaumaturgo, 10.3188°S, 67.1813°W, 130m, 1962–02, Herbst, P. (MPEG); **Amapá**: Parque Nacional Montanhas do Tumucumaque , 1.61667°N, 52.4833°W, 150m, 2017–07–25, Feitosa, R.; et al. (DZUP); **Amazonas**: 1 Km W Taruma falls, 3.00809°S, 60.07°W, 44m, 1981–03–02, Young, C. (MPEG), 30 Km N Manaus, CEPLAC, 2.83065°S, 60.0201°W, 49m, 1976–11–26 (INPA), Conjunto Villar Câmara, 3.03154°S, 59.9267°W, 65m, 1987–09–22, Daniel, P.; Diniz, L (DZUP), Instituto Nacional de Pesquisas da Amazôna (INPA), BR 174, KM 70, 3.09424°S, 59.9893°W, 100m,

1977–12–21, Soares, A. (INPA), Instituto Nacional de Pesquisas da Amazônia (INPA), Est. Aleixo Campus I, 3.09393°S, 59.9888°W, 82m, 1973–06–07, Castriloh, A. (MPEG), Manaus, 3.11863°S, 60.0217°W, 56m,, Roger (DZUP), Reserva Florestal Adolpho Ducke, Instituto Nacional de Pesquisas da Amazônia (INPA), 2.93333°S, 59.9667°W, 106m, 1982–08–27, Rafael, J., Malaise (INPA), São Francisco, 3.12267°S, 58.433°W, 17m, 2009–10–02, Fernandes, I. (INPA), Tapurucuara, 0.4°S, 65.0333°W, 64m, 1962–07–01, Oliveira, F. M. (DZUP), UFAM, 3.1°S, 59.9667°W, 80m, 2008–07–28, Oliveira, C. S. N. (DZUP); **Ceará**: Reserva Particular do Patrimônio Nacional Serra das Almas, 5.14141°S, 40.916°W, 624m, 2011–06–05, Nunes, F. A., pitfall (DZUP); **Goiás**: 20 km S of Padre Benardo, Fazenda Lagoa Santa, 15.3918°S, 48.3156°W, 881m, 1976–12–30, Kunze (DZUP); **Mato Grosso**: 85km W of Alta Floresta, rio dos Apiacás, 9.9°S, 56.9°W, 209m, 2017–11, Lopes, F. J. A.; Araujo, C. B. (DZUP), Chapada dos Guimarães, 15.45°S, 55.7333°W, 726m, 1983–11–18 (DZUP), Fontes e Lacerda, 15.3167°S, 59.2333°W, 295m, 2014–01–03, Queiroz–Santos, L. (DZUP), Nossa Senhora do Libramento, 15.7714°S, 56.3443°W, 224m, 2015–07, Thomas, E. O., pitfall (CPDC), Pantanal de Cáceres, 16.08°S, 57.6778°W, 100m, 1984–11, Elias, C., Malaise (DZUP), Parque Estadual Cristalino (PPBio), 9.53333°S, 55.5333°W, 272m, 2013–05–01, Vicente, R. E., pitfall (DZUP), Vila Bela da Santíssima Trinidade, 15.05°S, 59.7667°W, 216m, 2014–02–06, Maravalhas, J.; Vasconcelos, H. (DZUP); **Mato Grosso do Sul**: Fazenda Retiro Conc., 21.6833°S, 57.7667°W, 93m, 2012–08, De Souza, B., pitfall (DZUP); **Pará**: 54 km W Oeiras do Pará, 2.1°S, 50.35°W, 31m, 2015–06–22, Raveta, A. (MPEG), 65 km W Oeiras do Pará, 2.08333°S, 50.4667°W, 17m, 2015–06–16, Silva, R.; Siqueira, E. (MPEG), Alter do Chão, 2.5°S, 54.95°W, 85m, 2009–01–23, Ulyssea, M. A. (DZUP), Buena Vista, Ilha Arapiranga, 1.33319°S, 48.5669°W, 15m, 1992–11–21, Dias, J., arboreal Malaise (MPEG), Curionopolis, 6.2°S, 49.75°W, 343m, 2017–08–07, Tavares, M., pitfall (MPEG), Fazenda Florentino, 7.11667°S, 55.3833°W, 226m, 2010–12–12, Krinsk, D., pitfall (DZUP), Floresta Nacional Caxiuanã, 1.73333°S, 51.45°W, 21m, 2012–01, Cunha, D. et al., pitfall (MPEG), Floresta Nacional Caxiuanã, Estação Científica Ferreira Pennna – ECFPn, 1.75°S, 51.5167°W, 44m, 2003–10–28, Souza, J.; Moura, C., pitfall (INPA), Floresta Nacional de Carajas, Mina do Arenito, 6.08563°S, 50.2313°W, 653m, 2017–10–14, Albuquerque, E.; Monteiro, M., hand collected (MPEG), Floresta Nacional de Saracá–Taquera, 1.85°S, 56.45°W, 70m, 2016–08–25, Feitosa, R. M.; et al. (DZUP), Ilha Taboca, 2.88548°S, 52.0126°W, 16m, 2000–11–21, Santos, R.; Dias, J., hand collected (MPEG), Jarí–Amazônia, 0.88333°S, 52.6°W, 18m, 2011, Silva, E. A. (DZUP), Mina do Palito, 6.31667°S, 55.7833°W, 224m, 2018–02–02, Silva, R.; Prado, L., hand collected (MPEG), Serra das Andorinhas, 6.23333°S, 48.4667°W, 271m, 2000–07–23, Mascarenhas, B. (MPEG); **Paraíba**: Rio Tinto, 6.8083°S, 35.0775°W, 17m, 1999–03, Henriques, A., hand collected (DZUP); **Piauí**: Estação Ecológica Uruçuí–Una, 8.85996°S, 45.2001°W, 570m, 1980–12–02, Almeida, A. J. F. (DZUP); **Rondônia**: 16 km SE de Vilhena, 12.8333°S, 60.0333°W, 580m, 2012–08–14, Cavichioli, R.; et al. (DZUP), Área de Mata, quadrante 1, 11.45°S, 61.4333°W, 182m, 2013–07–01, Silva, L. S., hand collected (DZUP), Área de Mata, quadrante 8, 11.4167°S, 61.4333°W, 196m,

2013–08–01, Silva, L. S., hand collected (DZUP), Flona do Jamarí, 9.13333°S, 63°W, 114m, 2013–06–07, Bueno, L.; Williams (DZUP), Floresta Nacional de Jamari, 9.21225°S, 62.9406°W, 111m, 2017–12–19, Aurea; et al., hand collected (INPA), Jaci Paraná, Rio Madeira, 9.54037°S, 64.3728°W, 85m, 2011–10–03, Santana, F. D. (CPDC), Jaci Paraná, Três Praias, 9.54037°S, 64.3728°W, 85m, 2011–10–07, Santana, F. D. (CPDC), Parque Estadual do Guajara–Mirim, 18 km SW of Nova Dimensão, 10.3167°S, 64.55°W, 152m, 1998–02–20, Santos, J. R. M., hand collected (DZUP), Reserva Biológica de Ouro Preto do Oeste, 10.7°S, 62.2333°W, 287m, 2009–07–13, Fernandes, I. (INPA); **Roraima**: Estação Ecológica de Maracá, 3.41667°N, 61.65°W, 127m, 1981–05–27 (MPEG); **São Paulo**: Rio Claro, 22.4°S, 47.55°W, 615m, 2004–12–10, Bacau, L. S. R. (DZUP). **COLOMBIA**: **Amazonas**: 11 km Via Tarapacá, 4.10068°S, 69.9292°W, 90m, 2002–04–27 (ICN), Amancayu, 1989–07, Castillo, R. (MUSENUV); **Meta**: Parque Nacional Natural Serranía de La Macarena, 8 SW San Juan de Arama, 2.96922°N, 73.9004°W, 1257m, 1986–12–01, Fernández, F. (ICN), Parque Nacional Natural Serranía de La Macarena, Vereda Caño Curia, 3.40672°N, 73.9537°W, 520m, 2004–03–05, Villalba, W., Malaise (MEPN), San Juan de Arama, 3.34643°N, 73.8894°W, 430m, 1986, Fernández, F. (MUSENUV). **ECUADOR: Orellana**: Estación Chiruisla, 0.61389°S, 75.8761°W, 200m, 2005–12–05, Donoso, D., fogging (QCAZ); **Pastaza**: Montalvo, 2.04987°S, 77.0072°W, 314m, 1985–07–16 (MECN); **Sucumbíos**: Limoncocha, 0.39983°S, 76.6002°W, 280m, 1967–11–17, Rettenmeyer, G. W. (QCAZ), Reserva de Producción Faunística Cuyabeno, Cooperativa Flor de Oro, 0.08667°S, 76.7147°W, 227m, 2010–04–20, Guerra, P., pitfall (MECN). **FRENCH GUIANA**: **Cayenne**: 1km E Nouragues Station, Grand Plateau, Nouragues Natural Reserve, 4.08885°N, 52.6749°W, 120m, 2009–09, Groc, S., pitfall (CPDC), 9km W of Kaw Camp Patawa, Kaw Mountains, 4.53419°N, 52.1516°W, 284m, 2008–09, Groc, S.; Dejean, J., Winkler (CPDC), CSG, P62, 5.24142°N, 52.8386°W, 28m, 2015–04–20, Orivel, J.; Fichaux, M.; Petitclerc, F.;, Pitfall72h (EcoFoG), Petit Saut, 5.06667°N, 53.0333°W, 75m, 2002–11–01, Orivel, J. (DZUP); **Saint–Laurent–du–Maroni**: Belvedere de Saul, 3.61667°N, 53.2°W, 326m, 2010–07, SEAC (DZUP), Itoupe, P1, 3.26391°N, 53.7616°W, 800m, 9/11/14, Orivel, J.; Fichaux, M., Pitfall72h (EcoFoG), Itoupe, P5, 3.22583°N, 53.9692°W, 600m, 2014–11–11, Orivel, J.; Fichaux, M., Pitfall72h (EcoFoG), Itoupe, P6, 3.12221°N, 53.9932°W, 600m, 11/15/14, Orivel, J.; Fichaux, M., Pitfall72h (EcoFoG), Laussat, P6, 5.4683°N, 53.5809°W, 50m, 2015–08–28, Orivel, J.; Fichaux, M.; Jackie; N. Milhom, Winkler48h (EcoFoG), Mitaraka, P1, 2.24362°N, 54.4588°W, 385m, 2015–03–03, Orivel, J.; Petitclerc, F., Winkler48h (EcoFoG), Mitaraka, P10, 2.21636°N, 54.457°W, 392m, 2015–02–28, Orivel, J.; Petitclerc, F., Pitfall72h (EcoFoG). **PERU**: **Cusco**: Estación Biológica Villa Carmen, 1.5 Km N Pillcopata, 12.8833°S, 71.4°W, 521m, 2013–08–05, Ant course 2013 (DZUP); **Loreto**: 3 km NE of Genato Herraro, Estación Genaro Herrera, 4.83333°S, 73.65°W, 121m, 2011–01–13 (ICN); **Madre de Dios**: Greenhouse at the Universidad Nacional Amazónica, 12.5833°S, 69.2°W, 207m, 2011–04–14, Salcedo, J. M. C. (DZUP), Reserva Nacional Tambopata, Sachavacayoc, Condenado I trail, 12.85°S, 69.3663°W, 186m, 2012–07–20, Fernandes, I., Winkler (INPA), Sachavacayoc Centre, 12.85°S, 49.3667°W, 209m,

2012–07–19, Feitosa, R. M.; Probst, R. S. (DZUP). **VENEZUELA**: **Amazonas**: Caño Panaben, Marurucu, 4.5 Km NE Santa Bárbara, 3.965°N, 67.024°W, 110m, 2000–10, García, D. (MIZA), Parque Nacional Parima Tapirapecó, Cerro Delgado Chalbaud, 2.277°N, 63.362°W, 1000m, 11/2/92, Clavijo, J.; Chacón, A. (MIZA), Yutajé, 5.611°N, 66.118°W, 120m, 10/19/88, Chacón, A. (MIZA); **Bolívar**: 40 Km E La Paragua, 6.826°N, 62.986°W, 290m, 6/11/83, Bordón, C. (MIZA), Alto Caura region, Cuchime, 5.8°N, 64.66°W, 280m, 4/7/63, La Salle expedition (MIZA), Amarawai Tepuy, Talud Norte, 6.083°N, 62.25°W, 500m, 5/1/86, Lattke, J. (MIZA), Canaima, 6.239°N, 62.852°W, 390m, 10/17/88, Mackay, W. (MIZA), Caura river, 7.611°N, 64.9118°W, 18m, 1899–02–11, Klages, E. (MPEG), El Dorado a Santa Elena de Uairen, Km. 17, 6.715°N, 61.637°W, 120m, 6/28/84, Lattke, J. (MIZA), El Dorado a Santa Elena de Uairen, Km. 88, 6.148°N, 61.431°W, 150m, 1998–11–10, Chacón, A. (MIZA), El Hormiguero, Altiplanicie de Nuria, 7.666°N, 61.333°W, 190m, 1974–12–03 (MIZA), El Playón, Caura river, 6.3151°N, 64.4899°W, 250m, 1980–09–08, Osuna, E.; Clavijo, J. (MIZA), Gran Sabana, San Ignacio, 5.033°N, 60.95°W, 1100m, 1993–03–01, Osborn, F. et al. (MIZA), Guri, 7.779°N, 63.026°W, 200m, 1988–06–27, Joly, L.; et al. (MIZA), Hato El Amparo, Cachipo river, 8.203°N, 63.31°W, 20m, 1984–04–15, Chacón, M. (MIZA), Icabarú, 4.3332°N, 61.7413°W, 500m, 1957–06–18, Bernardi, J. (MIZA), Las Bonitas, Caroní river, 7.866°N, 61.661°W, 34m, 1984–12–18, Osuna, E. (MIZA), Los Pijiguaos, 6.572°N, 66.811°W, 87m, 1987–03–23, Lan, D. (MIZA), Los Pijiguaos, Bauxilum mine, 6.483°N, 66.766°W, 690m, 2004–11–02, Lattke, J. (MIZA), Mantecal, Cuchivero river, 6.866°N, 65.633°W, 150m, 1970–03–23, Fernández, F.; Rosales, C. J. (MIZA), Mariposa, camp. Corocate, between Caura river and Sipao river, 7.5703°N, 65.2782°W, 50m, 1990–08–12, Alemán, M. (MIZA), Paragua river, E Chiguao river, 6.8478°N, 63.0475°W, 425m, 1983–04–02 (MIZA), Paraitepuy, Vía Roraima, 5.055°N, 60.934°W, 1200m, 1978–02–25, Escobar, A. (MIZA), Parque Nacional El Caura, 6.108°N, 64.716°W, 340m, 1986–08–28, Ayala, J. (MIZA), Quebrada Jaspe, 4.907°N, 61.092°W, 920m, 1986–08–19, Gill, B. (MIZA), Salto Las Babas, Caroní river, 6.519°N, 62.877°W, 425m, 1983–04–08 (MIZA), San Ignacio de Yuruaní, Gran Sabana, 4.984°N, 61.15°W, 910m, 1986–12–30, Hernández, J. (MIZA), San Juan de Manapiare, carretera Caicara, Suapure river, 6.027°N, 66.2549°W, 400m, 1971–12–27, García, J. (MIZA), San Juan de Manapiare, km. 170, carretera Caicara, 6.3091°N, 66.1882°W, 300m, 1973–12–21, García, J. (MIZA), Santa Elena, 4.59503°N, 61.1094°W, 1000m, 1975–03–01, Ross, E. S. (CASC), Santa Elena de Uairén, 4.606°N, 61.105°W, 1000m,, Revelo (MIZA), Santa María de Erebato, 5.15°N, 64.833°W, 330m, 1963–04–09, La Salle expedition (MIZA); **Monagas**: Caripito, 10.107°N, 63.103°W, 36m, 1963–07–17, Rosales, C.; Requena, J. (MIZA).

Geographic range.: Bolivia, Brazil, Colombia, Ecuador, French Guiana, Guyana, Paraguay, Peru, Suriname, Venezuela.

***Neoponera gojira* sp. nov.**

ZooBank: https://zoobank.org/D146DCC3-6FE5-4BEF-9E2A-009BAAD12740

Figs 19: a–g (☿); 29: a (distribution)

Type material. ***Holotype.*** 1♀; **BRAZIL**: **Minas Gerais**: Pandeiros, Efeito antropização no Cerrado APA REVISE (Project), 511m (alt.), 15°29'58.15"S, 44°45'39.94'O, 07.i.2016, Santiago et al. (leg.), Area 9, Local APA, pitfall epigéico (col. method), ponto 1, repetição D, quadrante 1. (DZUP: DZUP549444).

Etymology. The specific name honors the French metal band Gojira, in recognition of their altruistic activism for the conservation of nature, as well as for supporting the rights of ancestral indigenous peoples living across Amazonia. Through their lyrics the band promotes an increasing awareness of our paramount, nonetheless usually neglected, biological diversity. The name is a noun in apposition, thus invariable.

Worker diagnosis. Antennal scape surpassing posterior margin of head by ca. one apical scape width; head in frontal view trapezoid, slightly wider posteriorly than anteriorly (Fig. 19d); dorsal masticatory margin of mandible uneven, with shallow, irregular rim (Fig. 19b); masticatory margin of mandible with three comparatively large blunt teeth alternating with blunt denticles (Fig. 19b); posteroventral cuticular flap at metapleural gland opening reduced to narrow carina, orifice of gland completely visible in posterolateral view (Fig. 2d); petiolar node laterally lacking striae, though very tenuous lines are present near its ventral margin (Fig. 19e); prora tiny, barely discernible laterally (Fig. 19e); posterior region of abdominal sternites 5–7 showing significantly more piligerous punctures compared to the rest of species in the *N. laevigata* group.

Worker description. Measurements (*n* = 1): HW: 2.19; HL: 2.5; EL: 0.66; SL: 1.94; WL: 3.72; PrW: 1.63; MsW: 0.97; MsL: 0.87; PW: 1.17; PH: 1.28; PL: 1.12; GL: 5.1; A3L: 1.43; A4L: 1.48; A3W: 1.73; A4W: 1.89; TLa: 10.26; TLr: 12.45; **Indices**. CI: 87.76; OI: 30.23; SI: 88.37; MsI: 111.76; LPI: 88; DPI: 104.55.

Head. *Frontal view*: trapezoidal, with posterior margin wider than anterior margin. Masticatory margin of mandible with four large, blunt teeth interspersed with four denticles, basal margin edentate. Prementum with clear transverse dome. Labral dorsum mostly smooth. Posterolateral margin of torular lobe rounded. Malar carina absent, though swelling is present. Eye convex, relatively flat, not surpassing lateral margin of head, placed anterior to cephalic mid–length. Posterior margin of head concave. Occipital carina absent. *Lateral and/or frontal view*: Scape when pulled back, surpasses posterior margin of head by close to one apical scape width. **Mesosoma**. *Lateral view*: Pronotum with weak, blunt, barely distinguishable humeral carina. Metanotal groove present, though not depressed, usually clearly separating mesonotum and propodeum. Anapleural sulcus present, completely merged with surrounding striae. Posterior face of propodeal declivity flat. Posterolateral margin of propodeal declivity with feeble, blunt carina, almost devoid of crenulae. Pheromone venting canal at metapleural gland opening well–developed, smooth. Propodeal lateral margins subparallel in posterodorsal view. Ventrolateral propodeal declivity with deep transverse groove just dorsad to metapleural gland opening. *Ventral view*: Probasisternal posterior projection acute. Space between apices of mesosternal process wider than width of each apex. **Petiole**. *Lateral view*: Anterior and posterior margins of node nearly straight and semi-parallel, posterior margin slightly convex; posterodorsal margin slightly higher than anterodorsal margin; mid-dorsal margin mostly flat. Lateral projection of anteroventral nodal carina well-developed, with slightly blunt tip moderately bent dorsad.

Dorsal view: Anterior margin of petiolar node roughly as broad as width of posterior margin. Anteroventral nodal carina incomplete, feebly concave medially. *Lateral view*: Subpetiolar process subtriangular, with acute anterior cusp, keel-shaped, followed by posterior relatively straight slope (ca. 30°). **Gaster**. *Lateral view*: Prora present, though poorly developed, similar to a cuticular lip, usually hardly discernible. Meeting of anterior margin of abdominal tergum 3 with its dorsal margin relatively angled. Cinctus moderate. *Dorsal view*: Tergum of A3 slightly shorter than A4. Posterior dorsum of epipygium smooth, feeble striations and punctae present but hardly discernible and requires rotation of specimen to get better angle of observation. **Legs**. Mesofemur thickened medially, thicker than metafemur, in dorsal or ventral view. Ventral surface of meso– and metafemora flattened roughly on distal two–thirds, bearing longitudinal shallow groove. **Color**. Appendages including antennae and mandibles black to ferruginous black, mandibles feebly lighter than remaining integument of body. **Pilosity**. Erect hairs on body dorsum about as long as maximum eye length. Posterior dorsum of epipygium surrounded by ca. 20, long flexuous hairs. **Sculpture**. Striae on head present, only dorsally, covering most of surface except posterior third, anepisternum, katepisternum, metapleuron and lateral side of propodeum bearing strong striae; striae on petiolar node almost absent.

Queen and male. Unknown.

Natural history notes. Unknown. The holotype was collected in January 2016 in a project aiming to analyze anthropogenic disturbance in the Brazilian Cerrado. The ecosystem where this species was found is composed of tropical savannas, deciduous and semi–deciduous forests, and highly disturbed areas used mostly for agriculture (IBGE 2004, Soterroni et al. 2019; García et al. 2021)

Comments. *Neoponera. gojira* **sp. nov.** is currently known from a single specimen, nonetheless, various morphological features clearly separate it from its potential closest species: *N. laevigata* and *N. mashpi* **sp. nov.** The following characters are useful for separating the workers: the dorsal masticatory mandibular region shows a depressed rim (Fig. 19b) which is absent in *N. laevigata* and *N. mashpi* **sp. nov.**, this feature is not to be confused with the strongly excavated mandibular groove of *N. marginata*, which runs uninterrupted posterad along the entire mandibular base (Fig. 12a); posterior margin of head in full-face view clearly concave, with relatively salient posterolateral corners (Fig. 19d), while in *N. laevigata* this margin is straight or feebly concave (Figs 20c, 21d), and straight or slightly convex in *N. mashpi* **sp. nov.** (Fig. 25c); flap at metapleural gland opening strongly reduced to a narrow, but sharply delineated carina, in posterolateral view, while in both *N. laevigata* and *N. mashpi* **sp. nov.** this flap is well-developed and runs uninterrupted along the ventrolateral margin of the metapleuron until reaching its anterior lobe (Fig. 2d); clypeus and internal side of frontal lobes heavily sculpted with foveae and striae (Fig. 12b), in *N. laevigata* and *N. mashpi* **sp. nov.**, on the other hand, the clypeus is feebly striated, and the frontal lobes almost always lack sculpture, except for two shallow foveae on the internal side. Heavily impressed clypeal sculpture is also typical in *N. marginata*, and to a lesser degree in *N. commutata*. However, impressed sculpture (foveae and striae) on the frontal lobe area has only been seen in *N. gojira* **sp. nov.** Compared to the workers of similarly sized species, e.g.,

DOI 10.1163/1876312X-bja10034

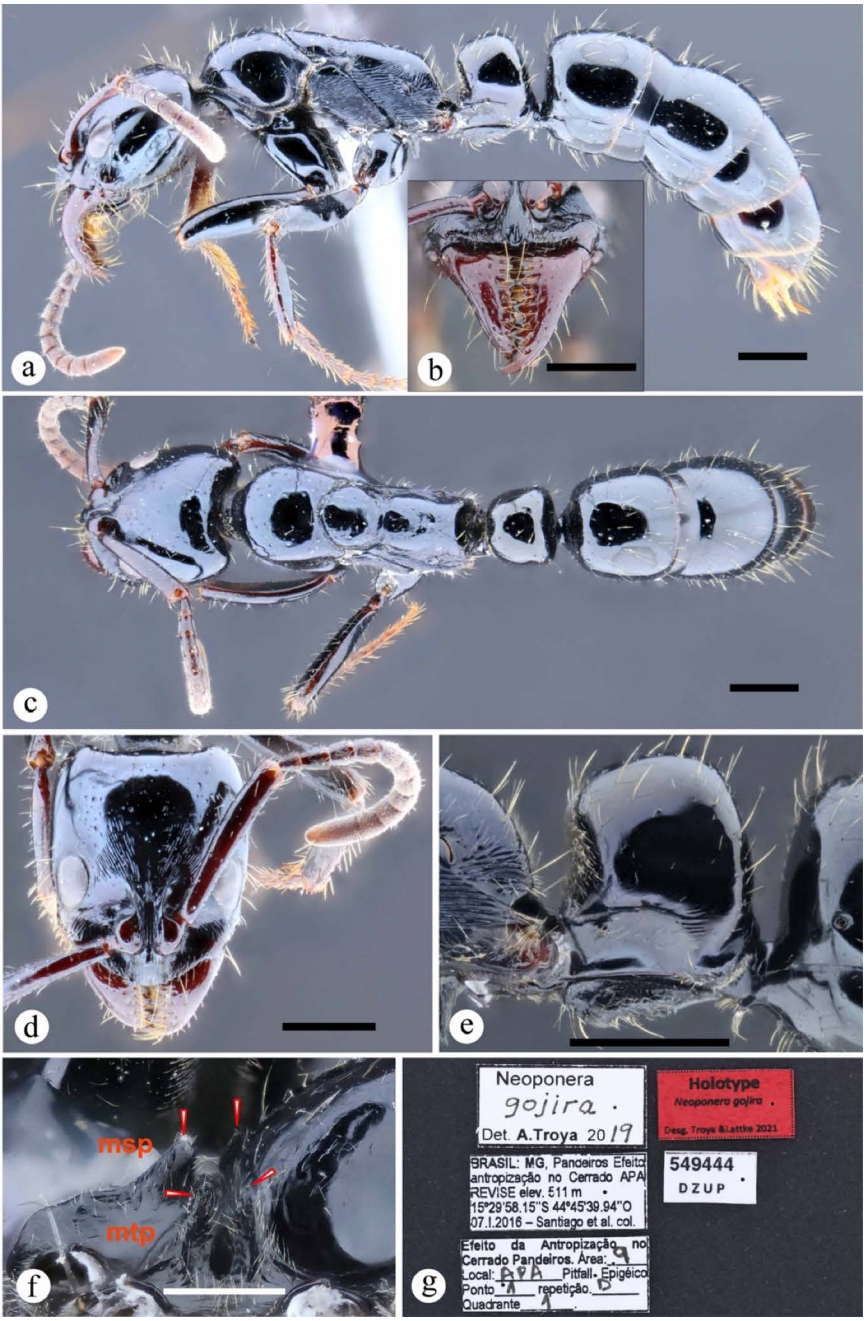

Fig. 19. *Neoponera gojira* **sp. nov.** Holotype ☿ (DZUP: DZUP549444), Brazil, Minas Gerais. **a.** Lateral view; **b.** Mandibles in frontal view; **c.** Head in frontal view; **e.** Petiole in lateral view; **f.** Meso– and metasternal processes (red arrowheads) in posteroventral view; **g.** Collection labels. Scales bars: 1 mm (**a**–**e**); 0.25 mm (**f**).

N. laevigata (WL= 2.45–3.57 mm; TLa= 7.88–10.03 mm) and *N. marginata* (WL= 2.75–3.59 mm; TLa= 7.41–10 mm), the holotype of *N. gojira* **sp. nov.** is thus far the second largest worker in the *N. laevigata* group (WL = 3.72 mm; TLa = 10.26 mm), only oversized by workers of *N. commutata*. It is assumed that the still unknown conspecifics (but see below) may have a similar size showing the characteristic continuous polymorphic size variation that is present in its closest lineages.

Geographic range. Eastern Brazil.

Phenotypic variant of *N. gojira* **sp. nov.**

In the northeastern Brazilian states of Piauí and Bahia we found ten workers morphologically similar to *N. gojira* **sp. nov.** and *N. laevigata*. This variant shares morphospace with these two species, but also with *N. marginata* (Fig.. 3). Until additional material is discovered we leave this morphotype as *Neoponera* nr. *gojira* which shows the following diagnostic traits: dorsal margin of mandibles, near the masticatory region, with shallow fossulae; antennal scape surpassing posterior margin of head by approximately one apical scape width (Fig. 13b); flap at metapleural gland orifice present, though not strongly curved anterad, so that the orifice is easily visible in posterolateral view (Fig. 2b); petiolar node mostly smooth, though with feebly impressed striae laterally (Fig. 22b); prora tiny (Figs 13d, 19e).

Neoponera nr. *gojira* differs from *N. gojira* **sp. nov.** in the following: relatively smaller (WL = 3.24–3.32 mm; TLa = 8.78–8.93 mm); four to five teeth on mid masticatory margin of mandibles clearly smaller and more acute (*N. gojira* **sp. nov.** bears three relatively large, blunt teeth, Fig. 19b); posterior margin of head less concave than in Figure 19d). *Neoponera* nr. *gojira* differs from *N. laevigata* in the following: dorsal mandibular surface, near masticatory margin, bearing fused, shallow fossulae (we saw these fossulae in some workers of *N. laevigata,* though clearly less impressed); petiolar node with tenuously impressed striae (node strongly striate laterally in *N. laevigata,* especially specimens from Amazonian populations); flap at metapleural gland orifice well–developed but not strongly curved anterad (this flap is also well–developed in *N. laevigata* but is strongly curved anterad, partially hiding the gland orifice, Fig. 2a).

Measurements (n = 3) of *Neoponera* nr. *gojira*: HW: 1.73–1.84; HL: 2.09–2.19; EL: 0.56–0.56; SL: 1.58–1.73; WL: 3.24–3.32; PrW: 1.3–1.33; MsW: 0.84–0.92; MsL: 0.69–0.77; PW: 1.02–1.07; PH: 1.07–1.07; PL: 0.82–0.97; GL: 2.91–4.13; A3L: 1.1–1.22; A4L: 1.33–1.43; A3W: 1.53–1.58; A4W: 1.68–1.71; TLa: 8.78–8.93; TLr: 9.26–10.46. **Indices**. CI: 79.07–87.8; OI: 30.56–32.35; SI: 88.57–100; MsI: 116.67–122.22; LPI: 76.19–90.48; DPI: 105.26–128.13.

Material examined for *Neoponera* nr. *gojira*: 10☿: **BRAZIL**: **Bahia**: Barreiras, 12.1333°S, 45.1333°W, 527m, 2011–05–15, Carvalho, K. S. (DZUP); **Piauí**: Ribeiro Gonçalves, 8.85996°S, 45.2001°W, 570m, 1980–12–10, Almeida, A. J. F. (DZUP), 1980–12–13, Almeida, A. J. F. (DZUP), 1980–12–16, Almeida, A. J. F. (DZUP), 1980–12–12, Almeida, A. J. F. (DZUP), 1980–12–15, Almeida, A. J. F. (DZUP), 1980–12–18, Almeida, A. J. F. (MPEG), 1980–12–11, Almeida, A. J. F. (DZUP), 1980–12–14, Almeida, A. J. F. (DZUP), 1980–12–17, Almeida, A. J. F. (MPEG).

***Neoponera laevigata* (Smith, 1858)**

Figs 20: a–f (☿); 21: a–f (♀); 29: a (distribution)

Ponera laevigata Smith, 1858: 98. BRAZIL (Amazonas), Ega (currently Tefé), (3.3°S, 64.7°W, 57m), (*Bates, H. W.*). Type material: 1 ☿ syntype (BMNH) (not examined), and 1 ☿, **lectotype** (present designation), BMNH(E)1015554, AntWeb CASENT0902510 (image examined).

Combinations. In *Euponera* (*Mesoponera*): Emery, 1901: 47. In *Termitopone*: Wheeler, 1936: 159. In *Pachycondyla*: Mayr, 1886: 358; Brown, 1995: 306; In *Neoponera*: Schmidt & Shattuck, 2014: 151.

Status as species. Mayr, 1863: 448; Wheeler, 1936: 161 (redescription); Mackay & Mackay, 2010: 414 (redescription).

Senior synonyms. *Neoponera gagatina* (Emery): Emery, 1892: 167; *Neoponera laevigata* var. *whelpleyi* (Wheeler): Wheeler, 1936: 164 [type material: 1 ☿ **paralectotype** (present designation), Trinidad & Tobago, Caparo, 1910-02-12, Whelpley, P.B., MCZENT20454. (image examined)].

Worker and queen diagnosis. Antennal scape, when pulled back, surpasses posterior head margin by about one apical scape width (Fig. 13b); longitudinal striae present around internal margin of eye and between frontal carinae, diverging posterad and usually vanishing at vertex, but reaching lateral head margin just posterior to eyes (Figs 13b, 21d); dorsum of head in smaller workers significantly less sculpted than larger workers to almost devoid of striae; lateral face of petiolar node always with oblique, usually strongly impressed striae (Fig. 20d); subpetiolar process, in lateral view, subtriangular, with acute anterior cusp, usually followed by relatively flat surface posterad (Figs 13d, 20d); prora absent or very small, lip–shaped (Fig. 13d).

Worker description. Measurements (n = 10): HW: 1.43–2.12; HL: 1.71–2.45; EL: 0.41–0.61; SL: 1.35–1.94; WL: 2.45–3.57; PrW: 0.94–1.53; MsW: 0.69–1.04; MsL: 0.55–0.97; PW: 0.69–1.07; PH: 0.78–1.25; PL: 0.73–1.05; GL: 2.61–4.34; A3L: 0.98–1.48; A4L: 0.98–1.48; A3W: 1.06–1.76; A4W: 1.1–1.69; TLa: 6.9–10.03; TLr: 7.55–11.4. **Indices**. CI: 79.18–90.57; OI: 28.13–31.17; SI: 88.89–101.3; MsI: 105.26–126.47; LPI: 76.92–94.74; DPI: 94.44–117.65.

Head. *Frontal view*: subrectangular. Masticatory margin of mandible with four to five teeth interspersed with three to six denticles, basal margin edentate. Prementum with clear transverse dome. Labral dorsum mostly smooth, posterolateral margin rounded. Malar carina absent, though swelling present. Eye convex, relatively flat, not surpassing lateral margin of head, placed anterior to cephalic mid–length. Posterior margin of head straight to slightly concave. Occipital carina absent. Scape when pulled back, surpasses posterior margin of head by close to one apical scape width. **Mesosoma**. *Lateral view*: Pronotum with weak, blunt, barely distinguishable humeral carina. Metanotal groove present, though not depressed, usually clearly separating mesonotum and propodeum. Anapleural sulcus present, though usually merged with surrounding striae. Posterior face of propodeal declivity mostly flat. Posterolateral margin of propodeal declivity with feeble, blunt carina, sometimes with crenulae. Pheromone venting canal at metapleural gland opening well-developed, smooth. Propodeal lateral margins

subparallel in posterodorsal view. Ventrolateral propodeal declivity with deep transverse groove just dorsad to metapleural gland opening, in posterolateral view. *Ventral view*: Probasisternal posterior projection acute. Space between mesosternal process lobes approximately equal to width of each. Metasternal process inclined posterad 20°–30° in lateral view. **Petiole**. *Lateral view*: anterior and posterior margins of node usually nearly straight and semi–parallel, sometimes posterior margin slightly convex; posterodorsal margin slightly higher than anterodorsal margin; mid-dorsal margin mostly flat. Lateral projection of anteroventral nodal carina well-developed, with acute or slightly blunt tip moderately bent dorsad. *Dorsal view*: Anterior margin of petiolar node slightly shorter than width of posterior margin. Anteroventral nodal carina incomplete, with feeble concavity medially. *Lateral view*: Subpetiolar process subtriangular, usually with keel-shaped, acute anterior cusp, followed by posterior straight slope (ca. 20° or less). **Gaster**. *Lateral view*: Prora present, though poorly developed, similar to a cuticular lip, usually hardly discernible. Meeting of anterior margin of abdominal tergum 3 with its dorsal margin relatively angled. Cinctus moderate. *Dorsal view*: Tergum of A3 slightly shorter than A4. *Posterior view*: Posterior dorsum of epipygium smooth, though feeble striations and punctae may be present. **Legs**. Mesofemur thickened medially, thicker than metafemur, in dorsal or ventral view. Ventral surface of meso– and metafemora flattened roughly on distad two thirds, usually bearing longitudinal shallow groove. **Color**. Appendages including antennae and mandibles brown to ferruginous brown, occasionally legs yellowish and mandibles lighter than remaining integument of body. **Pilosity**. Most erect hairs on body dorsum approximately as long as maximum eye length. Scape hairs about as long as apical scape width. Posterior dorsum of epipygium surrounded by ca. 20, long flexuous hairs. **Sculpture**. Striae on head present, only dorsally, covering most of surface except posterior third, anepisternum, usually part of katepisternum, metapleuron, lateral and part of dorsal side of propodeum with strong striae, on petiolar node always present, oblique and strongly impressed.

Queen description. Measurements (n = 2). HW: 2.48–2.41; HL: 2.79–2.73; EL: 0.73–0.73; SL: 2.13–2.1; WL: 4.95–4.7; PrW: 2.29–2.1; MsW: 2.22–2.19; MsL: 2.79–2.6; PW: 1.59–1.68; PH: 1.59–1.68; PL: 1.21–1.08; GL: 6.6–6.1; A3L: 1.97–2.1; A4L: 1.97–1.97; A3W: 2.6–2.54; A4W: 2.73–2.7; TLa: 12.89–12.57; TLr: 15.56–14.6. **Indices**. CI: 88.37–88.64; OI: 29.49–30.26; SI: 85.9–86.84; MsI: 79.55–84.15; LPI: 64.15–76; DPI: 131.58–155.88.

Morphology as in worker except for: **Head**. *Frontal view*: Anterior ocellus maximum diameter subequal to that of posterior ocelli. Distance from posterior ocellar margin to posterior margin of head close to twice apical scape width. Distance between anterior and posterior ocelli approximately 1.5 times anterior ocellus diameter. Posterior margin of head straight to slightly concave. **Mesosoma**. *Dorsal view*: Mesoscutum about as long as broad, close to 2.5 times as long as mesoscutellum. Transscutal line feebly developed. Scutoscutellar sulcus shallowly impressed, formed by scrobiculate sculpture. Mesoscutellum subquadrate, slightly flat dorsally. Posterior face of propodeal declivity flat. Posterolateral margin of propodeal declivity slightly rounded to barely carinate, not forming crenulae. Anterodorsal median propodeal sulcus present, weakly impressed. Probasisternal posterior projection with spine. **Wings**. Forewing

venation: Rs–M approximately one half larger than 2M. Forewing evenly covered by fine setose layer. Hindwing venation: 1Rs highly reduced. Hindwing bearing 10–13 hamuli. **Petiole**. *Lateral view*: anterior and posterior margins of node nearly straight at base and slightly tapering dorsad, with posterior margin slightly convex and with more pronounced slope than anterior margin which is almost perpendicular to horizontal body axis. **Gaster.** Prora absent. **Color**. Appendages, including antennae and mandibles, dark brown to black. **Pilosity**. Meso- and metatarsi bearing abundant spines and stiff setae interspersed with abundant suberect hairs. **Sculpture**. Striae on head present only dorsally, covering most of surface except posterior third; strong striae on posterolateral margin of pronotum, usually anepisternum and part of katepisternum, axillula, metapectus, and propodeum laterally; petiolar node always with oblique, strong striae laterally.

Male description. Not available, but see Wheeler (1936), and Mackay and Mackay (2010). These authors possibly revised male material of both *N. laevigata* and *N. mashpi* **sp. nov.** Since these two species are probably closely related, the male of *N. laevigata* might likely be very similar to that of *N. mashpi* **sp. nov.** If the male is finally found in the future we strongly recommend extracting and illustrating its genitalia, in particular the penisvalva which shows interesting differing features among the species here examined (see Fig. 28).

Natural history notes. Since *N. laevigata* is probably closely related to *N. mashpi* **sp. nov.** we consider the possibility that it could display a similar behavior, such as a diet based on termites. Borgmeier (1959) cites the observation "formando fila" (making a row) from P. Telles who collected specimens in Linhares, Espírito Santo, southeastern Brazil. Schmid-Hempel (1998) noted that the phorid fly *Ecitomyia juxtaposita* Borgmeier is associated with colonies of this species in Brazil. Mackay and Mackay (2010) collected winged gynes in March and October, also in Brazil. These are the only published sources which could potentially be associated with N. *laevigata*. However, since we could not find the vouchers of these studies no confirmation is currently possible. In regards to Baroni Urbani (1993) who includes this species in an overall analysis of the evolution of recruitment behavior in ants, it is uncertain whether this is in fact *N. laevigata* as no details about the voucher material is mentioned.

Comments. Workers of this species, which are much more commonly encountered in the field than other castes, are very similar to those of *N. mashpi* **sp. nov.** Even for a trained eye it is sometimes uneasy to differentiate both forms. However, upon recognizing the specific body features that vary between these two taxa, the task becomes easier. The queens of both species, however, are not so similar and proper examination allows separation without much trouble. We were fortunate in finding a nest series with close to 300 individuals from Pará, Monte Dourado (MPEG) which allowed us to associate workers with queens, but also to examine size polymorphism among workers, which is less variable than in its closest species *N. mashpi* **sp. nov.** (Fig. 3). For instance, the difference in size observed mainly in the variables WL and HL is less extended in the morphospace than in *N. mashpi* **sp. nov.**

The morphological characters allowing a differentiation of the known castes of *N. mashpi* **sp. nov.** and *N. gojira* **sp. nov.** which, based on their examined morphology,

we assume are the most closely related species to *N. laevigata*, are detailed in the 'comments' section of those species.

Wheeler (1922) in his work of "Ants of Trinidad", upon studying a specimen collected by P. Whelpley at Caparo, Trinidad and Tobago, mentions for the first time the lateral petiolar node striations and decides to erect *Neoponera* [= *Euponera* (*Mesoponera*)] *laevigata* var. *whelpleyi*. Later, in 1936, this author synonymizes it under *Termitopone laevigata*. We examined the image of Wheeler's (1922) syntype (MCZENT20454) and confirm this is *N. laevigata* since it matches the diagnostic traits specified in this study, whose populations are mostly distributed in Amazonian habitats. Together, with the record of *N. marginata* (voucher at American Museum of Natural History) by Mackay and Mackay (2010), these are the only records from the *N. laevigata* group for a Caribbean island. Although this specimen was collected more than a century ago, the forests of Trinidad and Tobago are relatively well-preserved (Baksh-Comeau et al. 2016) making it likely to find populations of this species in the present. Surprisingly, we could not find a single *N. laevigata* specimen from Venezuela, yet it is very likely that this species is also present in a number of habitats and regions in that country. AntWeb record CASENT0249152 identified as *N. laevigata* from the Venezuelan state of Bolívar, represents in fact *N. mashpi* **sp. nov.**

Distribution notes. This species is distributed only in South America, with most of the records coming from the Amazonian biome. The remaining scant records belong to the Caribbean forests of Trinidad, the tropical Andean forests of the Cordilleras Central and Occidental of Colombia, and the Pacific forests of the Chocó-Darien, also in Colombia. Although no records of this species were found for any bioregion in Bolivia, Ecuador and Peru, its populations are probably present there. For example, a *N. laevigata* record in the extremely isolated western Amazonian site of Estirão do Equador in Brazil, lies just at the political border with the northern Peruvian Amazon. Increasing sampling in these regions will likely unveil records for this species.

Material examined. 32 ☿, 7♀: **BRAZIL**: **Acre**: Parque Nacional da Serra do Divisor, Formosa, 7.43328°S, 73.65°W, 245m, 2016–11–15, Feitosa, R.; et al. (DZUP); **Amazonas**: Br. 174, Km 70, 2.46726°S, 60.0307°W, 123m, 1995–04–05, Matsuo, A.; Vasconcelos, H. (INPA), Estirão do Equador, 4.53583°S, 71.6236°W, 114m, 1979–10, Alvarenga, M. (MPEG), Presidente Figueiredo, 2.07361°S, 60.0148°W, 138m, 1994–02–25, Queiroz, hand collected (INPA), Reserva Florestal ZF3, Km 41, 2.41667°S, 59.8°W, 118m, 1996–09–20, Macedo, A. (INPA), ZF2, 2.6°S, 60.2°W, 89m, 1997–07–29, Cabini, G.; et al. (INPA); **Mato Grosso**: 65 Km S Sinop, 12.5167°S, 55.6167°W, 430m, 1974–10, Alvarenga, M. (MPEG); **Pará**: 30 Km E Belén, 1.27417°S, 48.2742°W, 30m, 2020–08–05, Oliveira, A. M.; Manne, W. S., hand collected (DZUP), Conceição do Araguaia, 8.26187°S, 49.2696°W, 177m, 1979–11–07, Overal, W. (MPEG), Mina do Palito, 6.3°S, 55.8°W, 229m, 2018–01–31, Silva, R.; Prado, L., hand collected (MPEG), Monte Dourado, 0.867652°S, 52.5348°W, 76m, 1979–10–31, Overal, W.; Neto, R. (MPEG), Utinga, 1.42424°S, 48.4454°W, 18m, 1979–07–10, Overal, W. (MPEG); **Roraima**: Estação Ecológica de Maracá, 3.41667°N, 61.65°W, 127m, 1976–03, Negre, R. (DZUP). **COLOMBIA**: **Amazonas**: Parque Nacional Natural Amacayacu, Matamata, 3.68333°N, 70.25°W, 150m, 2000–05–18,

DOI 10.1163/1876312X-bja10034

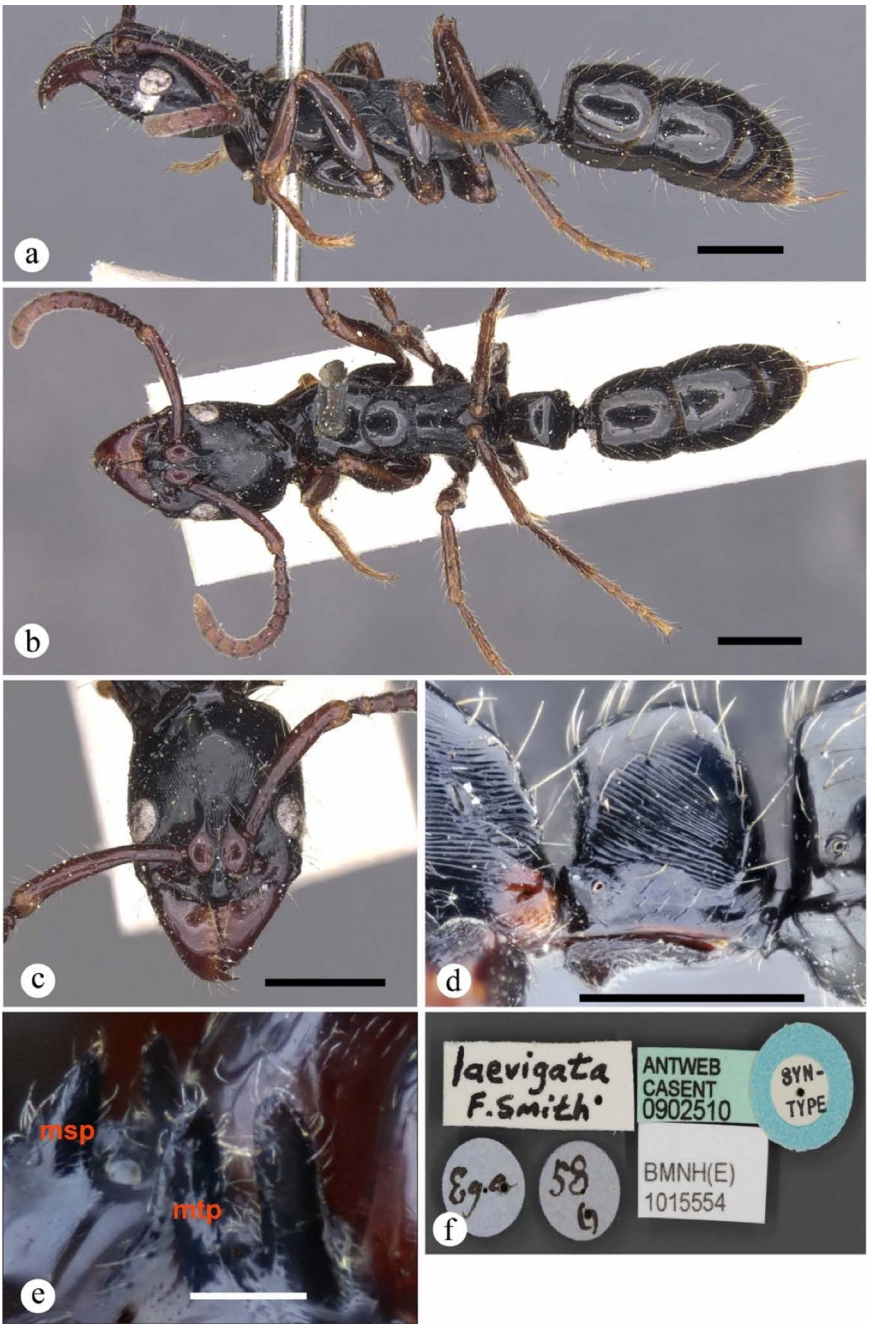

Fig. 20. *Neoponera laevigata*. Lectotype ☿ (BMNH: BMNH(E)1015554), Brazil, Amazonas. **a.** Lateral view; **b.** Dorsal view; **c.** Head in frontal view; **f.** Collection labels. Images **d, e**: non-type ☿ (MPEG: ATPFOR2027), Brazil, Roraima. **d.** Petiole in lateral view; **e.** Mesosternal (msp) and metasternal (mtp) processes in posteroventral view. Scale bars: 1 mm (**a**–**d**); 0.2 mm (**e**).

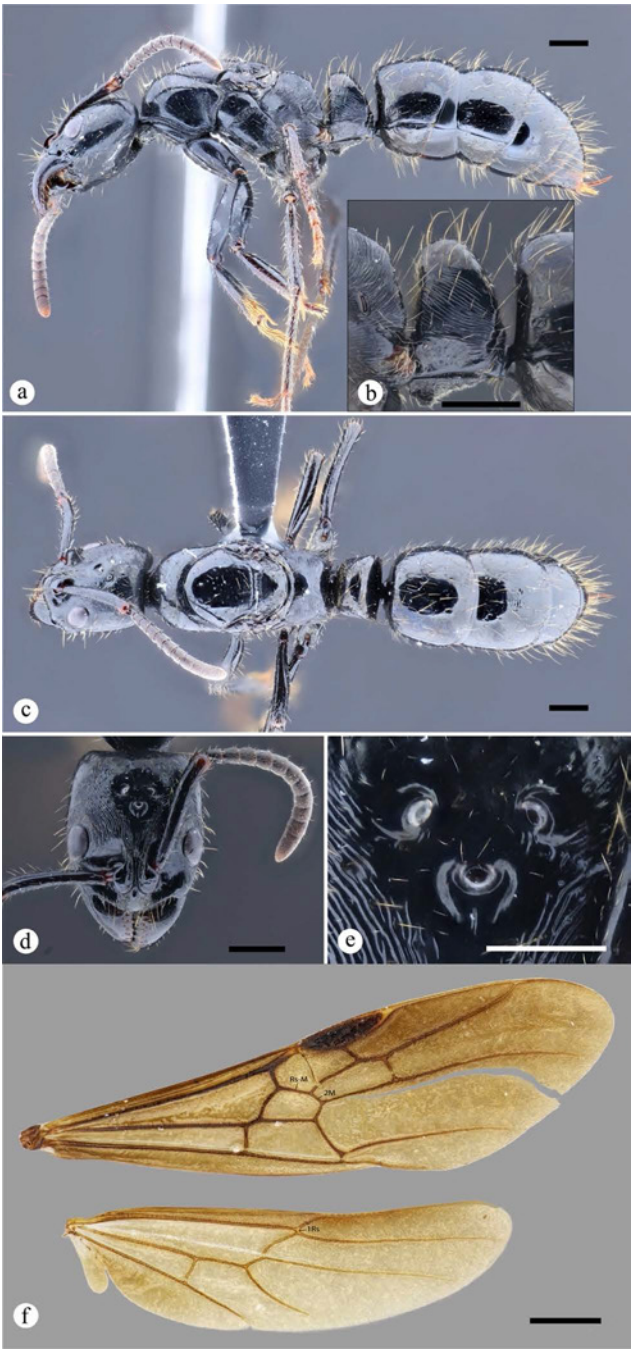

Fig. 21. *Neoponera laevigata*. ♀ (MPEG: ATPFOR2049), Brazil, Pará. **a.** Lateral view; **b.** Petiole in lateral view; **c.** Dorsal view; **d.** Head in frontal view; **e.** Ocelli in frontal view; Fore and hind wings. Scale bars: 1 mm (**a**–**d**, **f**); 0.5 mm (**e**).

Parente, A., Winkler (IAvH); **Boyacá**: San Luís de Gaceno, 4.81966°N, 73.1696°W, 400m, 2007–03–20, Campos, D. (ICN); **Chocó**: Parque Nacional Natural Utría, 6.01673°N, 77.3334°W, 390m, 1993, Baena, M., Malaise (IAvH); **Meta**: Parque Nacional Natural Serranía de La Macarena, Vereda Caño Curia, 3.40672°N, 73.9537°W, 520m, 2003–12–13, Villalba, W., Malaise (MEPN); **Valle del Cauca**: Campo–Tronco, 3.93333°N, 76.6667°W, 550m, 1994–04–01, Aldana, R. (IAvH), Parque Nacional Natural Farallones de Cali, Anchicaya, 3.43333°N, 76.8°W, 1455m, 2001–05–08, pitfall (IAvH). **FRENCH GUIANA**: **Cayenne**: Montagne des Singes, 5.07327°N, 52.7005°W, 127m, 2016–05–02, Petitclerc, F.; et al. (CPDC); **Saint–Laurent–du–Maroni**: Belvedere de Saul, 3.61667°N, 53.2°W, 326m, 2011–03–22, Team, S. E. A. G. (DZUP). **GUYANA**: **Upper Essequibo**: Parabara, 2.1819°N, 59.3371°W, 240m, 2013–11–05, Helms, J. A. (USNM). **TRINIDAD AND TOBAGO**: **Caroni**: Caparo, 10.4494°N, 61.3286°W, 90m, 1910–02–12, Whelpley, P. B. (MCZC).

Geographic range. Brazil, Colombia, French Guiana, Guyana, Peru, Trinidad and Tobago.

***Neoponera marginata* (Roger, 1861)**

Figs 22: a–e (☿); 23: a–c (♀); 24: a–e (♂); 28: d–f, k (♂ genitalia); 29: b (distribution)
Ponera marginata Roger, 1861: 8. Brazil, (Minas Gerais), São Joao del Rey. Type material (syntypes): 1 ☿, 1 ♀(MNHU), 1 ☿, 1 ♂ (ZSBS) [not examined]. Combinations. In *Euponera* (*Mesoponera*): Emery, 1901: 47. In *Termitopone*: Wheeler, 1936: 166. In *Pachycondyla*: Roger, 1863: 18; Brown, 1995: 307; In *Neoponera*: Schmidt & Shattuck, 2014: 151.
Status as species. Roger, 1863: 18; Gallardo, 1918: 67 (redescription); Wheeler, 1936: 166 (redescription); Mackay & Mackay, 2010: 455 (redescription).

Worker and queen diagnosis. Head rectangular (usually workers), and trapezoid or subquadrate (usually queens), when trapezoid the posterior margin is broader than anterior margin (Fig. 23c); dorsal masticatory margin of mandible with deep longitudinal groove (Fig. 22e); dorsoanterior clypeal margin usually strongly striated, sometimes bearing piligerous foveae (Fig. 22e); scape, when pulled back, almost reaching posterior margin of head, space between tip of scape and posterior head margin usually less than half apical scape width (Figs 22d, 23c); prora well–developed, directed ventrad (Figs 22b, 23d).

Worker description. Measurements (n = 16): HW: 1.59–2.25; HL: 1.84–2.57; EL: 0.39–0.53; SL: 1.25–1.88; WL: 2.75–3.59; PrW: 1.12–1.65; MsW: 0.72–1.1; MsL: 0.63–0.98; PW: 0.78–1.12; PH: 0.86–1.2; PL: 0.72–0.94; GL: 2.9–5.1; A3L: 0.98–1.39;A4L: 1.06–1.51; A3W: 1.14–1.71; A4W: 1.22–1.88; TLa: 7.41–10; TLr: 8.53–12.21; **Indices**. CI: 79.63–97.03; OI: 22.73–30.23; SI: 71.15–95.35; MsI: 89.58–118.75; LPI: 71.43–92; DPI: 90.48–122.22.

Head. *Frontal view*: Rectangular. Masticatory margin of mandible with four to five large teeth interspersed with denticles, usually posterior half bearing only four to six tiny denticles, basal margin edentate. Prementum with clear transverse dome. Labral dorsum mostly smooth. Torular lobe posterolateral margin rounded. Malar carina

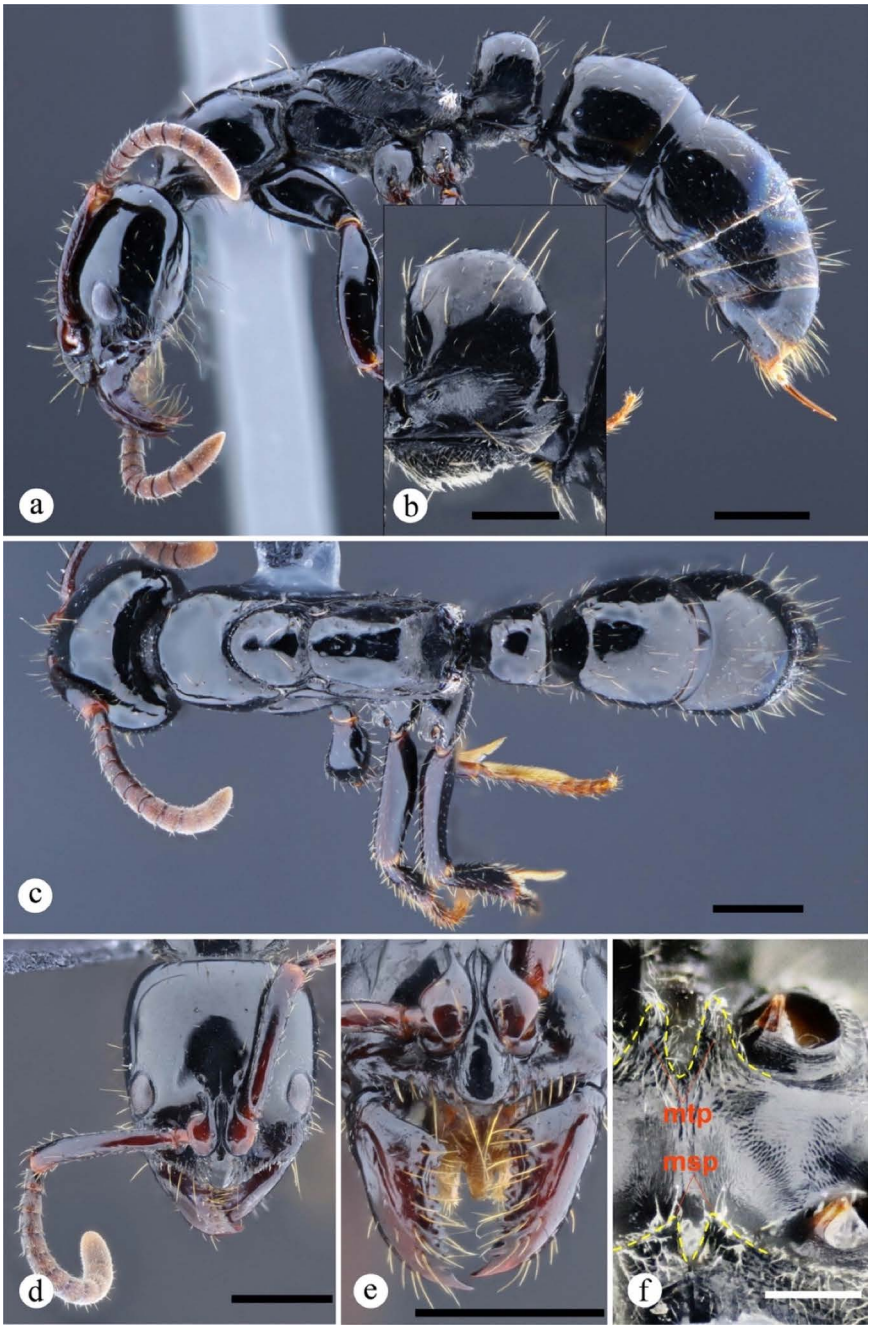

Fig. 22. *Neoponera marginata*. ☿ (MEPN: CASENT0649897), Brazil, Paraná. **a.** Lateral view; **b.** Petiole in lateral view; **c.** Dorsal view; **d.** Head in frontal view; **e.** Mandibles in frontal view; **f.** Mesosternal (msp) and metasternal (mtp) processes (dashed red line) in anteroventral view. Scale bars: 1 mm (**a**–**d**); 0.5 mm (**e**); 0.25 mm (**f**).

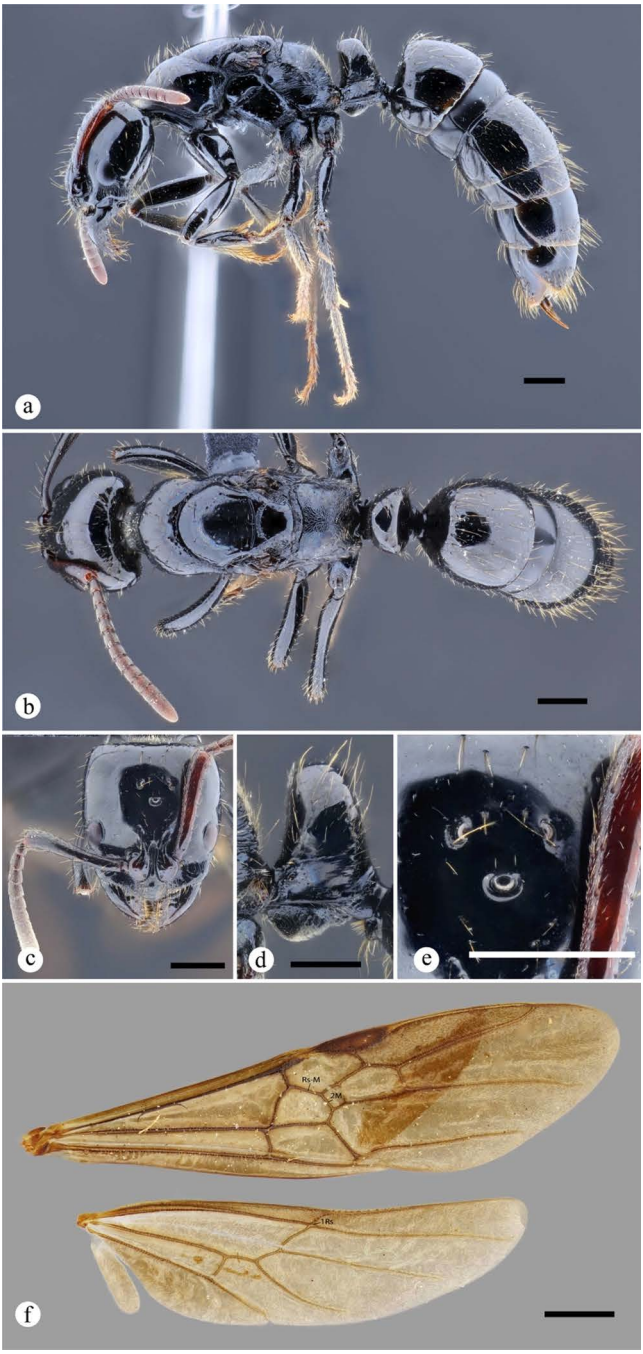

Fig. 23. *Neoponera marginata*. ♀ (MPEG: ATPFOR2028), Brazil, Espírito Santo. **a.** Lateral view; **b.** Dorsal view; **c.** Head in frontal view; **d.** Petiole in lateral view; **e.** Ocelli in frontal view; **f.** Fore and hind wings. Scale bars: 1 mm (**a**–**d**, **f**); 0.5 mm (**e**).

absent, though a swelling is present. Eye convex, relatively flat, not surpassing lateral margin of head, placed anterior to cephalic mid–length. Posterior margin of head straight. Occipital carina absent. **Mesosoma**. *Lateral view*: Pronotum with weak, blunt, barely distinguishable humeral carina. Metanotal groove present, slightly depressed, mesonotum and propodeum clearly separated. Anapleural sulcus present, though usually merged with surrounding striae. Posterior face of propodeal declivity mostly flat. Posterolateral margin of propodeal declivity with feeble, blunt carina, sometimes with crenulae. Propodeal lateral margins subparallel in posterodorsal view. Ventrolateral propodeal declivity with deep transverse groove just dorsad to metapleural gland opening. Pheromone venting canal at metapleural gland opening well–developed, slightly striated. *Ventral view*: Probasisternal posterior projection with spine. **Petiole**. *Lateral view*: anterior and posterior margins of node usually nearly straight and semi–parallel, sometimes posterior margin slightly convex. Petiolar node anterior and posterior dorsal margins equal in length vertically. Petiolar node dorsal margin mostly flat. Lateral projection of anteroventral nodal carina well–developed, with acute or slightly blunt tip moderately bent dorsad. *Dorsal view*: Anterior margin of petiolar node roughly as broad as width of posterior margin. Anteroventral nodal carina incomplete, with feeble concavity medially. *Lateral view*: Subpetiolar process subtriangular, with acute anterior cusp, sometimes keel–shaped, followed by posterior straight slope (ca. 30°). **Gaster**. *Lateral view*: Prora well–developed, with blunt tip projecting ventrad. Meeting of anterior margin of abdominal tergum 3 with its dorsal margin relatively angled. Cinctus moderate. *Dorsal view*: Tergum of A3 slightly shorter than A4. Posterior dorsum of epipygium smooth, though feeble striations and punctae may be present. **Legs**. Mesofemur thickened medially, thicker than metafemur, in dorsal or ventral view. Ventral surface of meso- and metafemora flattened roughly on distad two–thirds, usually bearing longitudinal shallow groove. Arolium roughly 0.5 times the length of pretarsal claw. Pretarsal claw with strong, median tooth. **Color**. Appendages including antennae and mandibles black to ferruginous black, mandibles feebly lighter than remaining integument of body. **Pilosity**. Most erect hairs on body dorsum approximately same as long as maximum eye length. Scape hairs about as long as apical scape width. Meso- and metatarsi bearing abundant spines and stiff setae interspersed with abundant suberect hairs. Posterior dorsum of epipygium surrounded by ca. 20 long, flexuous hairs. **Sculpture**. Striae on head mostly absent, though when present only anteriorly on dorsum, laterally on clypeus, and malar area; anepisternum, usually part of katepisternum, metapleuron, lateral and posterior surface of propodeum strongly striated; sometimes propodeal dorsum with longitudinal, feeble, broken line of tiny foveae; striae on petiolar node usually weak and only posterolaterally.

Queen description. Measurements (n = 5). HW: 2.54–2.79; HL: 2.79–2.92; EL: 0.63–0.73; SL: 1.95–2.1; WL: 4.25–4.75; PrW: 1.97–2.2; MsW: 1.78–1.95; MsL: 2.48–2.63; PW: 1.33–1.46; PH: 1.4–1.52; PL: 0.95–1.11; GL: 4.51–6.03; A3L: 1.78–1.91; A4L: 1.84–2.03; A3W: 2.29–2.37; A4W: 2.35–2.54; TLa: 11.84–12.67;

TLr: 12.7–14.63; **Indices**. CI: 90.91–97.78; OI: 23.86–26.74; SI: 70.45–77.5; MsI: 71.79–75.41; LPI: 66.67–76.47; DPI: 130.77–143.75.

Morphology as in worker except for: **Head**. *Frontal view*: Head usually trapezoidal. Anterior ocellus maximum length subequal to that of posterior ocelli. Distance from posterior ocellar margin to posterior margin of head close to 2.5 times apical scape width. Distance between anterior and posterior ocelli close to 2.5 times anterior ocellus maximum length. **Mesosoma.** *Dorsal view*: Mesoscutum about as long as broad, 2.5 times as long as mesoscutellum. Transscutal line well–developed. Scutoscutellar sulcus shallowly impressed, formed by scrobiculate sculpture. Mesoscutellum sub–trapezoid, flat dorsally. Posterior face of propodeal declivity flat. Posterolateral margin of propodeal declivity slightly round to barely carinate, not forming crenulae. Anterodorsal median propodeal sulcus present, weakly impressed. **Wings**. Forewing venation: Rs–M approximately one fifth longer than 2M. Forewing evenly covered by fine setose layer. Hindwing venation: 1Rs highly reduced. Hindwing bearing 10–14 hamuli. **Petiole**. *Lateral view*: anterior and posterior margins of node nearly straight at base and slightly tapering at top. **Gaster.** *Dorsoposterior view*: Posterior dorsum of epipygium with feeble striations and punctae. **Color**. Appendages, including antennae and mandibles, mostly black. **Pilosity and sculpture**. Mostly as in worker (but see general synoptic description).

***Neoponera marginata* male diagnosis.** Antennal scape trapezoidal (Fig. 24e); mesoscutum dorsally with weakly impressed, median longitudinal line (Fig. 15a); median tooth on pretarsal claw well–developed; sternum of A8 with dorsoventrally depressed spine, with blunt (somewhat round) posterior tip.

Male description. Measurements (n = 2). HW: 1.51–1.75; HL: 1.73–1.9; EL: 0.69–0.76; SL: 0.35–0.38; WL: 3.52–4; PrW: 1.95–2.16; MsW: 1.7–1.9; MsL: 2.23–2.54; PW: 0.91–1.08; PH: 1.13–1.33; PL: 0.82–0.89; GL: 5.08–5.91; A3L: 1.26–1.46; A4L: 1.42–1.59; A3W: 1.57–1.9; A4W: 1.82–2.16; TLa: 8.74–9.84; TLr: 11.87–11.98; **Indices**. CI: 87.27–91.67; OI: 43.64–45.83; SI: 20–25; MsI: 75–76.06; LPI: 66.67–72.22; DPI: 111.54–121.43.

Head. *Frontal view*: Mandibular apex, when closed, barely touches lateral margin of labrum. PF: 6,4. Clypeus anteromedially straight to slightly concave, dorsally inflated, with somewhat globular-shaped dome, always covering anterior clypeal margin. Area between posterior margin of clypeus and supraclypeal area with evident depression. Posterior supraclypeal area acute. Supraclypeal area slightly protruding from cuticle, followed posteriorly by tenuously impressed longitudinal carina. Distance between internal margins of antennal sockets approximately one socket diameter. Torular lobe strongly reduced. Eye suboval, slightly notched medially, maximum diameter ca. one-third of head length, placed slightly anterior to cephalic mid–length. Ocellar area positioned at vertex. Distance from posterior ocellar margin to posterior margin of head close to two–thirds apical scape width. Distance between anterior and posterior ocelli approximately equal to 1.5 times anterior ocellus maximum length. Scape trapezoidal, twice as long as pedicel. **Mesosoma**. As in queen with the following differences: *Dorsal view*: Mesoscutum close to 2.5 times as long as mesoscutellum, anterior triangular impression vestigial, with faint median longitudinal line. Parapsidal lines weakly

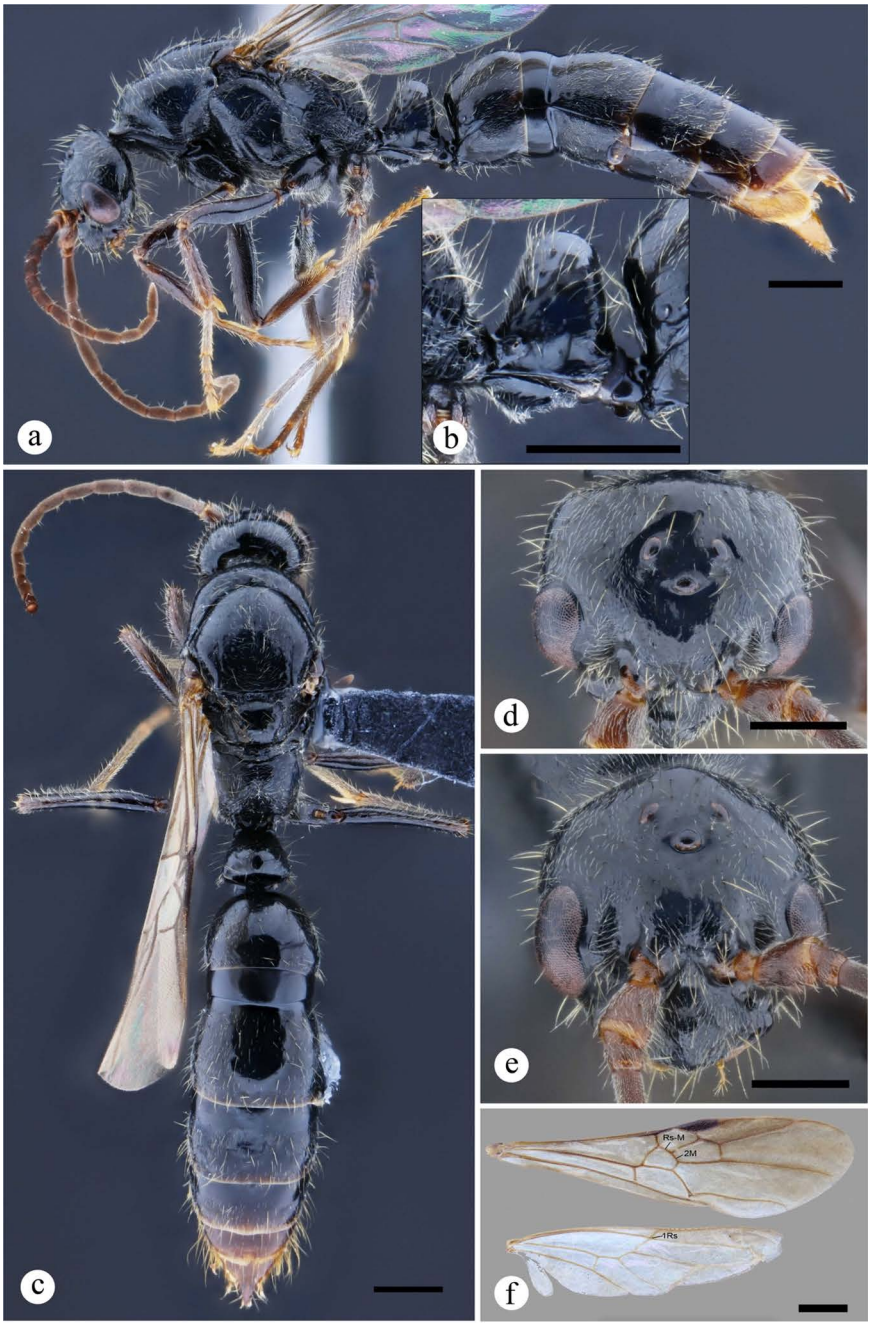

Fig. 24. *Neoponera marginata*. ♂ (DZUP: UFVLABECOL010414), Brazil, Minas Gerais. **a.** Lateral view; **b.** Petiole in lateral view; **c.** Dorsal view; **d.** Had in dorsal view; **e.** Head in frontal view; **f.** Fore and hind wings. Scale bars: 1 mm (**a**–**c**, **f**); 0.5 mm (**d**, **e**).

impressed, slightly divergent. Scutoscutellar sulcus slightly arched posterad. *Dorsolateral view*: Anterior subalar area shorter than tegular maximum width. Metanotum surface even, convex. Pheromone venting canal at metapleural gland opening poorly developed, striate. *Dorsoposterior view*: Metapleuropropodeal groove relatively shallow. Posterolateral margin of propodeal declivity slightly rounded, rugose midventrally. *Ventral view*: Probasisternal posterior projection round. Mesosternal process vestigial or absent. **Wings**. As in queen, except for Rs–M approximately as long as 2M. **Petiole.** *Lateral view*: anterior and posterior margins of node nearly straight at base and slightly tapering at top. Lateral projection of anteroventral nodal carina well–developed, with acute or slightly blunt tip moderately bent dorsad. *Dorsal view*: Anterior margin of petiolar node approximately four–fifths (0.8 times) shorter than width of posterior margin. *Lateral view*: Subpetiolar process subtriangular, with rounded cusp at middle of process, mostly smooth, though few striae may be present. **Gaster**. Morphology mostly as in worker and queen with the following differences: *Lateral view*: Abdominal sternum 7 showing even surface with no sulci, anterior half glabrous, posterior half with semicircular patch bearing abundant, appressed, stout hairs. Spine at posterior margin abdominal tergum 8 blunt, slightly flattened dorsoventrally. Pygostyles close to three times longer than broad. Ventral view: Abdominal sternum 9 roughly as long as broad. **Color**. Appendages, including antennae and mandibles, dark brown to black with slightly light brown tarsi. **Genitalia**. *Ventral view*: Cupula: posterior margin of medial invagination narrow. Lobular process vestigial. Basivolsella externally nearly straight. *Lateral view*: Gonopod subtriangular posterior half strongly directed ventrad, dorsolateral margin relatively straight medially, with medial, oblique, weak incision. Dorsal view: Gonopod subtriangular (subrectangular in lateral view). Gonostylus subacute apically, dorsointernal margin with rounded, tooth–shaped, swelling. Digitus spatulate, with outer margin round in ventral view. Penial sclerites overall outline axe–shaped, dorsal surface convex anteriorly, with an abrupt slope posteriorly. Dorsoapical third of penial sclerite surface with strong flap. **Sculpture**. Striae absent on head; axillula, metapleuron and lateral propodeal surface rugose; posterior and dorsopropodeal surface strongly striated; striae on petiolar node usually feeble and only posterolaterally.

Natural history notes. This is a relatively common, surface ground forager, termite feeding species (Wheeler 1936; Leal & Oliveira 1995; Hölldobler et al. 1996). The workers are usually collected through pitfall traps or by hand. Alate females and queens are much less commonly captured, unless searching for underground colonies. Males are quite rare, though they might be present in bulk Malaise samples. Due to their similarity to males of *N. mashpi* **sp. nov.**, and likely also to males of *N. laevigata* (which were not examined here), they can be misidentified as such. In warm morning hours the workers can be quite active around the nest entrance on the ground surface: while taking photos of them at a tourist trail, in Reserva Guartelá, southern Brazil, Adrian Troya observed ca. 10–20 workers removing soil particles from underground and piling them some 30 cm near the entrance. None of the ants showed aggressiveness when clearing part of the surrounding grass in order to get a clearer view, nor even when collecting some specimens.

Despite being comparatively easy to identify, and commonly collected in the field, most of what is known about the behavioral biology of *N. marginata* is basically summarized in three studies. In the first, Leal and Oliveira (1995) provided a comprehensive account on the group-raiding and migratory habits of this species in a semi-deciduous region of the state of São Paulo in southeastern Brazil. The authors recorded more than 200 raids, all of them directed against the termite species *Neocapritermes opacus* (Hagen). Within the *N. laevigata* group this "extreme diet specialization" has been documented only in this species, so far (but see Krishna & Araujo 1968; Mill 1982b). Leal and Oliveira (1995) also concluded that *N. marginata* shows a rudimentary form of the "army ant syndrome", with colonies relocating their nests less frequently than other group–raiding taxa, as for example, some Dorylinae. On the other hand, in regards to the communication system, Hölldobler et al. (1996) found that the pygidial gland of *N. marginata* produces Citronelal, the main monoterpenoid responsible for triggering trail-recruitment in ants. The third main contribution came from Acosta–Avalos et al. (1999) who found magnetic iron oxides in the head and gaster of *N. marginata* (but see also Wajnberg et al. 2017). Based on this result, they proposed that colonies of this species use the geomagnetic field during migrations, i.e., nest relocations. Two years later, Acosta-Avalos et al. (2001) linked that hypothesis to their observations of *N. marginata* colonies displaying a preferred directional migration which is deviated ca. 12° from the magnetic North–South axis.

Comments. Workers and queens of *N. marginata* are morphologically similar only to those of *N. gojira* **sp. nov.**, *N. mashpi* **sp. nov.**, and *N. laevigata*. These four lineages share traits like, for example, the relatively flattened eyes placed anterior to cephalic mid–length (Figs 20c, 21d, 22d, 23f, 25c, 26d); absence of malar carina; pronotal humerus feebly angled (not completely rounded as in *N. commutata*); a cuboid petiolar node, in lateral view; polymorphic workers, and presumably so in *N. gojira* **sp. nov.** for whom a single individual is known. However, *N. marginata* workers and queens are unique among these other lineages in showing a strongly carved, longitudinal groove on the inner side of the mandibular surface (absent in *N. mashpi* **sp. nov.** and *N. laevigata*, while *N. gojira* **sp. nov.** shows a shallow rim). Another useful feature, which helps identify queens of *N. marginata*, is its trapezoidal head which is broader posteriorly than anteriorly, in frontal view, though this character is more evident in the queens. The head in queens of *N. mashpi* **sp. nov.** and *N. laevigata* is subquadrate. In regards to known males, those of *N. marginata* could only be confused with those of *N. mashpi* **sp. nov.** The easiest way to distinguish both forms is using the following combination of traits: a feebly impressed, longitudinal line present medially on the mesoscutal dorsum (Fig. 15a), while in *N. mashpi* **sp. nov.** such line is absent; scape trapezoidal (Fig. 24e), whereas in *N. mashpi* ***sp. nov.*** it is cylindrical; pretarsal claws bearing subapical teeth, while those of *N. mashpi* **sp. nov.** lack teeth; blunt tipped spine on posterior margin of tergum of A8, while in *N. mashpi* **sp. nov.** the spine tip is acute. The male caste of *N. commutata* is quite dissimilar to that of *N. marginata* and *N. mashpi* **sp. nov.** Some unique features of the males in the *N. laevigata* group were already discussed under the treatment for that species, however, the user may also find the following useful: a roughly round head in frontal view (subquadrate in remaining species); dorsoposterior

propodeal margin strongly carinate (carina lacking in remaining species); forewing with glabrous subbasal and basal cells (setose in remaining species).

Distribution notes. Our records confirm an exclusively South American distribution for *N. marginata*, with an elevational range varying between 10 m to around 1700 m. Most of these records lie in the southern limit of its range represented mainly by three biomes: the southern Humid Chaco in Paraguay; the Atlantic Forest in Argentina (Misiones), northern Paraguay, and Brazil (Paraná and São Paulo); and the Cerrado in Brazil (Goias, Mato Grosso do Sul, São Paulo, Minas Gerais). Although highly anthropized (Ribeiro et al. 2009; Da Ponte et al. 2017) the remaining vegetation cover in these regions is mostly represented by ombrophyllous dense and open broadleaf forests, and tropical and subtropical grasslands, savannas, and shrublands (Sena-Souza et al. 2020). We found scant records of *N. marginata* in Amazonian regions, namely in northwestern Bolivia, western Brazil (Rondônia), and eastern Ecuador. The latter is the northwestern limit range for this species in the continent. However, as there are no large geographic barriers, e.g., mountain ranges, separating Amazonian regions between northern Ecuador and southern Colombia, we might expect *N. marginata* populations to be present at least in Colombian southern lowland rain forests. Mackay and Mackay (2010) list a record from the northeastern side of the continent, at Arima Reserve (voucher at the American Museum of Natural History), from the island of Trinidad, Trinidad and Tobago. The record of Wheeler (1936) from Churubamba (not 'Charubamba'), a Bolivian region in the Department of La Paz, is possibly wrong since its elevation surpasses 3400 m. This record is probably related to that from the same author (1925) from Ixiamas at 260 m (voucher at Natural History Museum Sweden), located in the same Bolivian Department.

As in *N. mashpi* **sp. nov.** and *N. laevigata*, *N. marginata* workers show gradual size polymorphism, though less marked than in the former two. Across its distribution range we did not notice major morphological variations in size, nor in coloration departing from the average ground plan of this species, as diagnosed here. Specimens from Bolivian Amazonian habitats were virtually identical to those examined from wet broadleaf forests in the Atlantic, and from the semi–dry grasslands and savannas in Paraná, southeast Brazil.

Material examined. 99☿, 5♀, 2♂: **ARGENTINA**: **Misiones**: Parque Nacional Iguazú, 25.6801°S, 54.4528°W, 180m, 2018–11–01, Troya, A., hand collected (MEPN), Parque Provincial Teyú Cuaré, 27.284°S, 55.594°W, 140m, 2015–01–20, Hanisch, P. (MACN), Reserva Natural Osonunu, 27.2797°S, 55.5702°W, 92m, 2015–01–19, Hanisch, P. (MACN). **BOLIVIA**: **Santa Cruz**: Las Gamas, P. N. Noel Kempff Mercado, 14.8°S, 60.3833°W, 700m, 1993–12–02, Ward, P. (PSWC). **BRAZIL**: **Distrito Federal**: IBGE Ecological Reserve, 15.932°S, 47.8997°W, 1031m, 2013–11–14, Rabeling, C. (MEPN); **Espirito Santo**: Reserva Biológica Santa Lucia, 19.95°S, 40.5333°W, 600m, 2018–11–18, Formigas do Brasil, hand collected (MPEG); **Goiás**: Br–364,Km 192 , 17.9242°S, 51.7171°W, 673m, 1997–09–29, Diniz, J., light trap (DZUP), Serranópolis, 18.3064°S, 51.9577°W, 743m, 2003–10–12, Diniz, J. (DZUP); **Mato Grosso**: Pontes e Lacerda, 15.2333°S, 59.3167°W, 292m, 2013–07–28, Queiroz–Santos, L. (DZUP), Universidade Federal de Mato Grosso, 15.9167°S, 52.2667°W,

352m, 2011–07–19, Oliveira, C. X., pitfall (DZUP), Utiarití, 13.0167°S, 58.2667°W, 325m, 1966–11–06, Lenko, K.; Pereira (MPEG); **Mato Grosso do Sul**: Fazenda Retiro Conc., 21.6833°S, 57.7667°W, 93m, 2012–03–08, Souza, P. R.; Morais, E., pitfall (DZUP), Parque Nacional da Serra da Bodoquena, 21.1°S, 56.6333°W, 556m,, Silvestre, R. et al. (CPDC); **Minas Gerais**: Araxa, 19.5833°S, 46.9333°W, 979m, 1965–11–14, Elias, C. (DZUP), Betim, 19.9668°S, 44.201°W, 845m, 1980–06–18 (DZUP), Caraça, 20.1333°S, 43.4833°W, 1674m, 1965–07–11, Moure, J. S. (DZUP), Convento Santa Isabel, 19.9565°S, 44.1615°W, 840m, 1981–01–10 (DZUP), Estação ao Buriti, 19.3386°S, 48.0332°W, 940m, 1983–11–21, Binda, hand collected (INPA), Mina Tamanduá, 20.0667°S, 43.9333°W, 1254m, 2012–07–12, Queiroz, et al., pitfall (DZUP), Ouro Preto, 20.3333°S, 43.75°W, 981m,, Moura, M. N.; et al. (DZUP), Santuário de Caraça, 20.0982°S, 43.488°W, 1287m, 2000–12–22, Frey, M (CPDC), Universidade Federal de Viçosa, 20.7623°S, 42.8605°W, 708m,, Noqueira, S. B. (DZUP), Universidade Federal de Viçosa, forest at the faculty of Biology, 20.7572°S, 42.8608°W, 706m, 2012–11–30, Chaul, J. (DZUP), Viçosa, 20.8167°S, 42.8833°W, 760m, 1995–10–19, Frenéav, D. (CPDC), 1994–02, Sperber, et al. (DZUP), Viçosa, 20.7474°S, 42.8833°W, 648m, 1995–10–19, Frenéav, D. (CPDC), 1994–02, Sperber, et al. (DZUP); **Paraná**: Jardim das Américas, 25.4333°S, 49.2333°W, 933m, 2016–04–01, Escárraga, M., hand collected (DZUP), Palmeira, 25.4167°S, 50°W, 865m, 2015–09–15, Franco, W. (DZUP), Parque Estadual do Cerrado , 24.1667°S, 49.6667°W, 780m, 2017–03–31, Ferreira, C.; et al. (DZUP), Parque Estadual do Guartelá, 30 Km W Piraí do Sul, 24.5667°S, 50.25°W, 981m, 2018–10, Troya, A., hand collected (MEPN), 2015–09–20, Franco et al., pitfall (DZUP), Parque Estadual do Guartelá, 30 Km W Piraí do Sul, 24.55°S, 50.25°W, 985m, 2018–10, Troya, A., hand collected (MEPN), 2015–09–20, Franco et al., pitfall (DZUP), São José dos Pinhais, 25.6°S, 49.1833°W, 880m, 2016–07–09, Domahovski, A. C., Malaise (DZUP), Universidade Federal do Paraná, Centro Politécnico, 25.4333°S, 49.2333°W, 916m, 2007–07–09, Ribeiro, A., hand collected (DZUP); **Rondônia**: Jaci Paraná, Rio Madeira, 9.54037°S, 64.3728°W, 85m, 2011–10–10, Santana, F. D. (CPDC); **São Paulo**: Bálsamo, 20.7341°S, 49.5836°W, 547m, 2003–02–04 (DZUP), Campus da USP, 21.1667°S, 47.8°W, 517m, 1998–09–10, Melo (DZUP), Guarulhos, 23.4532°S, 46.5337°W, 763m, (DZUP), Mirassol, 20.8161°S, 49.5042°W, 572m, 1977–12–12, Diniz, J. (DZUP), Reserva Santa Ginebra, 22.8275°S, 47.105°W, 623m, 1993–05, hand collected Rio Claro, 22.4145°S, 47.565°W, 615m, 2013–06–05, Melo, A. (CPDC). **PARAGUAY**: **Cordillera**: Caacupé, Jack Norment camp, 25.38°S, 57.15°W, 190m.

Geographic range. Argentina, Bolivia, Brazil, Ecuador, Paraguay, Trinidad and Tobago.

***Neoponera mashpi* sp. nov.**

ZooBank: https://zoobank.org/956C245D-24BB-46CE-865D-621CC07C009D
Figs 25: a–f (☿); 26: a–e (♀); 27: a–e (♂); genitalia 28: g–i, l (♂); 29: a (distribution).

Type material. ***Holotype.*** 1☿; **FRENCH GUIANA**: (**Sinnamary)**: Paracou, PS-02-3, (12km East from the village of Sinnamary), (5.2666°N, 52.9166°W), Abril–2002, J. Orivel (leg.), CPDC ant collection: ATPFOR2054–2. ***Paratypes***. 12☿, 2♀, 2♂; **BRAZIL**: **Amazonas**: Reserva Florestal Adolpho Ducke, INPA, 2.93333°S, 59.96666°W, 106m, 1999–07–29, Melo, G. (BMNH: 1☿, ATPFOR1985); 2.96304°S, 59.92286°W, 111m, 1987–09–14, fotoeclector, Souza, J. (INPA: 1☿, INPAHYM033803); **Bahia**: Porto Seguro, 16.44545°S, 39.06579°W, 3m, 1997–09–23, Malaise, Santos, J. R. M (CPDC: 1♂, ATPFOR2077); Refugio da Vida Silvestre do Una, 15.2323°S, 39.1151°W, 70m, 1999–10–04, Santos, J. R. S. (DZUP: 2☿, DZUP549512; **Pará**: Fazenda Vitoria, 2.98345°S, 47.34994°W, 82m, 1991–12–21, Moutinho, P. (ICN: 1☿, ATPFOR2029); Floresta Nacional Caxiuana, 1.716667°S, 51.45000°W, 32m, 1998–03–24, Malaise, Silveira, O., Pena, J. (MPEG: 1☿, MPEG03006223); 1.73333°S, 51.45000°W, 21m, 2012–09, ex pitfall, Cunha, D. et al. (CASC: 1 ☿, MPEG03020126); **Rio Grande do Norte**: Tabatinga 6.06753°S, 35.10311°W, 12m, 2005–09, Martins, J. (MHNG: 1☿, ATPFOR2010); **Rondônia**: Area Caiçara, 9.433110°S, 64.80237°W, 103m, 2011–01–04, winkler, Silva, R., Probst, R. (MPEG: 1☿, AT2206). **COLOMBIA**: **Putumayo**: Parque Nacional Natural La Playa, 0.11667°S, –74.93333°W, 320m, 2001–05–14, Cobete, R. (IAvH: 1☿, IAVH–E–49610). **ECUADOR**: **Orellana**: Tiputini Biodiversity Station, 0.63333°S, 76.15°W, 236m, 2011–12–11, Donnell, S. O. (MCZC: 1☿, DZUP549443), **Pichincha**: Reserva de Biodiversidad Mashpi, 50 Km NW Quito, 0.1544°N, 78.8905°W, 746m, 2017–04, hand collected, Troya, A. (MEPN: 1☿, MEPNINV38315). **FRENCH GUIANA**: **Cayenne**: Nouragues Natural Reserve, 1km E of Nouragues Station, Grand Plateau, 4.0889°N, 52.6749°W, 120m, 2018–08–21, (USNM: 1☿, ATPFOR1976); Sinnamary, 12km East from the village of Sinnamary, Paracou Station, 5.26667°N, 52.91667°W, 50m, 2002–04, Orivel, J. (CPDC: 1♀, ATPFOR2054; MZSP: 1☿, ATPFOR2054–1). **PERU**: **Madre de Dios**: Sachavacayoc camp, 12.81667°S, 69.36667°W, 229m, 2012–07–26, Fernandes, I. (INPA:1♀, INPAHYM033802).

Etymology. The name is derived from the Kichwa word 'mash' meaning 'friend', and 'pi', from the ancient Yumbo people, meaning 'water'. We thus acknowledge the Reserva de Biodiversidad Mashpi, as well as its supporters, in northwestern Ecuador (where one of the paratypes was found), for their efforts in the preservation of one of the last remnants of a highly threatened and diverse tropical Andean forest in the Chocó-Darien Global Ecoregion. The species name is a noun in apposition, thus invariable.

Worker and queen diagnosis. Antennal scape, in smallest workers (WL= 1.66 mm) and queens, when pulled back, fails to reach posterior margin of head by about one apical scape width (Figs 13a, 25c, 26d), whereas the scape of largest workers (WL = 3.31 mm) usually reaches such head margin, but never surpasses it; head mostly smooth in workers only (Fig. 25c), while in queens the head dorsum shows feeble, divergent striae at posterior limits of frontal carina and posteriorly to eye, these striae vanish before reaching lateral head margin (Fig. 26d); anterior margin of petiole usually narrower than posterior margin in dorsal view (Figs 25b, 26c); lateral face of petiolar node

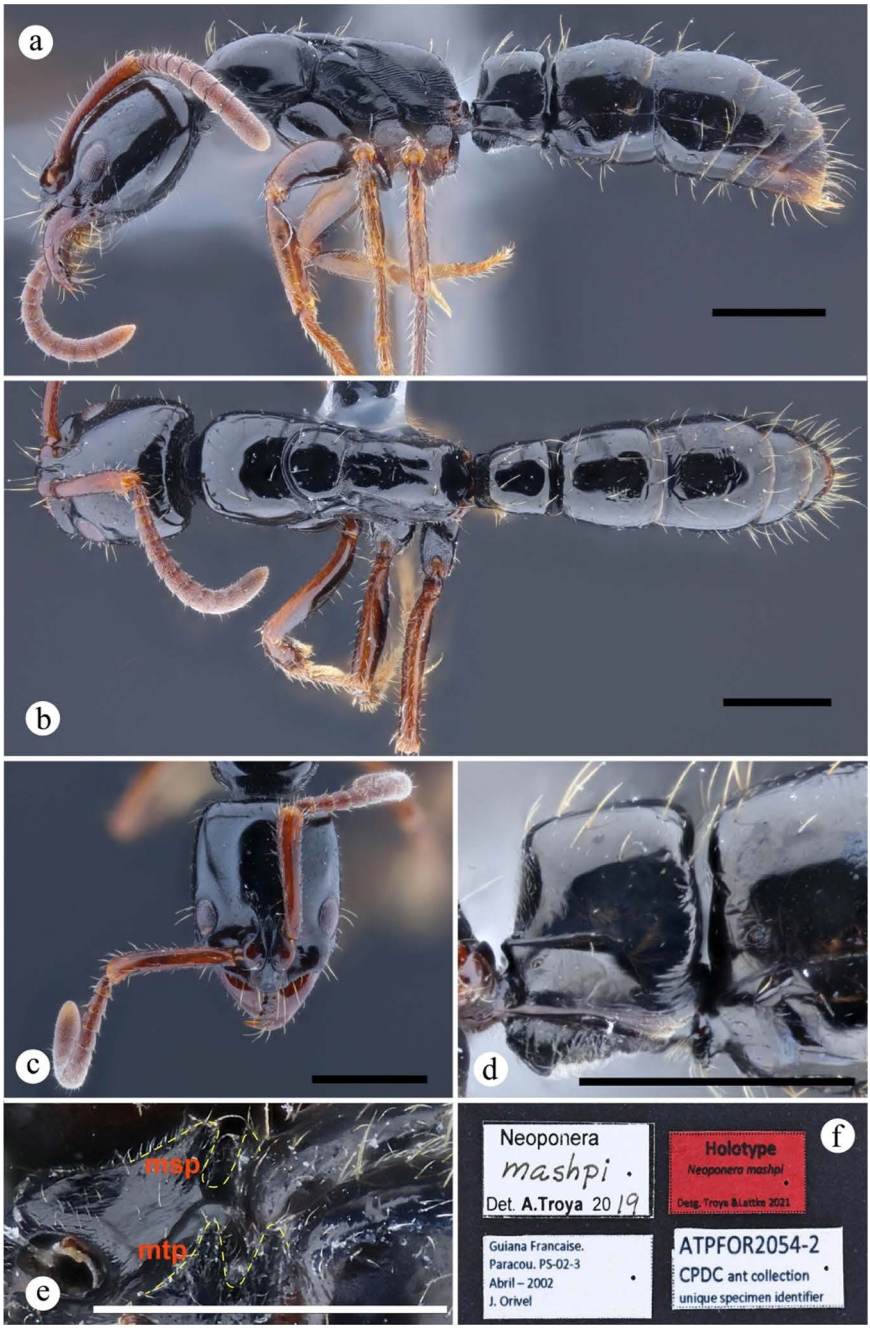

Fig. 25. *Neoponera mashpi* **sp. nov.** Holotype ☿ (CPDC: ATPFOR2054–2), French Guiana, Paracou. **a.** Lateral view; **b.** Dorsal view; **c.** Head in frontal view; **d.** Petiole in lateral view; **e.** Mesosternal (msp) and metasternal (mtp) processes (dashed yellow line) in posteroventral view. Scales bars: 1 mm (**a**–**d**); 0.6 mm (**e**).

completely lacking striae (Figs 25d, 26b), this is mostly seen in South American and Pacific Central American populations, while in Atlantic Central American populations the node bears slight striae laterally; subpetiolar process subtriangular with anterior acute cusp, in lateral view (Fig. 25d); prora with blunt, well–developed tip projecting ventrad (Figs 25d, 26b); workers of this species are the smallest within the *N. laevigata* group (WL = 1.66–3.31 mm), and among the smallest in *Neoponera*.

Worker description. Measurements (*n* = 21; holotype in parenthesis): HW: 0.88–1.84 (1.43); HL: 1.19–2.2 (1.8); EL: 0.25–0.53 (0.41); SL: 0.75–1.71 (1.22); WL: 1.66–3.31 (2.57); PrW: 0.66–1.22 (1.1); MsW: 0.38–0.88 (0.65); MsL: 0.3–0.78 (0.57); PW: 0.31–1.04 (0.73); PH: 0.53–1.03 (0.82); PL: 0.5–0.92 (0.73); GL: 1.72–3.76 (2.78); A3L: 0.56–1.22 (0.98); A4L: 0.69–1.39 (1.1); A3W: 0.59–1.57 (1.1); A4W: 0.67–1.71 (1.18); TLa: 4.67–9.02 (7.18); TLr: 5.2–9.84 (7.88). **Indices.** CI: 72.22–83.7 (79.55); OI: 27.78–30.77 (28.57); SI: 84.21–94.51 (85.71); MsI: 104.35–133.33 (114.29); LPI: 69.7–105.88 (90); DPI: 59.39–117.95 (100).

Head. *Frontal view*: Subrectangular. Masticatory margin of mandible with four to five large teeth interspersed with three to four denticles, basal margin edentate. Prementum with clear transverse dome. Labral dorsum mostly smooth. Torular lobe posterolateral margin rounded. Malar carina absent, though swelling is present. Eye convex, relatively flat, not surpassing lateral margin of head, placed anterior to cephalic mid-length. Posterior margin of head straight to slightly convex. Occipital carina absent. **Mesosoma**. Lateral view: Pronotum with weak, blunt, barely distinguishable humeral carina. Metanotal groove present, though not depressed, usually clearly separating mesonotum and propodeum. Anapleural sulcus present, though usually merged with surrounding striae. Posterior face of propodeal declivity mostly flat. Posterolateral margin of propodeal declivity with feeble, blunt carina, sometimes with crenulae. Propodeal lateral margins subparallel in posterodorsal view. Ventrolateral propodeal declivity with deep transverse groove just dorsad to metapleural gland opening. Probasisternal posterior projection acute. Metasternal process inclined posterad, 20°–30° in lateral view. **Petiole**. *Lateral view*: anterior and posterior margins of node usually nearly straight and semiparallel, sometimes posterior margin slightly convex; posterodorsal margin slightly higher than anterodorsal margin; mid–dorsal margin mostly flat. Lateral projection of anteroventral nodal carina well–developed, with acute or slightly blunt tip usually projecting anterad. *Dorsal view*: Anterior margin of petiolar node slightly shorter than width of posterior margin. Anteroventral nodal carina complete. *Lateral view*: Subpetiolar process subtriangular, with acute anterior cusp, sometimes keel–shaped, followed by posterior straight slope (ca. 30°). **Gaster**. *Lateral view*: Prora well–developed, with blunt tip projecting ventrad. Meeting of anterior margin of A3 tergum with its dorsal margin relatively angled. Cinctus moderate. *Dorsal view*: Tergum of A3 slightly shorter than A4. Posterior dorsum of epipygium smooth, though feeble striations and punctae may be present. **Legs**. Mesofemur thickened medially, thicker than metafemur, in dorsal or ventral view. Ventral surface of meso– and metafemora flattened roughly on distal two–thirds, usually bearing longitudinal shallow groove. **Color**. Appendages including antennae and mandibles brown to ferruginous brown, occasionally legs yellowish and mandibles lighter than remaining integument of body.

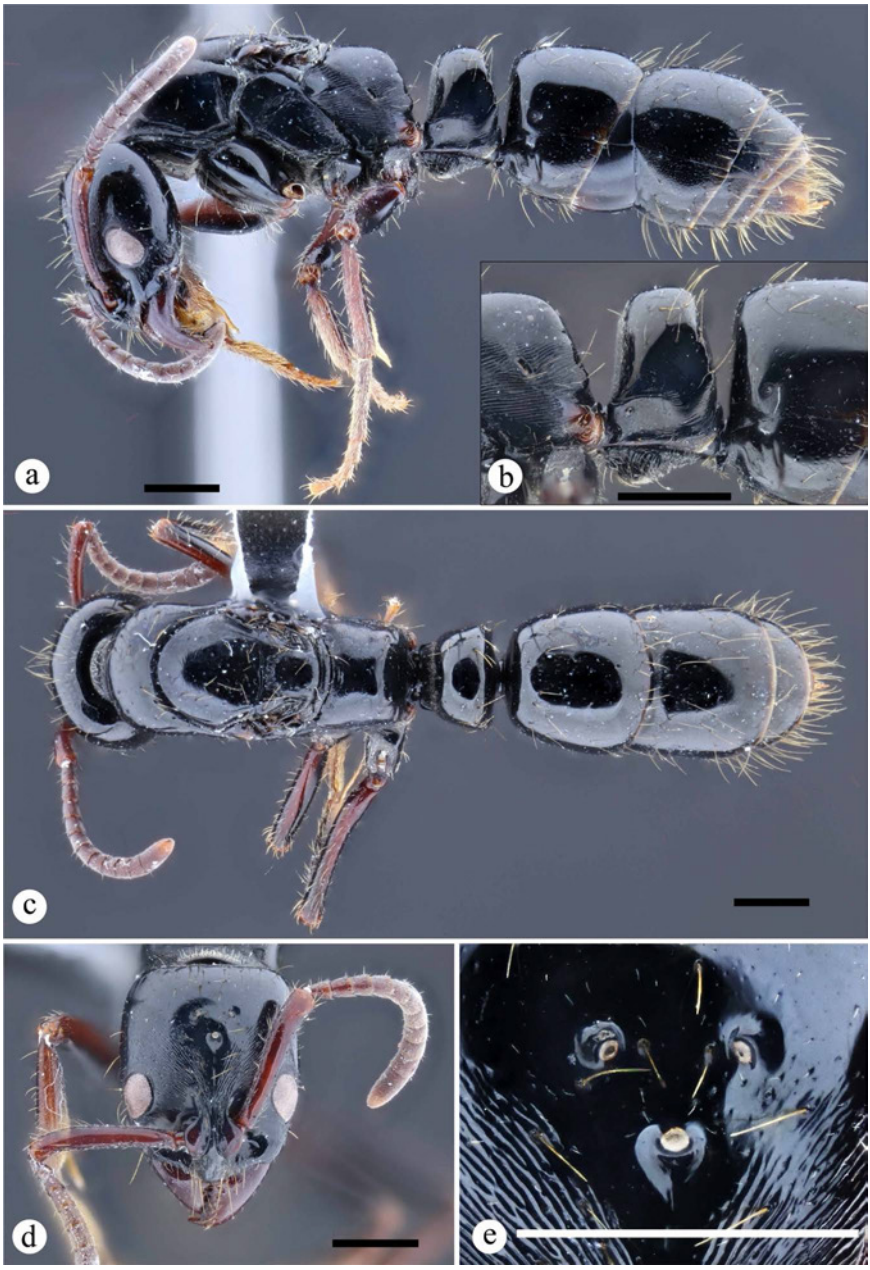

Fig. 26. *Neoponera mashpi* **sp. nov.** Paratype ♀ (CPDC: ATPFOR2054), French Guiana, Paracou. **a.** Lateral view; **b.** Petiole in lateral view; **c.** Lateral view; **d.** Head in frontal view; **e.** Ocelli in frontal view. Scale bars: 1 mm (**a**–**d**); 0.5 mm (**e**).

Pilosity. Most erect hairs approximately same length as eye maximum length. Scape hairs about as long as apical scape width. Posterior dorsum of epipygium surrounded by ca. 20, long flexuous hairs. Meso– and metatarsi bearing abundant spines and stiff

setae interspersed with abundant suberect hairs. **Sculpture**. Striae on head generally absent, though when present, very feeble and on dorsum only, laterally on clypeus, around frontal carinae, and malar area; anepisternum, metapleuron and lateral side of propodeum with strong striae; petiolar node usually devoid of striae, though when present feebly impressed on lateral face (but see diagnosis and comments).

Queen description. Measurements (*n* = 2): HW: 1.96–2.14; HL: 2.29–2.55; EL: 0.61–0.64; SL: 1.47–1.73; WL: 3.67–4.08; PrW: 1.63–1.84; MsW: 1.22–1.63; MsL: 1.98–2.22; PW: 1.17–1.18; PH: 1.43–1.48; PL: 0.98–1.07; GL: 4.29–4.34; A3L: 1.31–1.79; A4L: 1.39–1.73; A3W: 1.47–2.04; A4W: 1.55–2.14; TLa: 9.63–11.22; TLr: 11.23–12.04. **Indices.** CI: 84–85.71; OI: 29.76–31.25; SI: 75–80.95; MsI: 61.86–73.56; LPI: 68.57–72.41; DPI: 109.52–120.83.

Morphology as in worker except for: **Head**. *Frontal view*: Anterior ocellus maximum diameter subequal to that of posterior ocelli. Distance from posterior ocellar margin to posterior margin of head close to twice apical scape width. Distance between anterior and posterior ocelli close to 2.5 times anterior ocellus diameter. **Mesosoma**. *Dorsal view*: Mesoscutum about as long as broad, close to 2.5 times as long as mesoscutellum. Transscutal line well–developed. Scutoscutellar sulcus shallowly impressed, formed by scrobiculate sculpture. Mesoscutellum subquadrate, flat dorsally. Posterior face of propodeal declivity flat. Posterolateral margin of propodeal declivity slightly rounded to barely carinate, not forming crenulae. Anterodorsal median propodeal sulcus present, weakly impressed. *Ventral view*: Mesosternal process with internal margins slightly divergent. **Wings**. Unknown. **Petiole**. *Lateral view*: anterior and posterior margins of node nearly straight at base and slightly tapering dorsad. Lateral projection of anteroventral nodal carina slightly acute and moderately bent dorsad. **Color**. Appendages, including antennae and mandibles, dark brown to black. **Sculpture**. Striae on head present only dorsally, covering most of surface except posterior third; strong striae on posterolateral margin of pronotum, usually anepisternum and part of katepisternum, axillula, metapectus, and laterally on propodeum; petiolar node lacking striae, (see also general synoptic description).

Male diagnosis. Antennal scape cylindrical (Fig. 27d); mesoscutum lacking median longitudinal line (Fig. 15b); mesosternal process absent; forewing vein Rs–M feebly longer than 2M (Fig. 27f); hindwing with vein 1Rs incomplete or poorly developed (Fig. 27f); pretarsal claw arched, unarmed (without accessory teeth).

Male description. Measurements (*n* = 2): HW: 1.13–1.16; HL: 1.32–1.38; EL: 0.63–0.63; SL: 0.22–0.25; WL: 2.89–2.89; PrW: 1.26–1.45; MsW: 1.2–1.26; MsL: 1.76–1.76; PW: 0.75–0.75; PH: 0.88–0.94; PL: 0.69–0.75; GL: 4.4–4.53; A3L: 0.94–1.01; A4L: 1.2–1.29; A3W: 1.13–1.2; A4W: 1.32–1.42; TLa: 7.04–7.33; TLr: 9.31–9.56; **Indices**. CI: 81.82–88.1; OI: 54.05–55.56; SI: 18.92–22.22; MsI: 67.86–71.43; LPI: 78.57–80; DPI: 100–109.09.

Head. *Frontal view*: Mandibular apex, when closed, barely touches lateral margin of labrum. Prementum with clear transverse dome. PF: 6,4. Labral dorsum mostly smooth. Clypeus anteromedially straight to slightly concave, with weak dorsal dome, feebly swelling from cuticle and covering anterior clypeal margin. Area between posterior margin of clypeus and supraclypeal area with evident depression. Posterior

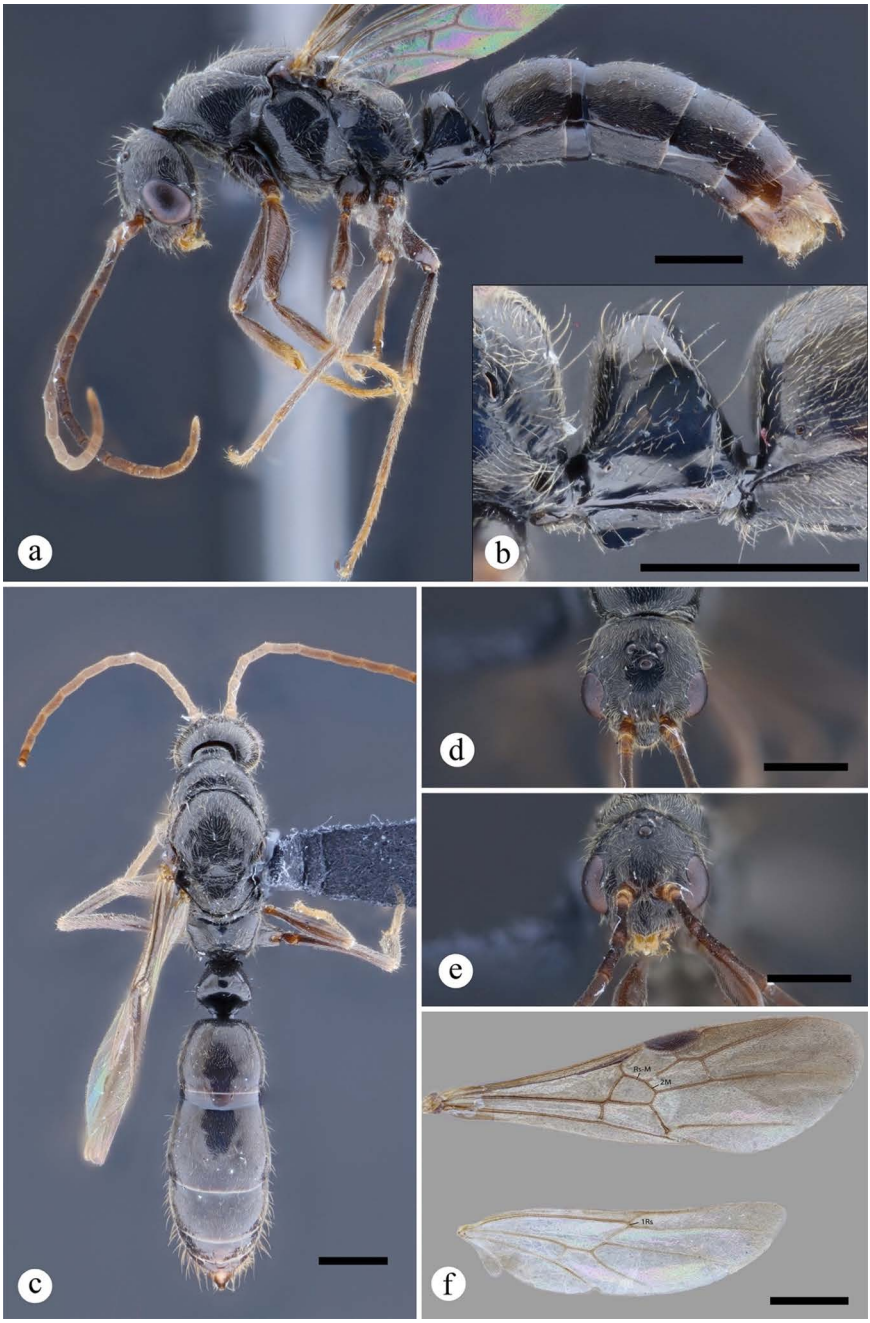

Fig. 27. *Neoponera mashpi* **sp. nov.** Paratype ♂ (CPDC: ATPFOR2077), Brazil, Bahia. **a.** Lateral view; **b.** Petiole in lateral view; **c.** Dorsal view; **d.** Head in dorsal view; **e.** Head in frontal view; **e.** Fore and hind wings. Scale bars: 1 mm.

supraclypeal area acute. Supraclypeal area slightly protruding from cuticule, followed posteriorly by tenuously impressed longitudinal carina. Distance between internal margins of antennal sockets less than one socket diameter. Torular lobe strongly reduced. Eye suboval, slightly notched medially, maximum diameter slightly less than half head length, placed slightly anterior to cephalic mid–length. Ocellar area positioned at vertex. Distance from posterior ocellar margin to posterior margin of head close to twice apical scape width. Distance between anterior and posterior ocelli varying between 1–1.5 times anterior ocellus maximum length. Scape cylindrical, one third longer than pedicel. **Mesosoma**. *Dorsal view*: Mesoscutum close to 3 times as long as mesoscutellum, anterior triangular impression weakly impressed, median longitudinal line absent. Parapsidal lines weakly impressed, slightly divergent. Scutoscutellar sulcus straight. Anterior subalar area shorter than tegular maximum width. Metanotum surface even, slightly flat. Metapleuropropodeal groove relatively shallow. Posterior face of propodeal declivity mostly flat. Anterodorsal median propodeal sulcus present, weakly impressed. *Lateral view*: Posterolateral margin of propodeal declivity slightly rounded to barely carinate, not forming crenulae. Pheromone venting canal at metapleural gland opening poorly developed, sightly striated. *Ventral view*: Probasisternal posterior projection acute. Mesosternal process vestigial. Metasternal process as in worker and queen. **Wings**. Forewing venation: Rs–M slightly longer than 2M. Forewing evenly covered by fine setose layer. Hindwing venation: 1Rs present, very short though. Hindwing bearing 8–10 hamuli. **Petiole**. *Lateral view*: anterior and posterior margins of node nearly straight at base and slightly tapering dorsad; dorsal margin convex. Lateral projection of anteroventral nodal carina well–developed, with acute or slightly blunt tip feebly projecting anterodorsad. *Dorsal view*: Anterior margin of petiolar node approximately two–thirds shorter than width of posterior margin. *Lateral view*: Subpetiolar process subtriangular, with rounded anterior cusp, followed by posterior straight slope (ca. 30°), with two slightly divergent longitudinal carinae separated by groove. **Gaster**. *Lateral view*: Meeting of anterior A3 margin with dorsal margin relatively angled. Cinctus moderate. Pygostyles close to three times longer than broad. *Dorsal view*: Tergum of A3 shorter than A4. *Ventral view*: Abdominal sternum 7 showing even surface with no ditches, anterior half glabrous, posterior half with semicircular patch bearing abundant, appressed, stout hairs. Spine at posterior margin of tergum of A8 acute, semitubular (not dorsoventrally flattened). Abdominal sternum 9 roughly as long as broad. **Legs**. Mesofemur thickened medially, thicker than metafemur, in dorsal or ventral view. Ventral surface of meso– and metafemora flattened roughly on distal two–thirds, surface even, without groove. **Genitalia**. *Ventral view*: Cupula: posterior margin of medial invagination narrow. Lobular process vestigial. Gonopod dorsally subtriangular, subrectangular in lateral view, with subtriangular posterior half strongly directed ventrad, dorsolateral margin relatively straight medially, with medial, oblique, weak incision. Gonostylus subacute apically, dorsointernal margin with rounded, tooth–shaped, swelling. Basivolsella externally nearly straight. Digitus spatulate, with outer margin round in ventral view. Penial sclerites overall outline axe–shaped, dorsally broadly round. Dorsoapical third of penial sclerite surface with strong flap. **Color**. Appendages including antennae and mandibles brown to ferruginous

brown, occasionally legs yellowish and mandibles lighter than remaining integument of body. **Sculpture**. Striae absent on head, axillula, metapleuron and lateral propodeal surface slightly rugose, on petiolar node usually absent, though when present, feebly impressed on lateral face.

Natural history notes. *Neoponera mashpi* **sp. nov.** has been collected mostly by hand and Malaise trapping. The elevation records vary from 3 to 746 m, being this species mostly found in preserved mature habitats from lowland and pre–montane rain forests in Central America, to Andean mountainous and Pacific lowland forests from the Chocó–Darien, to dense and open Amazonian and Atlantic ombrophyllous forests in South America. J. Longino (1999) observed this species raiding on unidentified termites in Costa Rica; he also briefly described a possible colony relocation of about 1400 to 1800 workers moving out from an underground nest into the remains of a termite nest, and over its entrance he noted a hovering cloud of unidentified fungus gnats. Adrian Troya observed a few foraging individuals approaching an unidentified termite nest built inside a fallen log in a tropical Andean cloud forest (Reserva de Biodiversidad Mashpi), northwestern Ecuador, the ant colony was located near their potential prey source some 5 m away.

Virtually all published observations on behavioral biology made by previous authors in the island of Barro Colorado (BCI), Panama, which have been attributed to *N. laevigata*, probably correspond to *N. mashpi* **sp. nov.**: Wheeler (1936): colony activity and diet (termite predation); Borgmeier (1959): diet (termite predation); Downing (1978): foraging and migratory behavior; Hölldobler and Traniello (1980): pheromone recruitment communication; Traniello (1981): behavior against termite deterrence; Longino (1999): foraging and migratory behavior; Mackay and Mackay (2010): sporadic gyne and male collections. Although we could not find vouchers from that specific Central American site, we did examine specimens of *N. mashpi* **sp. nov.** from the Panamanian regions of Coclé and Colón, which are in relative proximity to BCI.

Comments. *Neoponera mashpi* ***sp. nov.*** can only be confused with two species in the *N. laevigata* group: *N. laevigata* and *N. gojira* **sp. nov.** The remaining species, *N. commutata* and *N. marginata* are clearly different, with the worker caste in the former being much larger (WL = 5.59–5.68 mm), whereas the latter shows a strongly excavated dorsal groove on the mandible, in frontal view (Fig. 12a), this groove is absent in *N. mashpi* **sp. nov.** The following features facilitate separating *N. mashpi* **sp. nov.** from *N. laevigata* and *N. gojira* **sp. nov.** in the worker caste: when compared to the first, the scape is smaller, when pulled back it does not reach the posterior head margin by at least one apical scape width, this is usual in the smallest workers and queens, but see also diagnosis (Fig. 6a), while in *N. laevigata* the scape always surpasses said margin by close to one apical scape width (Fig. 6b); the lateral nodal face is smooth (Figs 25d, 26b), while that of *N. laevigata* always bears oblique striae. However, *N. mashpi* **sp. nov.** populations from Central American Atlantic forests may also show nodal striations laterally (see distribution notes below), though less strongly impressed than in *N. laevigata*. The subpetiolar process is subtriangular with an acute anterior cusp, in lateral view (Fig. 25d), in *N. laevigata* the subpetiolar process is also subtriangular but with an anterior keel–shaped cusp, followed posteriorly by a relatively flat or slightly concave

surface (Fig. 13d); prora well-developed (Fig. 15d), while in *N. laevigata* the prora is either absent or shaped as a tiny cuticular lip (Fig. 13d). Workers of *N. mashpi* **sp. nov.** differ from *N. gojira* **sp. nov.** in the following features: dorsal masticatory mandibular surface smooth, with few shallow piligerous fossulae medially (Fig. 12c), in *N. gojira* **sp. nov.** this region has a distinct longitudinal rim with piligerous foveae and longitudinal striae medially, Fig. 12b); flap at metapleural gland opening well–developed and strongly curved anterad so that the orifice of the gland is barely visible in posterolateral view (Fig. 2a), while in *N. gojira* **sp. nov.** the flap is reduced to a narrow, poorly discernible, blunt carina, leaving the gland orifice completely visible in posterolateral view, Fig. 2d; prora well–developed, while in *N. gojira* **sp. nov.** the prora is tiny and lip-shaped, Fig. 19e); clearly smaller (WL = 1.66–3.31 mm), whereas the holotype of *N. gojira* **sp. nov.** is the largest worker of the *N. laevigata* group (WL = 3.72 mm); the area of the pheromone venting canal at the metapleural gland opening in lateral view (Fig. 2a) is clearly less impressed than in *N. gojira* **sp. nov.** (Fig. 2d).

The queen: in *N. mashpi* **sp. nov.** the queen is smaller (WL = 3.67–4.08 mm) than that of *N. laevigata* (WL = 4.70–4.95), the ocelli are also smaller: ca. 0.085 mm vs ca. 0.14 mm. The scape in *N. mashpi* **sp. nov.**, when pulled back, fails to reach posterior head margin, whereas in *N. laevigata* the scape always surpasses said margin by approximately one apical scape width. The petiolar node of the currently known queens of *N. mashpi* **sp. nov.** is completely devoid of striae, while in *N. laevigata* those striae are always strongly impressed and present laterally on the nodal face. The queen of *N. gojira* **sp. nov.** is unknown.

The male: we only found two specimens of *N. mashpi* **sp. nov.** from the Brazilian Amazon, both bearing a well-developed prora which is one of the diagnostic features for the worker, and according to our observations of the current set of specimens in the *N. laevigata* group, the form and size of this structure is relatively conserved among all castes in each species. These males are virtually identical to the specimen identified as "*Pachycondyla*" *laevigata* by W. Mackay from the Pacific side of Costa Rica, Estación Pitilla (AntWeb record: INBIOCRI001099170, image examined). The Brazilian specimens slightly differ from this Costa Rican specimen in the following: outline of head feebly straight posterad to eyes (rounded in INBIOCRI001099170), and propodeal posterolateral surface more striated than in INBIOCRI001099170. Populations of *N. mashpi* **sp. nov.** from the Pacific regions of Central America do not show lateral nodal striae as is the case for INBIOCRI001099170. Thus, we can assign (for now) this Costa Rican male to *N. mashpi* **sp. nov.** Since the males of *N. commutata* greatly differ from the other known males examined in this study, e.g., in bearing torular lobes (absent in remaining known species), those of *N. mashpi* **sp. nov.** can only be confused with the males of *N. marginata*. Among other features, these two species can be distinguished mainly by the presence of a median longitudinal line (but can also be seen as a shallow groove) on the mesoscutum of *N. marginata* (absent in *N. mashpi* **sp. nov.**), and by the spine on the tergum of A8 being dorsoventrally depressed and with blunt posterior tip in *N. marginata* (conical and acute posteriorly in *N. mashpi* **sp. nov.**).

Neoponera mashpi **sp. nov.** is very similar to *N. laevigata* and since both occur in sympatry in several ecoregions, mostly in South America (Fig. 29a), they could well

be sister lineages as suggested by preliminary molecular analyses (Troya et al. unpubl. data). Additional insights from future studies, for example through population genetics, may potentially evidence a recent divergence. Some of the differential characters presented above, for example, the shape of the subpetiolar process in workers and queens, show certain degree of continuous variation in some examined populations (see distribution notes below). This may cause difficulty in its separation from correspondent castes of *N. laevigata*, however we consider these variations within the taxonomic limits of *N. mashpi* **sp. nov.** In prior treatments of the *N. laevigata* group, Wheeler (1936) and Mackay and Mackay (2010), these two forms were treated as a single species. The work of Wheeler partially depicts our definition of *N. laevigata*, nevertheless, the two workers illustrated in his plates (p. 161) show a developed, ventrally directed prora which we consider diagnostic for *N. mashpi* **sp. nov.** We assume that the specimens on which Wheeler (1936) based his descriptions were a mixture of both *N. mashpi* **sp. nov.** and *N. laevigata*. Mackay and Mackay (2010), on the other hand, represent in their descriptions mostly the morphology of *N. mashpi* **sp. nov.**, although without providing details on the prora, subpetiolar process, and the flap of the metapleural gland opening, the first two being key diagnostic characters.

Distribution notes. Populations of the Atlantic forests of Central America: Panama, Costa Rica, up to southern Nicaragua, show very tenuous to clear petiolar node striae, though not as strongly impressed as in the Amazonian populations of its known closest species, *N. laevigata*. The remaining examined populations of *N. mashpi* **sp. nov.**, including those from the Pacific forests of Costa Rica, south to Amazonia and the Atlantic forests of Brazil (Bahia), lack these striae. This gradual variation in sculpture, i.e., well-impressed striae turning into smooth surfaces, from South American regions north to Central America, has been observed in other ant groups as well (J. Longino, pers. comm.). Despite that, our observations on this trait do not support or suggest a lineage split between Central American and South American populations, though they could represent ongoing hybridization between both species.

Populations of *N. mashpi* **sp. nov.** and *N. laevigata*, are distributed in sympatry in several Amazonian and Chocó–Darien sites. Our current specimen set supports a Central American distribution up to northern Costa Rica only for *N. mashpi* **sp. nov.**, whereas *N. laevigata* populations reach up to the mid–western tropical regions of the Cordillera Occidental, up to approximately the Golfo de Cupica in the Chocó–Darien of Colombia. *N. mashpi* **sp. nov.** shows a broader range in South America, reaching the Atlantic Forest in northeast Brazil (Rio Grande do Norte and Minas Gerais), to the southern Peruvian Amazon.

Except for the petiolar node striae present in Central American *N. mashpi* **sp. nov.**, the diagnostic traits of this species are relatively stable across examined specimens from Amazonian and Atlantic forests. Costa Rican records from Guanacaste, to the northwestern Pacific, represent the northernmost distribution range of this species. Thus far no records of any species in the *N. laevigata* group have been found north of southern Nicaragua (J. Longino, pers. comm.), with the Hess Escarpment potentially acting as a biogeographic barrier not only for this group but for other biota as well (see Mendoza et al. 2019).

Other material examined. 67♀, 9♀, 4♂: **BRAZIL**: **Amapá**: Parque Nacional Montanhas do Tumucumaque , 1.61667°N, 52.4833°W, 150m, 2017–07–25, Feitosa, R.; et al. (DZUP); **Amazonas**: Reserva Florestal Adolpho Ducke, Instituto Nacional de Pesquisas da Amazônia (INPA), 2.96304°S, 59.9229°W, 111m, 1987–09–14, Souza, J., fotoecletor (INPA), 1999–07–29, Melo, G. (DZUP), Reserva Florestal Adolpho Ducke, Instituto Nacional de Pesquisas da Amazônia (INPA), 2.93333°S, 59.9667°W, 106m, 1987–09–14, Souza, J., fotoecletor (INPA), 1999–07–29, Melo, G. (DZUP), Reserva Florestal Adolpho Ducke, Instituto Nacional de Pesquisas da Amazônia (INPA), 2.93333°S, 59.9667°W, 106m, 1987–09–14, Souza, J., fotoecletor (INPA), 1999–07–29, Melo, G. (DZUP), Reserva Florestal ZF3, Km 27, 2.41667°S, 59.8°W, 118m, 1981–08–08, Harada, A. (INPA); **Bahia**: Itororó, 15.1158°S, 40.0646°W, 600m, 2001–10–04, Santos, J. R. M (CPDC), Japu, Fazenda Duas Barras, 14.8832°S, 39.1933°W, 130m, 1988–11–27, hand collected (DZUP), Porto Seguro, 16.4455°S, 39.0658°W, 3m, 1997–09–23, Santos, J. R. M, Malaise (CPDC), Refugio da Vida Silvestre do Una, 15.2323°S, 39.1151°W, 70m, 1999–10–04, Santos, J. R. S. (DZUP); **Pará**: Fazenda Vitória, 2.98345°S, 47.3499°W, 82m, 1991–12–21, Moutinho, P. (ICN), Floresta Nacional Caxiuanã, 1.73333°S, 51.45°W, 21m, 1998–03–24, Silveira, O.; Pena, J., Malaise (MPEG), 2012–09, Cunha, D. et al., pitfall (MPEG), Floresta Nacional Caxiuanã, 1.71667°S, 51.45°W, 32m, 1998–03–24, Silveira, O.; Pena, J., Malaise (MPEG), 2012–09, Cunha, D. et al., pitfall (MPEG); **Rio Grande do Norte**: Tabatinga, 6.06753°S, 35.1031°W, 12m, 2005–09, Martins, J. (DZUP); **Rondônia**: Area Caiçara, 9.43311°S, 64.8024°W, 103m, 2011–01–04, Silva, R.; Probst, R., Winkler (MPEG). **COLOMBIA**: **Chocó**: Aruzi, 5.56668°N, 77.4667°W, 49m, 1998–11–25, Jimenez, E., hand collected (MUSENUV); **Putumayo**: Parque Nacional Natural La Playa, Cabaña Viviano, 0.116667°N, 74.9333°W, 320m, 2002–05–14, Cobete, R., pitfall (IAvH); **Valle del Cauca**: Darien, 3.93371°N, 76.6833°W, 545m, 1994–07–15, Aldana, R., Winkler (MUSENUV). **COSTA RICA**: **Guanacaste**: Estación Pitilla, 9 Km S Santa Cecilia., 10.9926°N, 85.4295°W, 700m, 1989–12–01, C. Moraga & P. Rios (INBio); **Heredia**: 11km SE La Virgen, 10.3333°N, 84.0667°W, 500m, 2003–02–12, ALAS, Malaise (INBC); **Limón**: Reserva Biológica Hitoy Cerere, 9.65724°N, 83.0259°W, 530m, 2015–06–11, J. Longino, search (MUCR), 2015–06–11, ADMAC, maxiWinkler (MUCR), Reserva Biológica Hitoy Cerere, 9.65727°N, 83.026°W, 530m, 2015–06–11, J. Longino, search (MUCR), 2015–06–11, ADMAC, maxiWinkler (MUCR); **Puntarenas**: Cerro Rincon, Corcovado National Park, 8.55°N, 83.4833°W, 700m, 1981–02–27, J. Longino (JTLC), San Pedrillo, Corcovado National Park, 8.61667°N, 83.7333°W, 5m, 1980–06–14, J. Longino, hand collected (JTLC). **ECUADOR**: **Orellana**: Parque Nacional Yasuní, Tiputini Biodiversity Station, 288 km SE Quito, 0.633333°S, 76.15°W, 236m, 2011–12–11, Donnell, S. O. (DZUP); **Pastaza**: Parque Nacional Yasuní, Bameno, sendero Curaray 2, 1.301°S, 76.143°W, 240m, 2014–01–31, Troya, A.; Duque, P., fogging (MEPN); **Pichincha**: Reserva de Biodiversidad Mashpi, 50 Km NW Quito, 0.1544°N, 78.8905°W, 746m, 2017–04, Troya, A., hand collected (JTLC); **Sucumbíos**: Reserva de Producción Faunística Cuyabeno, Trocha Zábalo–Güepi, 0.25°S, 75.6833°W, 270m, 2000–08–08, Araujo, P., fogging (MEPN). **FRENCH GUIANA**: **Cayenne**: 12km East from the village of Sinnamary. Paracou Station, 5.26667°N, 52.9167°W, 50m,

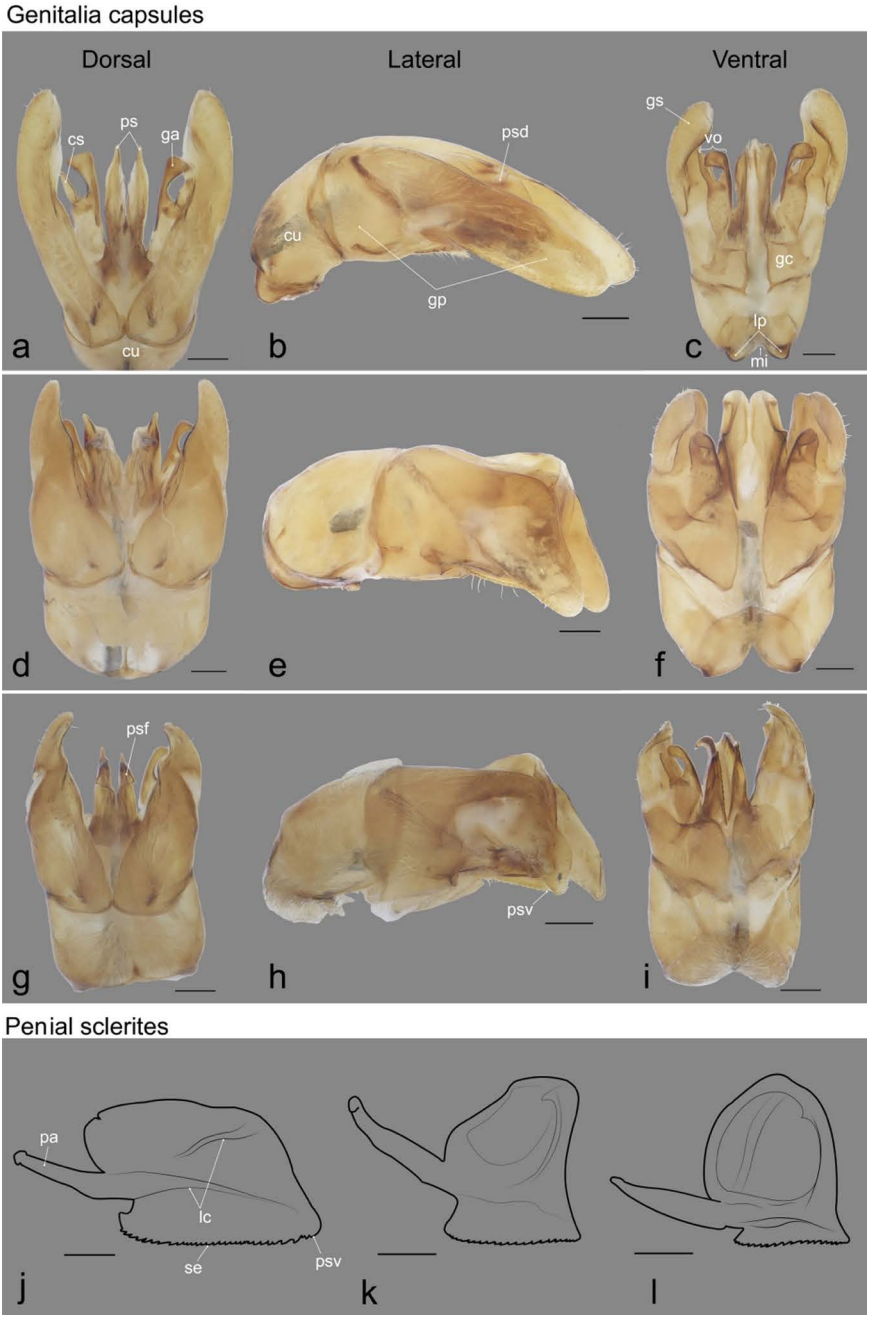

Fig. 28. *Neoponera laevigata* species–group, male genitalia capsules and right penial sclerites. *Neoponera commutata*, MEPN: ATPFOR2051 (**a–c**, **j**); *N. marginata*, UFVLABECOL: UFV–LABECOL010414 (**d–f**, **k**); *N. mashpi* **sp. nov.,** CPDC: ATPFOR2054–2 (**g–i**, **l**). Abbreviations: **cs** Cuspis; **cu** Cupula; **ga** Gonapophysis; **gc** Gonocoxa; **gp** Gonopod; **gs** Gonostylus; **lc** Lateral carina; **lp** Lobular process; **mi** Medial invagination; **pa** Penial apodeme; **ps** Penial sclerites; **psd** Penial sclerite dorsal apex; **psf** Penial sclerite flap; **psv** Penial sclerite ventral apex; **se** Serrated edge; **vo** Volsella. Scale bars = 0.2 mm.

DOI 10.1163/1876312X-bja10034

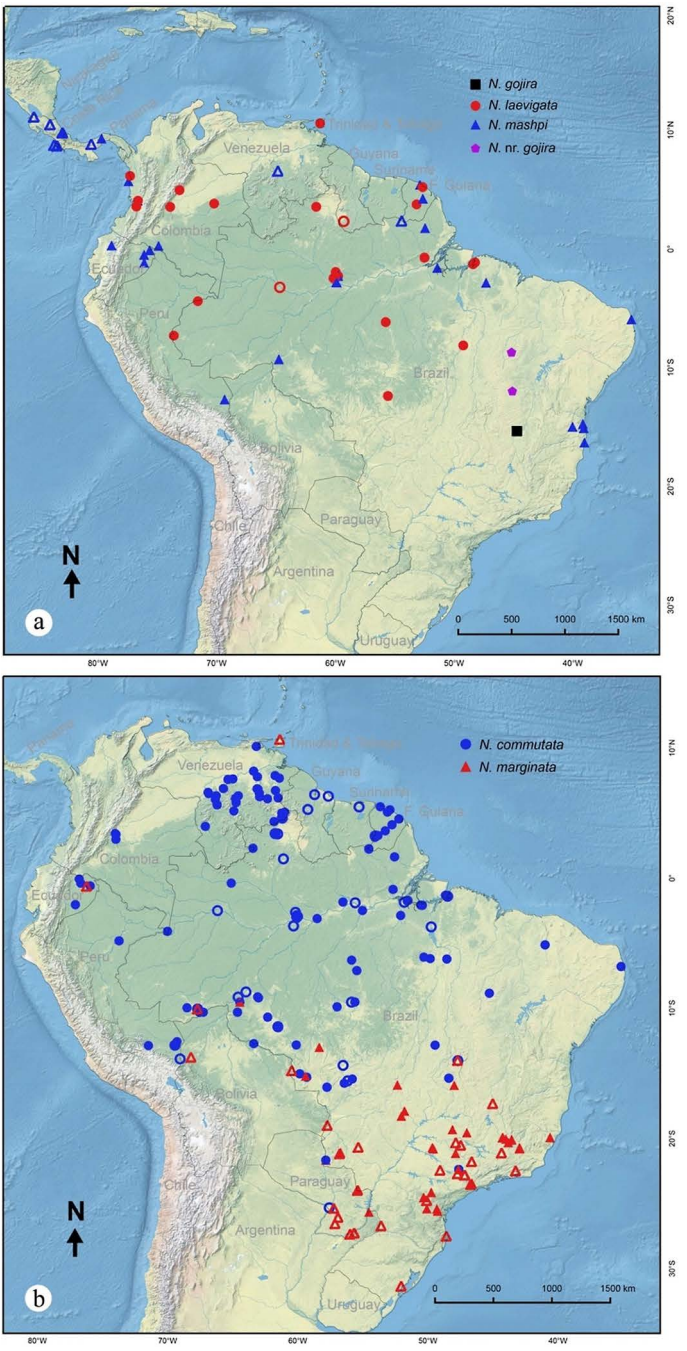

Fig. 29. Distribution of species in the *Neoponera laevigata* group. **a.** *Neoponera gojira* **sp. nov.**, *Neoponera* nr. *gojira*, *N. mashpi* **sp. nov.**, *N. laevigata*; **b.** *Neoponera commutata*, *N. marginata*. Empty icons (circles and triangles) belong to the same species as those with filled icons in each Figure, but these represent records obtained from the literature and AntWeb (see references below).

2002–04, Orivel, J. (CPDC), 1km E Nouragues Station, Grand Plateau, Nouragues Natural Reserve, 4.08885°N, 52.6749°W, 120m, 2018–08–21 (DZUP); **Saint–Laurent–du–Maroni**: Mitaraka, 2.22755°N, 54.4537°W, 335m, 2015–03–01, pitfall (EcoFoG). **PANAMA**: **Coclé**: 8 km NNW El Copé, Parque Nacional Omar Torrijos, 8.68543°N, 80.5989°W, 710m, 2015–01–22, hand collected (JTLC); **Colón**: Parque Nacional Soberanía, Pipeline road, La Seda, 9.15622°N, 79.7344°W, 60m, 2015–05–07, Schar, S., hand collected (MEPN). **PERU**: **Madre de Dios**: Reserva Nacional Tambopata, Sachavacayoc, 12.8167°S, 69.3667°W, 229m, 2012–07–26, Fernandes, I. (INPA). **VENEZUELA**: **Bolívar**: Nichare Field Station, Río Tawadu, 200m, 6.4333°N, 64.8833°W, 200m, 1996–02–10 (PSWC).

***Neoponera mashpi* sp. nov. geographic range.** Brazil, Colombia, Costa Rica, Ecuador, French Guiana, Panama, Peru, Suriname, Venezuela.

Acknowledgements

Adrian Troya and John Lattke are grateful to the following people who, in several ways, contributed either with general information, specimens, or with moral support. In alphabetical order, institutional affiliations in parentheses: Andrés Merino, Fernanda Salazar (PUCE, Ecuador); Carolina Londoño, Inge Armbrecht (Universidad del Valle, Colombia); Fernando Fernández, Andrés Meneses (Universidad Nacional de Colombia); Frank Azorsa (University of Boston); Itanna Fernandes (INPA, Brazil); Diana Espitia, Jhon Cesar–Neita (IAvH, Colombia); Jack Longino, Rodolfo Probst (University of UTAH, USA), Jacques Delabie, Priscila Silva, Alexandre Arnhold (CPDC, Brazil), Júlio Chaul (Universidade Federal de Viçosa, Brazil); Michelle Zavala (University of Pennsylvania); Mônica Ulysséa, Juan Pablo Botero (MZSP, Brazil); Lívia Pires, Rogério R. Silva, (MPEG, Brazil). Miguel Riera-Valera (Universidad Central de Venezuela, Venezuela) for organizing specimens in the MIZA collection. Also, special thanks to Jack Longino who kindly contributed sharing his knowledge on Central American *Neoponera*. We appreciate the comments and suggestions of three anonymous reviewers which certainly enhanced the quality of this manuscript. The following institutions contributed for the execution of this study: Escuela Politécnica Nacional, Ecuador; The Association of Systematic Biologists, USA; The Society for the Study of Evolution, USA; Conselho Nacional de Desenvolvimento Científico e Tecnológico – CNPq (Projeto 140995/2020– 0), Brazil.

Supplementary material

Supplementary material is available online at:
https://doi.org/10.6084/m9.figshare.20254404

References

Acosta–Avalos, D., Wajnberg, E., Oliveira, P.S, Leal, I., Farina, M. & Esquivel, D.M.S. (1999) Isolation of magnetic nanoparticles from *Pachycondyla* marginata ants. *Journal of Experimental Biology* **202**: 2687–2692. https://doi.org/10.1242/jeb.202.19.2687.

Acosta–Avalos, D., Esquivel, D.M., Wajnberg. E., Lins de Barros, H.G., Oliveira, P.S. & Leal, I. (2001) Seasonal patterns in the orientation system of the migratory ant *Pachycondyla marginata*. *Naturwissenschaften* **88**: 343–346. https://doi.org/10.1007/s001140100245.

Aili, S.R., Touchard, A., Koh, J.M.S., Dejean, A., Orivel, J., Padula, M.P., Escoubas, P. & Nicholson, G.M. (2016) Comparisons of Protein and Peptide Complexity in Poneroid and Formicoid Ant Venoms. *Journal of Proteome Research* **15**: 3039–3054. https://doi.org/10.1021/acs.jproteome.6b00182.

AntCat (2022) An online catalogue of the ants of the world by Barry Bolton. Available from: https://www.antcat.org. (accessed on Mar 2022).

AntWeb (2021) AntWeb. Available from: https://www.antweb.org. (accessed on Mar 2022).

Arnett, R., Samuelson, A.G. & Nishida, G.M. (2019) The Insect & Spider Collections of the World. CRC Press, Boca Ratón: 316 pp.

Arnold, M.L. (1992) Natural hybridization as an evolutionary process. *Annual review of Ecology and Systematics* **23** (1): 237–261. https://doi.org/10.1146/annurev.es.23.110192.001321.

Baksh–Comeau, Y.S., Maharaj, S.S., Adams, C.D., Harris, S.A., Filer, D.L. & Hawthorne, W.D. (2016). An annotated checklist of the vascular plants of Trinidad and Tobago with analysis of vegetation types and botanical 'hotspots'. *Phytotaxa* **250** (**1**): 1–431. https://doi.org/10.11646/phytotaxa.250.1.1.

Baroni Urbani, C. (1993) The diversity and evolution of recruitment behaviour in ants, with a discussion of the usefulness of parsimony criteria in the reconstruction of evolutionary histories. *Insectes Sociaux* **40**: 233–260. https://doi.org/10.1007/BF01242361.

Bolton, B. (1994) Identification guide to the ant genera of the world. Harvard University Press, Cambridge, Mass., United States: 232 pp.

Bolton, B. (1995) A new general catalogue of the ants of the world. Harvard University Press, Cambridge, Mass., United States: 504 pp. https://www.antcat.org/references/122860.

Borgmeier, T. (1959) Myrmecologische Studien. II. *Anais da Academia Brasileira de Ciencias* **31**: 309–319. https://antcat.org/references/122939.

Boudinot, B.E. (2013) The male genitalia of ants: Musculature, homology, and functional morphology (Hymenoptera, Aculeata, Formicidae). *Journal of Hymenoptera Research* **30**: 29–49. https://doi.org/10.3897/jhr.30.3535.

Boudinot, B.E. (2015) Contributions to the knowledge of Formicidae (Hymenoptera, Aculeata): a new diagnosis of the family, the first global male–based key to subfamilies, and a treatment of early branching lineages. *European Journal of Taxonomy* **120**: 1–62. https://doi.org/10.5852/ejt.2015.120.

Branstetter, M.G., & Longino, J.T. (2022) UCE Phylogenomics of New World *Cryptopone* (Hymenoptera: Formicidae) elucidates genus boundaries, species boundaries, and the vicariant history of a temperate–tropical disjunction. *Insect Systematics and Diversity* **6** (1): 6. https://doi.org/10.1093/isd/ixab031.

Brown, B.V. (2013) Automating the "Material examined" section of taxonomic papers to speed up species descriptions. *Zootaxa* **3683**: 297–299. https://doi.org/10.11646/zootaxa.3683.3.8.

Brown, W. (1973) A comparison of the Hylean and Congo–west African rain forest ants faunas. In: Meggers, B.J., Ayensu, E.S. & Duckworth, W.D. (Eds.), Tropical forest ecosystems in Africa and South America: a comparative review. Smithsonian Institution Press, Washington, D.C, pp. 350. https://www.antcat.org/references/search?reference_q=Brown%2C+W.+%281973%29.

Brown, W.L. (1995) [Untitled. Taxonomic changes in *Pachycondyla* and *Neoponera* attributed to William L. Brown]. In: Bolton, B. A new general catalogue of the ants of the world. Harvard University Press, Cambridge, pp. 504.

Cantone, S. (2017) Winged ants – The male. Dichotomous key to genera of winged male ants in the world. Behavioral ecology of mating flight. Autopubblicato, São Paulo, Brazil: 318 pp. https://antcat.org/references/143115.

Cantone, S., Von Zuben, C.J. (2019) The Hindwings of Ants: A Phylogenetic Analysis. *Psyche* **2019**: 1–11. https://doi.org/10.1155/2019/7929717.

Constantino, R. 2020. Termite Database. Brasília, University of Brasília. Available from: http://termitologia.net. (version Dec 2020).

Dallwitz, M. (1980) A general system for coding taxonomic descriptions. *Taxon* **29**: 41–46. https://doi.org/10.2307/1219595.

Da Ponte, E., Mack, B., Wohlfart, C., Rodas, O., Fleckenstein, M., Oppelt, N., ... & Kuenzer, C. (2017) Assessing forest cover dynamics and forest perception in the Atlantic Forest of Paraguay, combining remote sensing and household level data. *Forests* **8** (10), 389. https://doi.org/10.3390/f8100389.

Downing, H. (1978) Foraging and migratory behavior of the ponerine ant *Termitopone laevigata*. Smith College. Doctoral dissertation, Smith College, Northampton, Mass.

Emery, C. (1890) Voyage de M. E. Simon au Venezuela (Décembre 1887 - Avril 1888). Formicides. *Annales de la Société Entomologique de France* **10**: 55–76. https://www.antcat.org/references/124550.

Emery, C. (1892) ["1891"]. Note sinonimiche sulle formiche. *Bullettino della Società Entomologica Italiana* **23**: 159–167. https://antcat.org/references/124557.

Emery, C. (1901) Notes sur les sous–familles des dorylines et ponérines (famille des Formicides): 32–54. https://www.antcat.org/references/124641.

Emery, C. (1911) Hymenoptera. Fam. Formicidae. Subfam. Ponerinae. Genera Insectorum **118**: 1–25. https://www.antcat.org/references/124702.

Fernandes, I.O., De Oliveira, M.L & Delabie, J.H.C. (2014) Description of two new species in the Neotropical *Pachycondyla foetida* complex (Hymenoptera: Formicidae: Ponerinae) and taxonomic notes on the genus. *Myrmecological News* **19**: 133–163. https://www.antcat.org/references/142549.

Field, D.L., Ayre, D.J., Whelan, R.J., & Young, A. G. (2011) Patterns of hybridization and asymmetrical gene flow in hybrid zones of the rare *Eucalyptus aggregata* and common *E. rubida*. *Heredity*, **106** (**5**): 841–853. https://doi.org/10.1038/hdy.2010.127.

Gallardo, A. (1918) Las hormigas de la República Argentina. Subfamilia Ponerinas. *Anales del Museo Nacional de Historia Natural de Buenos Aires* **30**: 1–112. https://antcat.org/references/125422.

García, M., Rijk, G. & Piotrowski., M. (2021) Key Cerrado Deforesters in 2020 Linked to the Clearing of More Than 110,000 Hectares. *Chain Reaction Research*: 1–16. https://chainreactionresearch.com/wp-content/uploads/2021/03/Key-Cerrado-Deforesters-Linked-to-the-Clearing-of-More-than-110000-Hectares-2.pdf.

Google Maps (2021). Google. https://earth.google.com.

Gower, J. C. (1971) A general coefficient of similarity and some of its properties. *Biometrics* **27** (**4**): 857–871 https://doi.org/10.2307/2528823.

Harris, R.A. (1979) Glossary of surface sculpturing. *Occasional Papers in Entomology*: 32. http://bioguid.osu.edu/xbiod_pubs/4823.

Hermann, H.R. (1968) Group raiding in *Termitopone commutata* (Roger) (Hymenoptera: Formicidae). *Journal of the Georgia Entomological Society* **3**: 23–24. https://www.antcat.org/references/125869.

Hölldobler, B., Traniello, J.F.A. (1980) The pygidial gland and chemical recruitment communication in *Pachycondyla* (=*Termitopone*) *laevigata*. *Journal of Chemical Ecology* **6**: 883–893. https://doi.org/10.1007/BF00990472.

Hölldobler, B., Janssen, E., Bestmann, H.J., Leal, I.R., Oliveira, P.S., Kern, F. & König, W.A. (1996) Communication in the migratory termite–hunting ant *Pachycondyla* (= *Termitopone*) *marginata* (Formicidae: Ponerinae). *Journal of Comparative Physiology A*: Sensory, Neural, and Behavioral Physiology **178**: 47–53. https://antcat.org/references/131491.

IBGE (2004) Mapa da vegetação do Brasil. Ministerio do Planejamento, Orçamento e Gestão. Available from: https://www.ibge.gov.br/geociencias/informacoes–ambientais/vegetacao/15842–biomas.html?edicao=16060&t=acesso–ao–produto. (accessed on Oct 2020).

Janicki, J., Narula, N., Ziegler, M., Guénard, B. & Economo, E.P. (2016) Visualizing and interacting with large–volume biodiversity data using client–server web–mapping applications: The design and

implementation of antmaps.org. *Ecological Informatics* **32**: 185–193. https://doi.org/10.1016/j.ecoinf.2016.02.006l.

Kaiser, H.F. (1961) A Note on Guttman'S Lower Bound for the Number of Common Factors. *British Journal of Statistical Psychology* **14**: 1–2. https://doi.org/10.1111/j.2044–8317.1961.tb00061.x.

Keller, R.A. (2011) A phylogenetic analysis of ant morphology (Hymenoptera: Formicidae) with special reference to the poneromorph subfamilies. *Bulletin of the American Museum of Natural History* **2011**: 1–90. https://doi.org/10.1206/355.1.

Krishna, K., Araujo, R.L. (1968) A revision of the neotropical termite genus *Neocapritermes* (Isoptera: Termitidae: Termitinae). *Bulletin of the AMNH* **138**. http://hdl.handle.net/2246/1107.

Kruskal, J.B. (1964) Multidimensional scaling by optimizing goodness of fit to a nonmetric hypothesis. *Psychometrika* **29**: 1–27. https://doi.org/10.1007/BF02289565.

Lattke, J.E. (2012) Revision of the new world species of the genus *Leptogenys* Roger Insecta: Hymenoptera: Formicidae: Ponerinae. *Arthropod Systematics and Phylogeny* **70**: 71. https://www.antcat.org/references/132941.

Leal, I.R. & Oliveira, P.S. (1995) Behavioral ecology of the neotropical termite–hunting ant *Pachycondyla* (= *Termitopone*) *marginata*: colony founding, group–raiding and migratory patterns. *Behavioral Ecology and Sociobiology* **37**: 373–383. https://doi.org/10.1007/BF00170584.

Longino, J. (1999) Ants of Costa Rica. https://ants.biology.utah.edu/AntsofCostaRica.html (accessed on Aug 2021).

Longino, J.T. & Branstetter, M.G. (2020) Phylogenomic species delimitation, taxonomy, and 'bird guide' identification for the Neotropical ant genus *Rasopone* (Hymenoptera: Formicidae). Insect Systematics and Diversity **4** (**2**): 1–33. https://doi.org/10.1093/isd/ixaa004.

Mackay, E. & Mackay, W. (2010) The systematics and biology of the New World ants of the genus *Pachycondyla* (Hymenoptera: Formicidae). Edwin Mellen Press, Unites States: 642 pp. https://www.antcat.org/references/131785.

Mayr, E. (1942) Systematics and the Origin of Species. Columbia University Press, New York: 334 pp.

Mayr, G. (1863) Formicidarum index synonymicus. *Verhandlungen der Kaiserlich-Königlichen Zoologisch-Botanischen Gesellschaft in Wien* **13**: 385–460. https://antcat.org/references/127213.

Mayr, G. 1886. Notizen über die Formiciden-Sammlung des British Museum in London. Verhandlungen der Kaiserlich-Königlichen Zoologisch-Botanischen Gesellschaft in Wien 36: 353–368. https://antcat.org/references/127239.

Mendoza, A.M., Bolívar–García, W., Vázquez–Domínguez, E., Ibáñez, R. & Parra Olea, G. (2019) The role of Central American barriers in shaping the evolutionary history of the northernmost glassfrog, *Hyalinobatrachium fleischmanni* (Anura: Centrolenidae). *PeerJ* **2019**: 1–28. https://doi.org/10.7717/peerj.6115.

Mill, A.E. (1982a) Emigration of a colony of the giant termite hunter, *Pachycondyla commutata* (Roger) (Hymenoptera: Formicidae). *Entomologist's Monthly Magazine* **118**: 243–245. https://agris.fao.org/agris-search/search.do?recordID=US201302602888.

Mill, A.E. (1982b) Faunal studies on termites (Isoptera) and observations on their ant predators (Hymenoptera: Formicidae) in the Amazon Basin. *Revista Brasilera de Entomologia* **26**: 253–260.

Mill, A.E. (1984) Predation by the ponerine ant *Pachycondyla commutata* on termites of the genus *Syntermes* in Amazonian rain forest. *Journal of natural History* **18**: 405–410. https://doi.org/10.1080/00222938400770341.

National Geodetic Survey (2021) NGS Coordinate Conversion and Transformation Tool (NCAT). https://www.ngs.noaa.gov/NCAT/. (accessed on Jan 2021).

Ogata, K. (1991) A generic synopsis of the poneroid complex of the family Formicidae (Hymenoptera). Part II. Subfamily Myrmicinae. *Bulletin of the Institute of Tropical Agriculture*. Kyushu Univ. **14**: 61–149.

Oksanen, J., Blanchet, F.G., Kindt, R., Legendre, P., Minchin, P.R. & O' Hara, R.B. (2015) Vegan community ecology package: ordination methods, diversity analysis and other functions for community and vegetation ecologists. R package version 2.5–7. https://github.com/vegandevs/vegan.

Orivel, J., Redeker, V., Le Caer, J.P., Krier, K., Revol–Junelles, A.M., Longeon, A., Chaffotte, A., Dejean, A. & Rossier, J. (2001) Ponericins, new antibacterial and insecticidal peptides from the venom of the ant *Pachycondyla goeldii*. *Journal of Biological Chemistry* **276**: 17823–17829. https://doi.org/10.1074/jbc.M100216200.

Rakotonirina, J.C. & Fisher, B.L. (2013) Revision of the *Pachycondyla sikorae* species–group (Hymenoptera: Formicidae) in Madagascar. *Zootaxa* **3683**: 447–485. https://doi.org/10.11646/zootaxa.3683.4.8.

Ribeiro, M.C., Metzger, J.P., Martensen, A.C., Ponzoni, F.J. & Hirota, M.M. (2009) The Brazilian Atlantic Forest: How much is left, and how is the remaining forest distributed? Implications for conservation. *Biological Conservation* **142**: 1141–1153. https://doi.org/10.1016/j.biocon.2009.02.021.

Roger, J. (1860) Die *Ponera*–artigen Ameisen. Berliner *Entomologische Zeitschrift* **4**: 278–312. https://www.antcat.org/references/128087.

Roger, J. (1861) Die *Ponera*–artigen Ameisen (Schluss). *Berliner Entomologische Zeitschrift* **5**: 1–54. https://antcat.org/references/128088.

Roger, J. (1863) Verzeichniss der Formiciden-Gattungen und Arten. *Berliner Entomologische Zeitschrift* **7**: 1–65. https://antcat.org/references/128094.

Schmid–Hempel, P. (1998) Parasites in social insects. Princeton University Press: 393 pp. ISBN:9780691059242.

Schmidt, C. (2013) Molecular phylogenetics of ponerine ants (Hymenoptera: Formicidae: Ponerinae). *Zootaxa* **3647**: 201–250. https://www.antcat.org/references/142356.

Schmidt, C.A. & Shattuck, S.O. (2014) The Higher Classification of the Ant Subfamily Ponerinae (Hymenoptera: Formicidae), with a Review of Ponerine Ecology and Behavior. Zootaxa **3817**: 1–242. https://doi.org/10.11646/zootaxa.3817.1.1.

Schmidt, J.O. & Overal, W.L. (2009) Venom and task specialization in *Termitopone commutata* (Hymenoptera: Formicidae). *Journal of Hymenoptera Research* **18**: 361–367. https://antcat.org/references/132225.

Sena–Souza, J.P., Houlton, B.Z., Martinelli, L.A. & Bielefeld Nardoto, G (2020) Reconstructing continental–scale variation in soil δ15N: a machine learning approach in South America. *Ecosphere* **11** (**8**): e03223. https://doi.org/10.1002/ecs2.3223.

Serna, F. & Mackay, W. (2010) A descriptive morphology of the ant genus *Procryptocerus* (Hymenoptera: Formicidae). *Journal of Insect Science* **10** (**1**). https://doi.org/10.1673/031.010.11101.

Silva, T.S.R. & Feitosa, R.M. (2019) Using controlled vocabularies in anatomical terminology: A case study with *Strumigenys* (Hymenoptera: Formicidae). *Arthropod Structure and Development* **52**: 100877. https://doi.org/10.1016/j.asd.2019.100877.

Smith, F. (1858) Catalogue of hymenopterous insects in the collection of the British Museum. Part VI. Formicidae. London: British Museum, 216 pp. https://www.antcat.org/references/128685.

Soterroni, A.C., Ramos, F.M., Mosnier, A., Fargione, J., Andrade, P.R., Baumgarten, L., Pirker, J., Obersteiner, M., Kraxner, F., Câmara, G., Carvalho, A.X.Y. & Polasky S (2019) Expanding the soy moratorium to Brazil's Cerrado. *Science Advances* **5**. DOI: 10.1126/sciadv.aav7336.

Tozetto, L., Lattke, J.E. (2020) Revealing male genital morphology in the giant ant genus *Dinoponera* with geometric morphometrics. *Arthropod Structure and Development* **57**: 100943. https://doi.org/10.1016/j.asd.2020.100943.

Traniello, J.F.A. (1981) Enemy deterrence in the recruitment strategy of a termite: Soldier–organized foraging in *Nasutitermes costalis*. *Proceedings of the National Academy of Sciences* **78**: 1976–1979. https://doi.org/10.1073%2Fpnas.78.3.1976.

Wajnberg, E, Rossi, A.L. & Esquivel, D.M.S. (2017) Titanium and iron titanium oxide nanoparticles in antennae of the migratory ant *Pachycondyla marginata*: an alternative magnetic sensor for magnetoreception? *BioMetals* **30**: 541–548. https://doi.org/10.1007/s10534-017-0024-z.

Wheeler, W.M. (1922) The ants of Trinidad. American Museum Novitates 45: 1–16. https://antcat.org/references/130152.

Wheeler, W.M. (1936) Ecological relations of ponerine and other ants to termites. *Proceedings of the American Academy of Arts and Sciences* **71**: 158–243. https://www.antcat.org/references/130270.

Wild, A.L. (2005) Taxonomic revision of the Pachycondyla apicalis species complex (Hymenoptera: Formicidae). *Zootaxa* **834**: 1–25. https://doi.org/10.11646/zootaxa.834.1.1.

Wilson, E.O. (1955) A Monographic Revision of the Ant Genus Lasius. *Bulletin of the Museum of Comparative Zoology at Harvard College* **113**: 59–77. https://doi.org/10.5281/zenodo.25290.

Yoder, M.J., Mikó, I., Seltmann, K.C., Bertone, M.A. & Deans, A.R. (2010) A gross anatomy ontology for Hymenoptera. *PLoS ONE* **5**: e15991. https://doi.org/10.1371/journal.pone.0015991.

References for non–examined material included in the distribution maps

Demétrio, M.F., Silvestre, R., de Souza, P. R. & Aoki, C. (2017) Inventário da fauna de formigas (Hymenoptera, Formicidae) no Mato Grosso do Sul, Brasil. *Iheringia. Série Zoologia* **107**. https://doi.org/10.1590/1678-4766e2017126.

Emery, C. (1894) [Untitled.]. Pp. 373–401 in: von Jhering, H. 1894. Die ameisen von Rio Grande do Sul. Berliner Entomologische Zeitschrift **39**: 321–447. https://www.antcat.org/references/124581.

Fowler, H. G. (1981) Nuevos registros de hormigas para el Paraguay (Hymenoptera Formicidae). *Neotropica* **26**: 183–186. https://www.antcat.org/references/125297.

Harada, A.Y. (2016). State of art of ants (Hymenoptera: Formicidae) at Caxiuanã, Melgaco, Pará, Brazil. *Advances in Entomology* **4**: 115–132. http://dx.doi.org/10.4236/ae.2016.43013.

Hölldobler, B., Janssen, E., Bestmann, H. J., Kern, F., Leal, I. R., Oliveira, P. S., & König, W. A. (1996) Communication in the migratory termite–hunting ant *Pachycondyla* (= *Termitopone*) *marginata* (Formicidae, Ponerinae). *Journal of Comparative Physiology A* **178** (**1**): 47–53. https://antcat.org/references/131491.

Lutinski, J.A., Lopes, B.C. & de Morais A.B.B. (2013) Diversidade de formigas urbanas (Hymenoptera: Formicidae) de dez cidades do sul do Brasil. *Biota Neotropica* **13**: 332–342. https://doi.org/10.1590/S1676-06032013000300033.

Mackay, E. & Mackay, W. (2010) The systematics and biology of the New World ants of the genus Pachycondyla (Hymenoptera: Formicidae). Edwin Mellen Press, Unites States: 642 pp. https://www.antcat.org/references/131785.

Oliveira, M.A., Della Lucia, T.M.C., Marinho, C.G.S., Delabie, J.H.C., & Morato, F.F. (2009) Ant (Hymenoptera: Formicidae) diversity in an area of the Amazon forest in Acre, Brazil. Sociobiology **54** (**1**): 243–267.

Rosumek, F.B., Ulysséa, M.A., Lopes, B.C., Steiner, J., & Zillikens, A. (2008) Formigas de solo e de bromélias em uma área de Mata Atlântica, Ilha de Santa Catarina, sul do Brasil: Levantamento de espécies e novos registros. *Biotemas*, **21** (4): 81–89. https://doi.org/10.5007/2175–7925.2008v21n4p81.

Santos–Silva, L., Vicente, R. E. & Feitosa, R.M. (2016) Ant species (Hymenoptera, Formicidae) of forest fragments and urban areas in a Meridional Amazonian landscape. *Check List* **12**: 1885. https://doi.org/10.15560/12.3.1885.

Souza, J.L.P., Baccaro, F.B., Landeiro, V.L., Franklin, E., Magnusson, W.E.L., Pequeno, P.A.C. & Fernandes, I.O. (2016) Taxonomic sufficiency and indicator taxa reduce sampling costs and increase monitoring effectiveness for ants. *Diversity and Distributions* **22**: 111–122. https://repositorio.inpa.gov.br/handle/1/17405.

Vicente, R.E., Prado, L.P. & Izzo, T.J. (2016) Amazon Rainforest Ant–Fauna of Parque Estadual do Cristalino: Understory and Ground–Dwelling Ants. *Sociobiology* **63**: 894. https://doi.org/10.13102/sociobiology.v63i3.1043.

Wheeler, W.M. (1936) Ecological relations of ponerine and other ants to termites. *Proceedings of the American Academy of Arts and Sciences* **71** (3): 159–243. https://www.antcat.org/references/130270.

Wheeler, W.M. (1925) Neotropical ants in the collections of the Royal Museum of Stockholm. *Arkiv för Zoologi* **17**: 1–55. https://www.antcat.org/references/130175.

Wilkie, K.T.R., Mertl, A.L. & Traniello, J.F. (2010) Species diversity and distribution patterns of the ants of Amazonian Ecuador. *PLoS One* **5** (10): e13146. https://doi.org/10.1371/journal.pone.0013146.